

**Synthesis and Characterization of Metal-Metal Multiply Bonded
Complexes and Catalytic Applications of Solvent Stabilized
Transition Metal Complexes for Polymerization of Olefins**

Guofang Zhang

Anorganisch-chemisches Institut der Technischen Universität München

Synthesis and Characterization of Metal-Metal Multiply Bonded Complexes and Catalytic Applications of Solvent Stabilized Transition Metal Complexes for Polymerization of Olefins

Guofang Zhang

Vollständiger Abdruck der von der Fakultät für Chemie der Technischen Universität München zur Erlangung des akademischen Grades eines

Doktors der Naturwissenschaften

genehmigten Dissertation

Vorsitzender:	Univ.-Prof. Dr. Klaus Köhler
Prüfer der Dissertation	1. Priv.-Doz. Dr. Fritz E. Kühn
	2. Univ.-Prof. Dr. Oskar Nuyken

Die Dissertation wurde am 18. 06. 2001 bei der Technischen Universität München eingereicht und durch die Fakultät für Chemie am 16. 07. 2001 angenommen.

Guofang Zhang

Synthesis and Characterization of Metal-Metal Multiply Bonded Complexes and Catalytic Applications of Solvent Stabilized Transition Metal Complexes for Polymerization of Olefins

Die vorliegende Arbeit entstand in der Zeit von April 1998 bis August 2001 am Anorganisch-chemischen Institut der Technischen Universität München.

I would like to express my deep gratitude to my academic supervisor

Priv.-Doz. Dr. Fritz. E. Kühn

for having always an open ear and patient instructions for all the chemical problems and others, for believing in me and in my work as well as having great interest in my work.

and

Prof. Dr. Dr. h.c. mult. Wolfgang A. Herrmann

for the opportunity to work in his laboratory, the excellent research conditions and the continuous support of my work.

Support of this research by the Katholischer Akademischer Ausländer-Dienst (KAAD) through a grant is greatly acknowledged.

Acknowledgements:

My sincere thanks go to Dr. Xue Wen-Mei for her close cooperation in the laboratory and for her partial contribution to this work as well as her invaluable help and discussion. To Prof. Dr. Oskar Nuyken, Dr. Jürgen R. Ismeier and Mr. Dirk Schön I am very grateful for the fruitful cooperation in the field of polymerization of olefins, as well as to Prof. Dr. Isabel S. Gonçalves, Dr. Paula Ferreira and other members in the group of Prof. Dr. Isabel S. Gonçalves for cooperation on derivatized MCM-41 mesoporous materials. To Prof. Dr. Klaus Köhler I give my deep thanks for his help in many things.

Dr. Eberhardt Herdtwerk is acknowledged for the X-ray structural determinations included in this work. Dr. Gabriele Raudaschl-Sieber is also acknowledged for her measurements of some Raman and Solid-state NMR spectra included in this work and for her friendly help in other things. Prof. Dr. Mink is also acknowledged for his measurements of some Raman and IR spectra of this work and their assignments as well as for his valuable discussions and suggestions.

Dr. Barth and his team are also acknowledged for the elemental analysis presented in this work. Frau R. Dumitrescu is acknowledged for the measurements of mass spectra and to Frau Romana Kuçi I would like to thank for her measurements of some NMR spectra presented in this work.

To Dr. Shi Jicheng, Dr. Zuo Jinglin, Dr. Liu Qiancai and Dr. Tang Yongjun I am grateful for their many helps and discussions in chemistry and non-chemical area. To PD. Dr. Reiner Anwander I would like to thank his friendly help in many cases.

Frau Donaubauer, Frau Grötsch, Frau Schuhbauer, Frau Kaufmann and Frau Huber of the secretary's office are acknowledged for their help with organization and many tedious matters.

To Dr. Xue Wen-Mei, Dr. Jürgen Schwarz, Dr. Ana Santos and Dr. Jörg Fridgen I would like to thank for the good working atmosphere. To Dipl. Chem. Klaus Lembacher give my thanks for his invaluable help in many matters.

To all the members of Prof. Herrmann's group, I am thankful for their cooperativeness and friendly working atmosphere, as well as all the people that in some way contributed to this thesis.

Personally my deep thanks to my friends in Munich and other cities of Germany should be expressed, particularly the family of Mr. Zhao Tianliang, of Dr. Lu Yafeng, of Dr. Wu Minyao, of Mr. Du Hailong, of Dr. Xue Wen-Mei, of Dr. Kuang Guokui, priest Johannes Chen, Mr. He Fan and my neighbor Mr. Luo Gang. It is just these friends that my life in Munich is of happiness and of colorfulness. Priest Johannes Chen is further acknowledged for his spiritual welfare and Mr. He Fan for computer care.

To my mother I don't know how to express my thanks, because she is now more than seventy years old and I am studying in a remote place and thus I cannot take care of her. To my brothers, sisters and relatives I am very grateful for their taking care of my mother and for their support to me.

Finally I would like to express my deepest gratitude to my wife, who shares laughs and tears with me all the time. She nearly bears all household duties so that I have more time to do my research work and gives me warm encouragements whenever I encounter difficulties in my work.

*To my mother, my wife and my son
with deep gratitude and love*

Contents

1	Introduction and Objectives	1
1A.	Introduction	1
1A.1	The Recognition of Metal-Metal Bond	1
1A.2	An Overview of the Quadruple Bond	2
1A.3	Quadruple Metal-Metal Bond Dimolybdenum (II) and Dirhodium (II) Compound	3
1A.4	Catalytic Applications of Dimolybdenum(II,II) Complexes Containing Multiple Metal-Metal Bonds	6
1A.4.1	Polymerization of Olefins	6
1A.4.2	Ring-Opening Metathesis Polymerization of Cyclo-Olefins	7
1A.4.3	Grafting of Dimolybdenum(II,II) Complexes on Metal Oxides	8
1A.4.4	Mechanistic Considerations	10
1B.	Objectives of This Work	12
2	Results and Discussion	14
Part A.	Synthesis and Characterization of Complexes with M -M Multiple Bonds	14
2A.1	Dimolybdenum(II) Complexes Linked by Cyano Bridges to Organic and Organometallic Ligands	14

2A.1.1	Introduction	14
2A.1.2	Results and Discussion.	15
2A.1.2.1	Synthesis	15
2A.1.2.2	Molecular Structures.	17
2A.1.2.3	Spectroscopy.	20
2A.2	Dimolybdenum(II) Complexes Linked by Pyridine and Its Derivatives	26
2A.2.1	Introduction	26
2A.2.2	Results and Discussion.	26
2A.2.2.1	Synthesis	26
2A.2.2.2	Structures	27
2A.2.2.3	Spectroscopy.	28
2A.3	Synthesis and Characterization of Dimolybdenum and Dirhodium Complexes Bearing 2-pyridylphosphine Ligands, PPhPy ₂ or PPy ₃ (Ph = Phenyl, Py = 2-Pyridyl)	33
2A.3.1	Introduction	33
2A.3.2	Results and Discussion	34
2A.3.2.1	Syntheses	34
2A.3.2.2	Molecular Structures	36

2A.3.2.3	Spectroscopy.	37
Part B	Cationic Polymerization of Olefins.	39
2B.1	Solvent Stabilized Transition Metal Cations as Initiators for Cyclopentadiene Polymerization	40
2B.1.1	Introduction	40
2B.1.2	Results and Discussion	42
2B.1.2.1	Effect of Reaction Time	44
2B.1.2.2	Effect of Concentration of the Initiator	45
2B.1.2.3	Effect of Solvents	46
2B.1.2.4	Effect of Aging Time	46
2B.1.2.5	Other Effects.	47
2B.2	Monometallic Solvent Stabilized Transition Metal Cations as Initiators for Cyclopentadiene Polymerization	52
2B.2.1	Introduction	52
2B.2.2	Results and Discussion	52
2B.3	Synthesis and Characterization of MCM-41-Supported Dimolybdenum Complexes	60
2B.3.1	Introduction	60

2B.3.2	Results and Discussion.	61
2B.3.2.1	Synthesis and Textural Characterization.	61
2B.3.2.2	Powder XRD.	63
2B.3.2.3	N ₂ Adsorption Studies	64
2B.3.2.4	Solid-State NMR and FTIR Spectroscopy	66
2B.4	XAFS Analysis and Catalytic Activity of MCM-41-supported Dimolybdenum Complexes Containing Metal-Metal Bonds	73
2B.4.1	Introduction	73
2B.4.2	Results and Discussion.	73
2B.4.2.1	XAFS Analysis	73
2B.4.2.2	Heterogeneous Polymerization of Methylcyclopentadiene	79
3	Summary	82
4	Experimental Part.	86
4.1	General	86
4.2	Characterization and Analysis of the Complexes	86
4.3	Syntheses of the Complexes.	91
4.3.1	Dimolybdenum(II) Complexes Linked by Cyano Bridges to Organic and Organometallic Ligand.	91

4.3.2	Dimolybdenum(II) Complexes Linked by Pyridine and Its Derivatives	96
4.3.3	Dimolybdenum(II) and Dirhodium Complexes Bearing 2- Pyridylphosphine Ligands, PPhPy ₂ and PPy ₃	101
4.3.4	Solvent Stabilized Metal-Metal Bond Complexes.	105
4.3.5	Solvent Stabilized Monomeric Complexes.	107
4.3.6	Mesoporous MCM-41	107
4.4	Grafting of Homogeneous Catalysts and Characterization of the Fixed Materials	107
4.5	Cationic Polymerization of Olefins	110
4.5.1	Polymerization of Cyclopentadiene	110
4.5.2	Polymerization of Methylcyclopentadiene.	111
5	Bibliography	112
	Chapter 1A	112
	Chapter 2A	115
	Chapter 2A.1	115
	Chapter 2A.2	116
	Chapter 2A.3	117
	Chapter 2B.	118

	Chapter 2B.1.	118
	Chapter 2B.2.	119
	Chapter 2B.3	120
	Chapter 2B.4	122
	Chapter 3.	122
	Chapter 4.	123
6	Appendix	125

Introduction

Abbreviation List:

Ac	acetato
AN	acetonitrile
BPh ₄	tetraphenylborate
ClAc	chloroacetato
Cl ₂ Ac	dichloroacetato
Cl ₃ Ac	trichloroacetato
Cp	η^5 -cyclopentadienyl
δ	chemical shift
DMF	dimethylformamide
DMSO	dimethylsulfoxide
dppm	bis(diphenylphosphino)amine
dppma	bis(diphenylphosphino)aminomethane
Et	ethyl
IR	Infrared Spectroscopy
L	ligand
MAS NMR	Magic Angle Spinning NMR
Me	methyl
ν	wave number
NMR	Nuclear Magnetic Resonance Spectroscopy
Ph	phenyl
PPh ₃	triphenylphosphine
PPh ₂ Py	diphenyl(2-pyridyl)phosphine
PPhPy ₂	bis(2-pyridyl)phenylphosphine
PPy ₃	tri(2-pyridyl)phosphine
ppm	parts per million
Py	pyridine or 2-pyridyl
PXRD	Powder X-Ray Diffraction

RT	room temperature
S	solvent
TFPB	tetrakis[3,5-bis(trifluoromethyl)phenyl]borate
THF	tetrahydrofuran
TMS	tetramethylsilane

Chapter 1A. Introduction

1A.1 The Recognition of the Metal-Metal Bond

From the time of Alfred Werner (*ca.* 1900) until the early 1960s, the chemistry of the transition metals was based entirely on the conceptual framework established by Werner ^[1]. This Wernerian scheme has as its essential feature the concept of a single metal ion surrounded by a set of ligands. Although many advances were made during that time, these expansions upon Werner's theme only are *evolutionary* progress, all referring to, in essence, *one-center coordination chemistry*.

As early as 1907 a compound, "TaCl₂·2H₂O", now known as Ta₆Cl₁₄·7H₂O with an octahedral cluster of Ta atoms, was reported, but its behavior could not be understandable in Wernerian terms. Although later the structural work of Brosset ^[2] showed the occurrence of Mo₆ clusters that explains the behavior of this special type of compounds. However, neither of this work, nor subsequent studies led to any comprehensive recognition of the existence of a new area of transition metal chemistry. It was only in 1963, when two different laboratories ^[3,4] at the same time observed that 'ReCl₄⁻' actually contains triangular Re₃ groups in which the Re-Re distances (2.47 Å) are significantly shorter than those (2.75 Å) in metallic rhenium and one of the groups ^[3] gave a complete description of its molecular structure and a detailed discussion of its electronic structure leading to the conclusion that the rhenium atoms are united by a set of three Re-Re double bonds, that the field of metal-metal bonds and clusters became a recognized, non-Wernerian field of inorganic chemistry. Since then, intense research was conducted in this type of chemistry and extended to all of the transition elements except for manganese, with highlights being the recognition of triple and quadruple bonds ^[5c].

1A.2 An Overview of the Quadruple Bond

After the recognition of Re-Re double bonds in the trinuclear cluster anion [Re₃Cl₁₂]³⁻ in mid-1963, further studies were being performed in this respect ^[6]. Despite the chloride and bromide

of Re^{III} had been often employed as starting materials for the preparation of Re^{III} clusters ^[1], the preparation of these starting materials was tedious and time-consuming. The chemists therefore paid their attention to reduction of readily available $[\text{ReO}_4]^-$ ion in aqueous solution for synthesis of the trinuclear complexes. The group of F. A. Cotton, while reexamining the rhenium complexes published by Soviet chemists ^[7], used hypophosphorous acid instead of high-pressure hydrogen gas as the reducing reagent to synthesize other rhenium compounds ^[8] and found that these complexes contain the identical $[\text{Re}_2\text{Cl}_8]^{2-}$ anion. They resolved the crystal structure of $\text{K}_2\text{Re}_2\text{Cl}_8 \cdot 2\text{H}_2\text{O}$ successfully, as shown in Fig. 1A.1. Consequently, they proposed and illustrated explicitly in September of 1964 the existence of a quadruple bond between the two rhenium atoms in the eclipsed structure of $[\text{Re}_2\text{Cl}_8]^{2-}$ ion. Later the quadruple bonds were discovered in other transition metals: Mo, Tc, Cr and W. Today the concept of quadruple bonds has become commonly and far more than one thousand such compounds have been published to date.

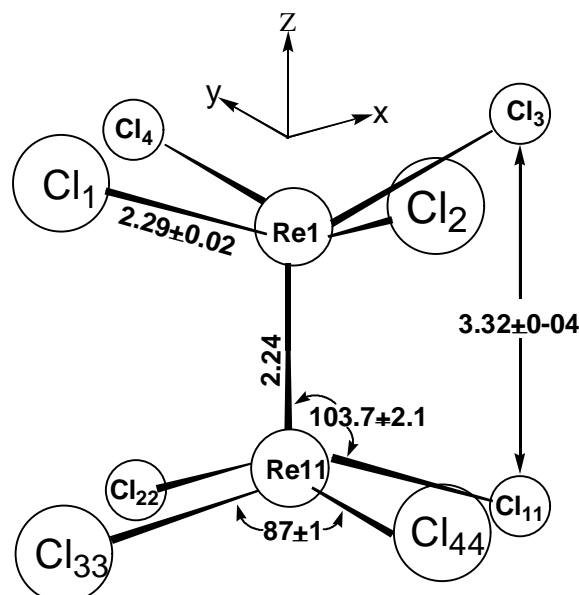


Fig. 1A.1 The structure of the $[\text{Re}_2\text{Cl}_8]^{2-}$ ion as originally reported in Ref. 8b with a Cartesian coordinate system.

For the formation of a quadruple bond, d -orbitals or higher (f , g , etc., orbitals) are required. In fact, contributions of only d -orbitals can formulate the quadruple bond, such as in the $[\text{Re}_2\text{Cl}_8]^{2-}$ ion shown in Fig. 1A.1. Taking $[\text{Re}_2\text{Cl}_8]^{2-}$ ion as an example, if we define the Re-Re axis as the z direction and the Re-Cl bond axes as $\pm x$ and $\pm y$, the eight lobes of the two $d_{x^2-y^2}$ orbitals are involved in the formation of rhenium-to-chlorine σ bonds; the remaining d orbitals are engaged

in the establishment of the Re-Re quadruple bond (one σ , two π , one δ orbital), the electron configuration of which is $\sigma^2\pi^4\delta^2$. Such a bond has two characteristic properties: (1) it is very strong, therefore very short, and (2) the $[\text{Re}_2\text{Cl}_8]^{2-}$ moiety displays an eclipsed structure due to an inherent dependence of the δ bond on the angle of internal rotation. In addition to these two properties, this type of compounds has a number of interesting chemical and spectroscopic characteristics. The most characteristic spectroscopic feature of them is their various bright colors such as royal blue of $[\text{Re}_2\text{Cl}_8]^{2-}$ ion, yellow of $\text{Mo}_2(\text{O}_2\text{CCH}_3)_4$, intense red $[\text{Mo}_2\text{Cl}_8]^{4-}$, due to the $\delta \rightarrow \delta^*$ transition.

1A.3 Quadruple Metal-Metal Bond Dimolybdenum (II) and Dirhodium (II) Compounds

At the present time the largest group of compounds that contain quadruple bonds remain those of molybdenum. The most generally useful access to this chemistry are shown in the following equations ^[10]:

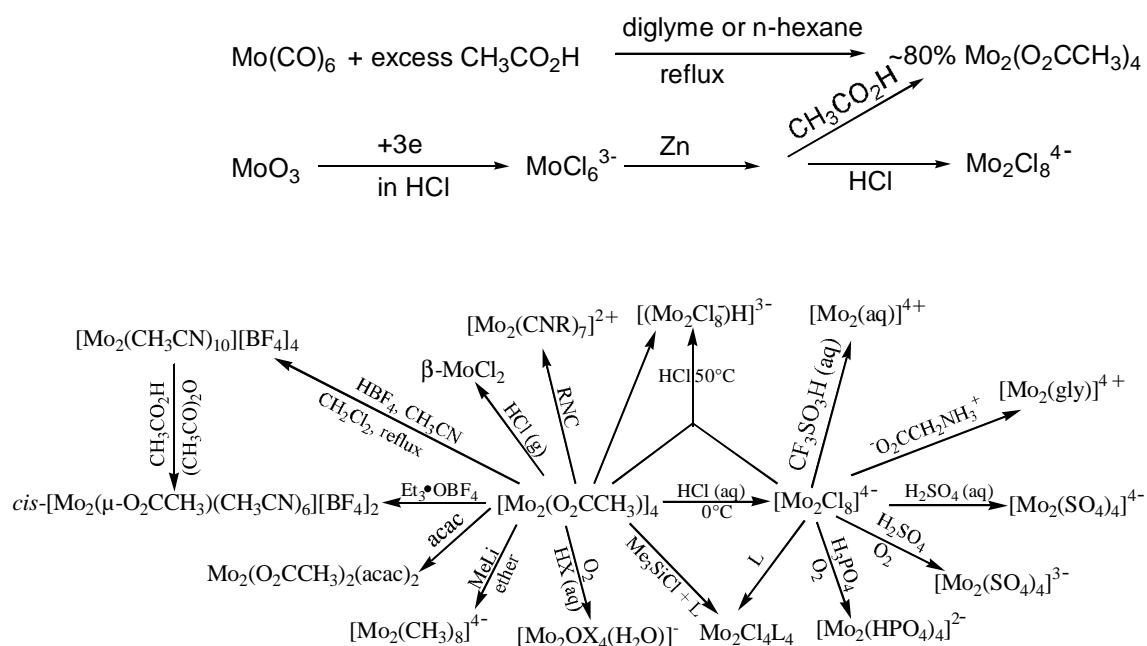


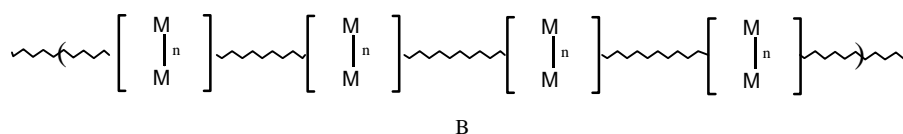
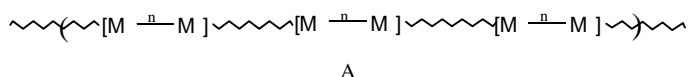
Fig. 1A.2

Yellow $\text{Mo}_2(\text{O}_2\text{CCH}_3)_4$ is thermally stable but very slowly decomposes in air with color change from light yellow to dull yellow. The purple $[\text{Mo}_2\text{Cl}_8]^{4-}$ ion can be isolated in a variety of air-stable salts. Some important reactions of these key complexes are shown in Fig. 1A.2.

Quite important derivatives are $[\text{Mo}_2(\text{CH}_3\text{CN})_{10}][\text{BF}_4]_4$ and *cis*- $[\text{Mo}_2(\mu\text{-O}_2\text{CCH}_3)_2(\text{CH}_3\text{CN})_6][\text{BF}_4]_2$, whose solvent ligands can be partly or totally replaced by a variety of ligands, e.g. carboxylates, pyridine derivatives, phosphine ligands, etc., to form a great number of compounds^[5,11]. Due to the easy replacement of the weakly coordinating solvent ligands, these compounds can be regarded as potential catalyst in organic transformations and other catalytic fields^[12].

Another type of reaction is the formation of compounds of the type $\text{Mo}_2(\text{O}_2\text{CR})_2\text{X}_2(\mu\text{-LL})_2$, where LL represents a diphosphine such as dppm, dppe or dppa and R a CH_3 , CF_3 , etc.. They are usually synthesized by the reaction of $\text{Mo}_2(\text{O}_2\text{CR})_4$ and $(\text{CH}_3)_3\text{SiX}$ in the presence of diphosphines. However, these compounds have generally been regarded as reactive and unstable^[13], for molecules of the type $\text{Mo}_2\text{X}_4(\mu\text{-LL})_2$ can be formed as byproducts or major products depending on the reaction conditions^[14]. The closely related compounds of the type $[\text{Mo}_2(\mu\text{-O}_2\text{CCH}_3)_2(\text{LL})_2(\text{CH}_3\text{CN})_n][\text{BF}_4]_2$ ($n = 0\text{-}2$)^[15] could be versatile building blocks for their axial-located acetonitrile ligands can be easily replaced by other organic or inorganic donor ligands.

One-dimensional polymers and mesogens incorporating multiple bonds between metal atoms have been studied in last decades to examine their electronic, nonlinear optical or other behaviors^[16]. They are prepared either by carboxylic exchange reaction between $\text{Mo}_2(\text{O}_2\text{CR})_4$ and a dicarboxylic HOOC-R-COOH or by the metathetic reaction between $[\text{Mo}_2(\text{O}_2\text{CR})_2(\text{NCCH}_3)_4][\text{BF}_4]_2$ and the sodium or tetrabutyl ammonium salt of a bridging ligand^[16e]. Two types of such polymers can be imaged as shown below in A and B, respectively ($M = \text{Mo}$, $n = 4$).



In A the Mo-Mo axis is parallel to the propagating axis, whereas in B the Mo-Mo axis is perpendicular. Control of the orientation of the Mo-Mo axis and the polymer propagation depends on the judicious selection of bridging ligands. The use of a bridging ligand derived from 2,7-dihydroxynaphthyridine gives a polymer of the type shown in Fig. 1A.3, taking as an example ^[16a,e]. This polymer is formed by substitution of the equatorial labile solvent ligands CH₃CN of two adjacent dimolybdenum moieties by a tetradentate ligand and classified as type A. In addition to the two general methods mentioned above, linkage of quadruple M-M bonded subunits by bridging ligands at *axial* position should be one of the efficient synthetic routes, too, although reports on this aspect are rare and only M₂(O₂CR)₄ (M = Cr, Mo, Rh; R = CH₃,) is employed as subunit ^[17]. Some of these polymers ^[17b] are unstable due to weak association between the bridging ligands and the metal centers. However, using appropriate bimetallic subunits with judicious selection of bridging ligands, more stable and manifold one-dimensional polymers could be produced by direct axial linkage between subunits and ligands.

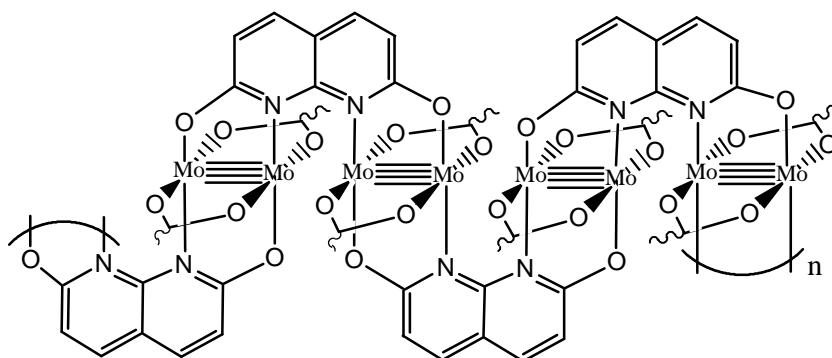


Fig. 1A.3

Dirhodium(II,II) compounds, containing a Rh-Rh bond, are structurally and electronically similar to those of their dimolybdenum counterparts. Dirhodium tetracarboxylates, Rh₂(μ-O₂CR)₄, are best known. Their derivatives Rh₂(μ-O₂CR)₄L_n (n = 1 or 2) maintain the largest class of dirhodium(II) compounds so far. The range of R groups and axial ligands L is very extensive. R groups includes CH₃, CF₃, C₂H₅, linear chain n-alkanoates, several optically carboxylate ligands, e.g. mandelate, α-methoxy-α-phenylacetate, and so forth. The axial ligand L may contain carbon, nitrogen, phosphorous, arsenic, antimony, oxygen, sulfur, and halogen donor atoms.

1A.4 Catalytic Applications of Dimolybdenum(II,II) Complexes Containing Metal-Metal Multiple Bond

A few years after the recognition of the existence of quadruple bond, the applications of metal-metal multiply bonded complexes as catalysts and precatalysts for organic transformations were extensively explored^[18]. As early as in 1969, Wilkinson *et al.*^[19] reported the dimolybdenum(II,II) acetato complex $[\text{Mo}_2(\mu\text{-O}_2\text{CCH}_3)_4]$ with noncomplexing acids (e.g., $\text{CF}_3\text{SO}_3\text{H}$, HBF_4) in methanol to give red solutions, upon addition of PPh_3 ($\text{PPh}_3 : \text{Mo} = 1 : 1$ mol), the resulting species are catalytically active for the homogeneous hydrogenation of alkenes and alkynes. However, their activity is lower than that of the corresponding dirhodium and diruthenium species. Then their applications were extended to many other organic transformations such as polymerization of olefins^[20], ring-opening metathesis polymerization (ROMP) of cyclic olefins^[21], metathesis of acyclic olefins^[22], desulfurization^[23], coupling and cross-coupling of ketones and aldehydes^[24], etc.. Typically, the complexes have bimetallic $[\text{M-M}]^{n+}$ core ($n = 4 - 6$) and carry either carboxylate, alkoxide, alkyl, allyl, halide, or nitrile ligands. In this chapter, the focus is on the recent progress of dimolybdenum(II,II) complexes containing quadruple metal-metal bond as initiators for polymerization and ROMP of olefins.

1A.4.1 Polymerization of Olefins

McCann and his coworkers^[20a] used a variety of dimolybdenum(II,II) complexes including dicationic salts of the type $[\text{Mo}_2(\mu\text{-O}_2\text{CR})_2(\text{MeCN})_4][\text{BF}_4]_2 \cdot x\text{H}_2\text{O}$ ($\text{R} = \text{CH}_2=\text{CH}$; $\text{CH}_2=\text{C}(\text{CH}_3)$; $\text{CH}_2=\text{CHCH}_2$; $\text{CH}_2=\text{CHCH}_2\text{CH}(\text{CH}_3)$; C_7H_9), neutral $[\text{Mo}_2(\mu\text{-O}_2\text{CCH}_3)_4]$ and the dianionic salt $(\text{Et}_4\text{N})_2[\text{Mo}_2(\mu\text{-O}_2\text{CCH}_3)_2\text{Br}_4]$ as initiators for polymerization of cyclopentadiene in acetonitrile. The results showed that the neutral and dianionic species do not lead to any reaction, and that $[\text{Mo}_2(\mu\text{-O}_2\text{C}(\text{CH}_3)\text{C}=\text{CH}_2)_2(\text{MeCN})_4][\text{BF}_4]_2 \cdot x\text{H}_2\text{O}$ is the most active among the dicationic initiators. The resulting polymer is insoluble in all common organic solvents and discolors slightly on standing. In another report^[20b], McCann *et al.* demonstrated that $[\text{Mo}_2((\text{MeCN})_8)[\text{BF}_4]_4]$ and $[\text{Mo}_2(\mu\text{-O}_2\text{CCH}_3)_2(\text{MeCN})_4][\text{BF}_4]_2$ are extremely efficient catalysts for the cationic polymerization of neat cyclopentadiene and for solutions of the monomer in dichloromethane. In contrast, the silica supported complexes $[\text{Mo}_2((\text{MeCN})_8)[\text{BF}_4]_4\text{-SiO}_2]$ and $[\text{Mo}_2(\mu\text{-O}_2\text{CCH}_3)_2(\text{MeCN})_4][\text{BF}_4]_2\text{-SiO}_2$ only gave small polymer yields unless dichloromethane is used as a monomer solvent; the catalysts could be used many times to polymerize successive

batches of monomer and gave approximately equal amounts of the 1,2- and 1,4-isomers/polymers in most cases. Soluble, ring-addition polydicyclopentadiene was formed in essentially quantitative yield when $[\text{Mo}_2((\text{MeCN})_8)[\text{BF}_4]_4]$ and $[\text{Mo}_2(\mu\text{-O}_2\text{CCH}_3)_2(\text{MeCN})_4][\text{BF}_4]_2$ were reacted with neat dicyclopentadiene at 170°C. In addition, McCann ^[15] mentioned that they used $[\text{Mo}_2((\text{MeCN})_8)[\text{BF}_4]_4]$ and $[\text{Mo}_2(\mu\text{-O}_2\text{CCH}_3)_2(\text{MeCN})_4][\text{BF}_4]_2$ and their silica supported derivatives for heterogeneous polymerization of neat styrene, too. The product is from orange to pale-yellow amorphous powders. Jufa *et al.* ^[20c] described in their patent a commercially applicable process for the production of linear polymers from alicyclic compounds having at least two double bonds in the ring, the Mo-Mo allyl complex $[\text{Mo}_2(\eta\text{-C}_3\text{H}_5)_4]$ being used as one of the initiators. It was claimed that the polymers produced could be used as general-purpose rubbers for tires since they simulate alternating copolymers of various olefins and dienes.

1A.4.2 Ring-Opening Metathesis Polymerization of Cyclo-Olefins

In 1985, McCann and his coworkers ^[21a, b], for the first time, reported the use of $[\text{Mo-Mo}]^{4+}$ complexes as initiators for the room-temperature ring-opening metathesis polymerization (ROMP) of the strained bicyclic monomers of the norbornene (bicyclo[2.2.1]hept-2-ene) family. In the presence of added AlEtCl_2 cocatalyst, the neutral and tetraanionic complexes $[\text{Mo}_2(\mu\text{-O}_2\text{CCR}_3)_4]$ (R = H, F) and $\text{K}_4[\text{Mo}_2\text{Cl}_8]$, respectively, catalyze the ROMP of (\pm)-1-methylnorbornene. The polymerization is both immediate and exothermic with ~50% yield of chloroform-soluble poly-1-methylnorbornene. The $^{13}\text{C}\{^1\text{H}\}$ NMR spectra of the polymers revealed that they all had a similar microstructure, indicative of no influence of the ancillary ligands of the molybdenum centers on the polymer microstructures. Furthermore, recent studies ^[21c] using inductively coupled plasma analysis have revealed that the addition of AlEtCl_2 to $[\text{Mo}_2(\mu\text{-O}_2\text{CCH}_3)_4]$ gives a mixture of heterogeneous (comprising Mo and Al) and homogeneous (comprising Mo and Al) catalyst species. These two Mo/Al catalyst systems, however, give polynorbornene with different weight-average molecular weight.

McCann *et al.* also exploited the activity of the complexes they used for polymerization of cyclopentadiene ^[20a,b] for ROMP of norbornene in conjunction with AlEtCl_2 . The results showed again that varying the ligands around the $[\text{Mo-Mo}]^{4+}$ core did not induce any significant structural changes in the polymer. Of these complexes, $[\text{Mo}_2(\text{CH}_3\text{CN})_8][\text{BF}_4]_4$ and $[\text{Mo}_2(\mu\text{-$

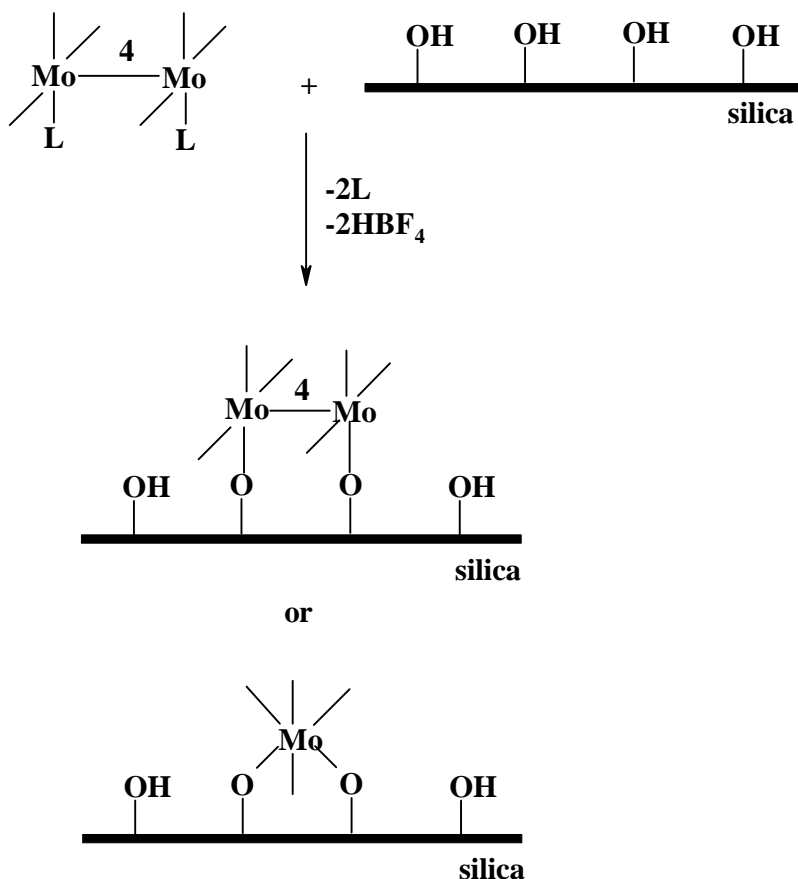
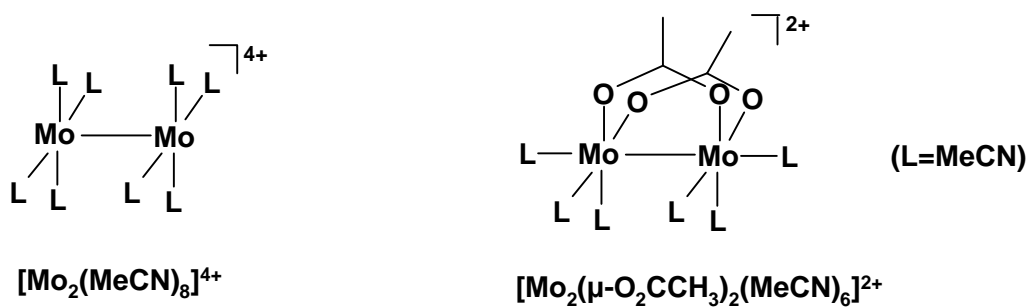
$\text{O}_2\text{CH}_3)_2(\text{CH}_3\text{CN})_6][\text{BF}_4]_2$ have been anchored on the silica to give materials represented as $[\text{Mo}_2(\text{CH}_3\text{CN})_8][\text{BF}_4]_4\text{-SiO}_2$ and $[\text{Mo}_2(\mu\text{-O}_2\text{CR})_2(\text{CH}_3\text{CN})_6][\text{BF}_4]_2\text{-SiO}_2$, respectively ^[20b]. These supported and unsupported complexes were each tested as heterogeneous catalysts for the polymerization of norbornene. In the absence of AlEtCl_2 cocatalyst $[\text{Mo}_2(\text{CH}_3\text{CN})_8][\text{BF}_4]_4\text{-SiO}_2$ was the only species found to be active at 90°C and a reaction time of 48h. The polymerization was essentially quantitative for the formation of chloroform-soluble ring-opened polymer; the other three complexes are completely inactive without cocatalyst AlEtCl_2 , even at elevated temperature. In contrast, in the presence of AlEtCl_2 $[\text{Mo}_2(\text{CH}_3\text{CN})_8][\text{BF}_4]_4\text{-SiO}_2$ was the only catalyst of the four that failed to polymerize the monomer at 20°C .

1A.4.3 Grafting of Dimolybdenum(II, II) Complexes on Metal Oxides

Even at the beginning of use of M-M multiple bonded complexes as homogeneous catalysts for organic transformations, intense research was carried out on heterogenization of such types of catalysts and on characterization of structures of the resulting heterogeneous systems as well as on their activity and selectivity. These systems can in fact potentially lead to a promotion of the catalytic activity and selectivity. Also, a heterogeneous catalytic process is easier to automatize, since the products obtained are more readily separated from the reaction mixture. Some examples found in the literature will be briefly mentioned here.

In 1974 Whan and his coworkers ^[22e] used a dry-mix impregnation of the tetracarboxylates $[\text{Mo}_2(\mu\text{-O}_2\text{CR})_4]$ ($\text{R} = \text{CH}_3$ or CF_3) on silica and alumina as catalysts for propene metathesis. ESR ^[22f,g] and EXAFS ^[22g] studies of the $[\text{Mo}_2(\mu\text{-O}_2\text{CH}_3)_4]\text{-SiO}_2$ system revealed that at activation temperatures below 350°C the active catalytic species comprised an $[\text{Mo-Mo}]^{5+}$ moiety and that at 450°C cleavage of the Mo-Mo bond occurred with consequent loss in catalyst performance.

Candlin ^[22i,j] prepared heterogeneous catalysts by impregnating Al_2O_3 and SiO_2 with solutions of the dimolybdenum(II,II) allyl complex $[\text{Mo}_2(\eta\text{-C}_3\text{H}_5)_4]$ and used them for the metathesis of hex-1-ene and also for the polymerization of ethylene. It was emphasized that the activity of the allyl complexes for olefin metathesis and ethylene polymerization was greatly improved when they were anchored to the inorganic oxide supports. No suggestions were made with respect to the exact structure of the supported species, however.



Scheme 1A.4.3

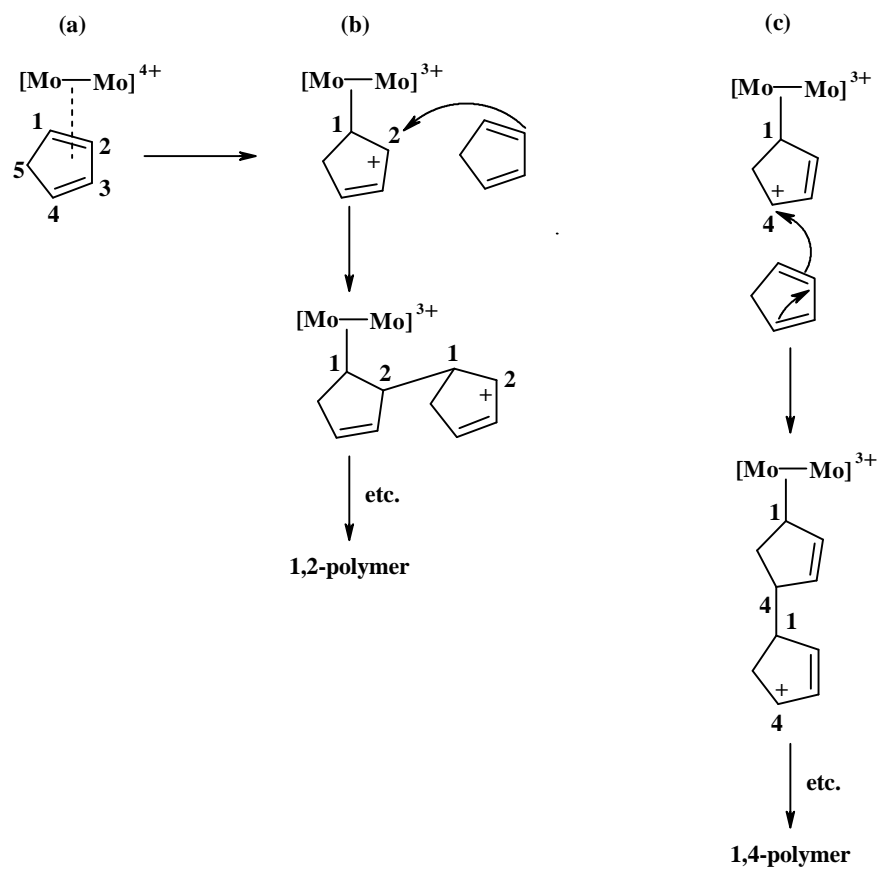
Iwasawa *et al.* ^[22k-0] also supported $[Mo_2(\eta-C_3H_5)_4]$ on Al_2O_3 and SiO_2 and reduced the supported complexes with H_2 , followed by exposure to O_2 . The resulting 'paired' oxo-bridged divalent molybdenum species acted as excellent catalysts for ethane hydrogenation at 200-293 K. They also conducted detailed physical studies on the structure of surface species obtained on reacting hexane solution of $[Mo_2(\eta-C_3H_5)_4]$ with silica and alumina. They claimed that the Mo-

Mo bond was broken after the deposition of the dimolybdenum complex on the surface of the refractory oxides.

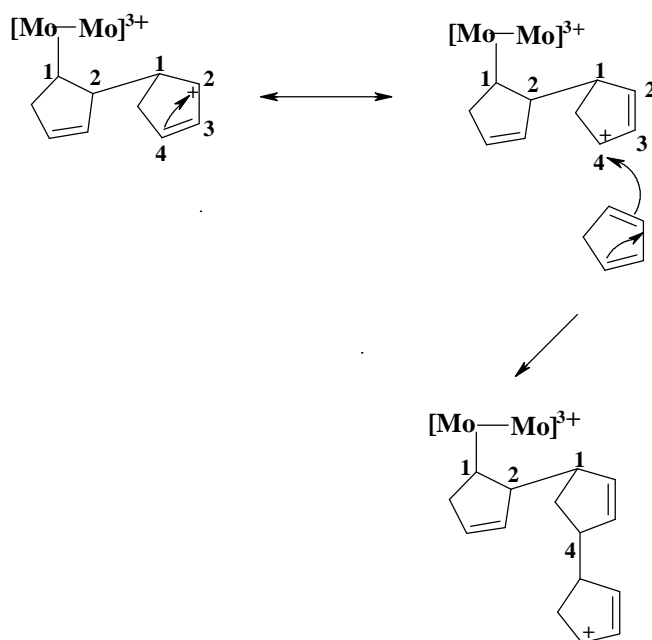
McCann and his coworkers^[20b, 21e] have anchored the salt $[\text{Mo}_2(\text{CH}_3\text{CN})_8][\text{BF}_4]_4$ and $[\text{Mo}_2(\mu\text{-O}_2\text{CR})_2(\text{CH}_3\text{CN})_6][\text{BF}_4]_2$ on silica and tested their activities for polymerization of cyclopentadiene and ROMP of norbornene. It was thought that the lability of the CH_3CN ligands attached to the supported and unsupported complexes was a contributory factor in these polymerizations^[25]. In a word, the binding of the Mo-Mo bonded complexes to SiO_2 was thought to occur at the surface OH groups upon removal of labile CH_3CN from the complexes (Scheme 1A.4.3). However, there was no direct physical evidences as to the exact structure of the silica-bound molybdenum complexes, namely, whether the Mo-Mo bond is retained on the silica surface (as observed for $[\text{Mo}_2(\mu\text{-O}_2\text{CCH}_3)_4]\text{-SiO}_2$ ^[22g]) or it ruptures to give mononuclear species (as reported for $[\text{Mo}_2(\eta\text{-C}_3\text{H}_5)_4]\text{-SiO}_2$ ^[22k-o]).

1A.4.4 Mechanistic Considerations

McCann and his coworkers^[20b] proposed a possible mechanism (Scheme 1.4.4) for the polymerization process of olefins using quadruply-bonded Mo^{4+} salts, $[\text{Mo}_2(\text{CH}_3\text{CN})_8][\text{BF}_4]_4$ and $[\text{Mo}_2(\mu\text{-O}_2\text{CCH}_3)_2(\text{CH}_3\text{CN})_6][\text{BF}_4]_2$, as initiators, taking cyclopentadiene as substrate. The first step involves the association of a cyclopentadiene molecule with the bimetallic $[\text{Mo-Mo}]^{4+}$ catalyst center to give species (a) in (1) of Scheme 1A.4.4. In the homogeneous reactions access to the bimetallic centers can be achieved by displacement of one or more of the labile CH_3CN ligands, whilst with the heterogeneous catalysts it may be that some surface $[\text{Mo-Mo}]$ sites may be exposed for attack by nucleophilic cyclopentadiene molecules. Then the cyclopentadiene molecule may bond to either one or both (i.e., bridging) molybdenum atoms of the bimetallic core to give the carbocation (b), which itself may isomerize to (c). Addition of cyclopentadiene molecule to (b) and (c) will produce separate 1,2- and 1,4-polycyclopentadiene chains, respectively. A single polymer chain containing a mixture of 1,2 and 1,4 units can form if there is isomerization of either (b) or (c) during the polymerization as in (2) of Scheme 1.4.4. At present it is unclear whether or not the present products are mixtures of separate 1,2- and 1,4-polymers, or if each polymer chain comprises a mixture of 1,2- and 1,4-units



(1)



(2)

Scheme 1A.4.4

1B. Objectives of this work

As mentioned in the introduction above, the compounds of the type $\text{Mo}_2(\text{O}_2\text{CR})_2\text{X}_2(\mu\text{-LL})_2$ (LL = diphosphine; R = CH_3 , CF_3) are usually prepared by the reaction of $\text{Mo}_2(\text{O}_2\text{CR})_4$ and $(\text{CH}_3)_3\text{SiX}$ in the presence of diphosphines. But these compounds have generally regarded as reactive and unstable^[13], for molecules of the type $\text{Mo}_2\text{X}_4(\mu\text{-LL})_2$ can be formed as byproducts or major products depending on the reaction conditions^[14]. The closely related compounds of the type *trans*- $[\text{Mo}_2(\mu\text{-O}_2\text{CCH}_3)_2(\text{LL})_2(\text{CH}_3\text{CN})_n][\text{BF}_4]_2$ (0 = 0-2)^[13b,g,h], prepared from the reaction of *cis*- $[\text{Mo}_2(\mu\text{-O}_2\text{CCH}_3)_2(\text{CH}_3\text{CN})_6][\text{BF}_4]_2$ with diphosphine, have each two labile acetonitrile ligands or are vacant at axial positions, which could be easily attacked by other inorganic or organometallic donor ligands to form new compounds. And most importantly, if bidentate ligands or building blocks with two donor atoms at trans position, one-dimensional polymers incorporating M-M backbone could be synthesized. Therefore, the tasks should be:

- (1) Use other donor ligands to prepare new complexes to exploit influences of different ligands on the bond strength of Mo-Mo quadruple bond;
- (2) Look for appropriate bidentate donor ligands in order to form stable one-dimensional polymers with M-M backbone and alter the carboxylato and/or phosphine groups to produce soluble polymers beneficial to the characterization of such polymers.

McCann *et al.*^[20] explored the activity of the quadruply-bonded $[\text{Mo}_2]^{4+}$ salts, $[\text{Mo}_2(\text{CH}_3\text{CN})_8][\text{BF}_4]_4$ and $[\text{Mo}_2(\mu\text{-O}_2\text{CCH}_3)_2(\text{CH}_3\text{CN})_6][\text{BF}_4]_2$, as initiators for polymerization of olefins in homogeneous and heterogeneous systems and found that they are of high efficiency. Then questions are:

- (1) Are other quadruply bonded $[\text{Mo}_2]^{4+}$ salts also active as initiators for polymerization of olefins?
- (2) Will other $[\text{M}_2]^{4+}$ salts, e.g., Rh, W, be efficient as initiators for polymerization of olefins?
- (3) Does the M-M bond play a very important role in the activity of such catalytic precursors?

For a cationic polymerization process the true initiating species is R^+ , which may, for example, be a proton, a carbenium, etc.. McCann *et al.* put forward the catalytic mechanism of cationic

polymerization of cyclopentadiene initiated by $[\text{Mo}_2]^{4+}$ salts that the first step should be the association of the cyclopentadiene with the Mo-Mo multiple bond. This seems that the M-M bond plays a crucial role in the polymerization course. Is this reasonable? And which one is the true initiator, the proton (coming from a little amount of water in the system) or the intermediate (produced by the displacement of a labile acetonitrile by an olefin molecule)?

As to the exact structures of $[\text{M-M}]^{4+}$ salts on the surface of metal oxides such as silica and alumina, it is known that there is always a controversy: whether the intact $[\text{M-M}]^{4+}$ is maintained during anchoring (as reported for $[\text{Mo}_2(\mu\text{-O}_2\text{CH}_3)_4]\text{-SiO}_2$) or it decomposes to give mononuclear species (as observed for $[\text{Mo}_2(\eta\text{-C}_3\text{H}_5)_4]\text{-SiO}_2$)?

Chapter 2 Results and Discussion

Part A. Synthesis of Complexes with M-M Multiple Bonds

Since the recognition of metal-metal bond in 1964 by the group of F. A. Cotton, many researchers came into this realm to exploit their physical and chemical properties, to examine their applications in the fields of catalysis and material science. So far the M-M quadruple bonds have been found to be existing between Cr, Mo, W, Re and Tc atoms. Dimolybdenum complexes containing quadruple bond maintain the largest one of this group due to relatively strong bond strength and easy accessibility. Thus, these complexes have been extensively studied and examined. This work focuses therefore primarily on synthesis and characterization of dimolybdenum complexes.

2A.1 Dimolybdenum(II) Complexes Linked by Cyano Bridges to Organic and Organometallic Ligands

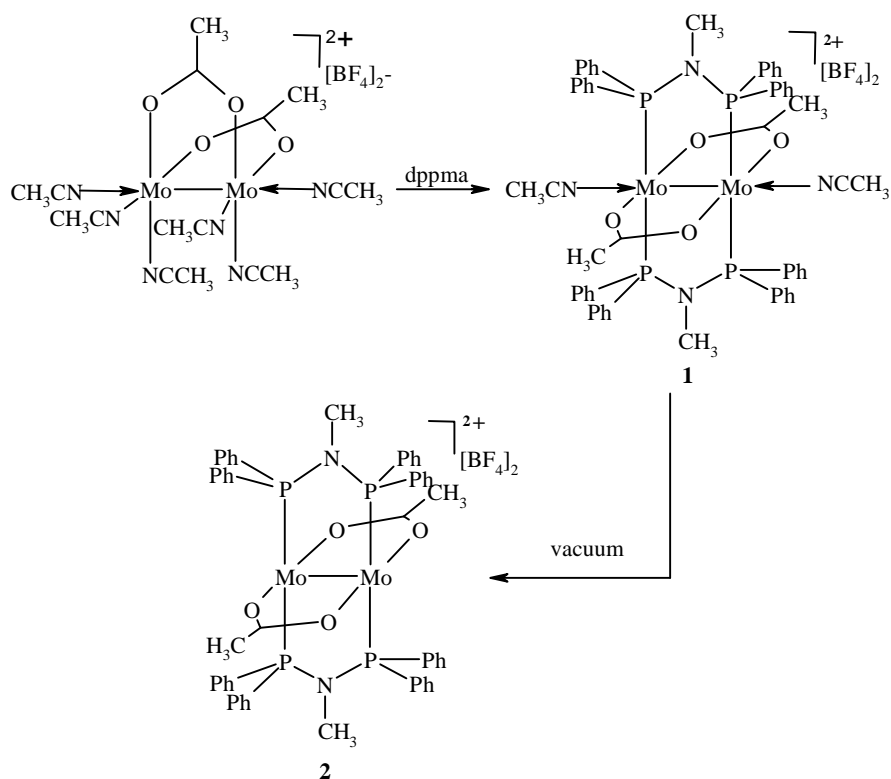
2A.1.1 Introduction

As stated in Chapter 1.3, numerous and varied molecules containing MoMo quadruple bonds are known. However, the number of compounds of the type $[\text{Mo}_2(\mu\text{-Ac})_2(\text{LL})_2]\text{X}_2$, where Ac is a bridging acetate ligand, is rather limited for these molecules have been regarded as difficult to handle^[1]. Nearly all of the structurally characterized complexes of this type have been described in the last decade^[2]. In these molecules the ligands X are in most cases halides, fixed in axial position to the metal center with rather long metal-halide bond distances^[2c]. The compounds are usually synthesized by the reaction of $\text{Mo}_2(\text{Ac})_4$ with $(\text{CH}_3)_3\text{SiX}$ in the presence of diphosphines. Molecules of the type $\text{Mo}_2\text{X}_4(\text{diphosphine})_2$ can be formed as byproducts or major products, depending on the reaction conditions^[2c, e, f]. Closely related to the $[\text{Mo}_2(\mu\text{-Ac})_2(\text{LL})_2]\text{X}_2$ complexes are compounds of the type $[\text{Mo}_2(\mu\text{-Ac})_2(\text{LL})_2(\text{S})_n](\text{BF}_4)_2$ ($n = 0-2$) where the halide ligands are replaced by usually not coordinating tetrafluoroborates. The axial position in these compounds can be occupied by solvent molecules S, in all cases described to date $\text{S} = \text{acetonitrile}$ ^[2a, b]. It should be possible to replace these solvent molecules by other

organic and inorganic donor ligands, both by neutral molecules and anions. Recently the first dirhenium complexes of the type $\text{Re}_2(\mu\text{-O}_2\text{CR})_4\text{L}_2$, where L is an organometallic ligand which was introduced by the replacement of axial halide ion was reported [3]. These reactions could only be achieved by organometallic anions as new axial ligands. In the present work the examinations are extended to Mo_2 complexes and report on the preparation, structures, and spectroscopic properties of compounds of the types $[\text{Mo}_2(\mu\text{-Ac})_2(\text{LL})_2(\text{L}')_2](\text{BF}_4)_2$ and $\text{Mo}_2(\mu\text{-Ac})_2(\text{LL})_2(\text{L}'')_2$ (L' and L'' are organic or organometallic ligands). It will be shown that the replacement of the axial solvent molecules enables the introduction of both neutral and anionic ligands and provides an easy access to a much broader variety of axial ligands than the rather limited $(\text{CH}_3)_3\text{SiX}$ /diphosphine route mentioned above.

2A.1.2 Results and Discussion

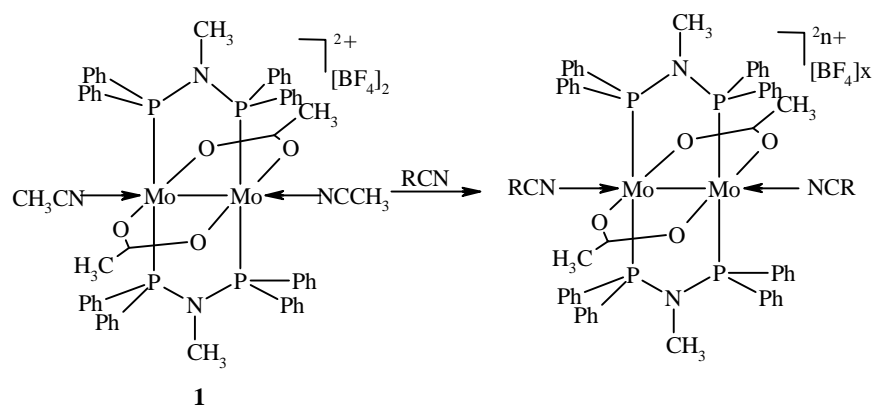
2A.1.2.1 Synthesis



eqn. 2A.1A

Reaction of the purple *cis*-[Mo₂(*m*-Ac)₂(NCCH₃)₆](BF₄)₂ with a two fold stoichiometric amount of the diphosphino ligand dppma in acetonitrile at room temperature leads to the formation of the pink *trans*-[Mo₂(*m*-Ac)₂(dppma)₂(CH₃CN)₂](BF₄)₂ (**1**) according to eqn. 2A.1A. Drying the compound in vacuum (1 mm Hg) for several hours causes a gradual removal of the two axial acetonitrile ligands. Finally a compound of the composition *trans*-[Mo₂(*m*-Ac)₂(dppma)₂](BF₄)₂ (**2**) remains. This behavior explains the difficulties in receiving a correct elementary analysis for complex **1**. Several related complexes are known, most prominently [Mo₂(CH₃CN)₈₋₁₀](BF₄)₄, which shows a similar behavior in vacuum, and will be examined as potential catalyst for polymerization of olefin based on its labile ligand CH₃CN.

Reacting derivative **1** in methylene chloride with an excess of *tert*-butylnitrile, benzonitrile, or *p*-nitroethynylbenzene leads to complete replacement of the acetonitrile ligand by the nitriles as shown in eqn. 2A.1B.



R	n	x	Complex
C(CH ₃) ₃	2	2	3
C ₆ H ₅	2	2	4
C ₆ H ₄ -CCH	2	2	5
M(CO) ₅	0	0	M = Cr 6 , Mo 7 , W 8
Fe(CO) ₂ Cp	2	2	9

eqn. 2A.1B

The complexes 1-5 are soluble in CH₂Cl₂, CHCl₃, THF, CH₃OH, and CH₃CN. In the latter solvent the axial ligands are partially exchanged by solvent molecules. In solid state the compounds decompose in the air within a few days. In solution they are only stable for a few hours when exposed to air or moisture. According to elementary analyses and IR spectroscopy of the brownish precipitates the main decomposition products are molybdenum oxides. Under inert gas atmosphere the compounds are stable for several weeks in solution and for more than one year in solid state.

Addition of a two fold stoichiometric amount of Na[NC-M(CO)₅] (M = Cr, Mo, W) to an acetonitrile solution of compound **1** at room temperature leads to a precipitate of red derivatives of formula *trans*-Mo₂(*m*-OAc)₂(dppma)₂[(NC-M(CO)₅)]₂ (**6-8**) according to eqn. 2A.1B. Addition of the neutral ligand NC-Fe(CO)₂Cp at room temperature quantitatively yields the pinkish-red *trans*-{Mo₂(*m*-OAc)₂(dppma)₂[NC-Fe(CO)₂Cp]₂}[BF₄]₂ (**9**).

While compounds **6-8** are only slightly soluble in CH₂Cl₂ and insoluble in all other common organic solvents, derivative **9** has good solubility in CH₂Cl₂, CHCl₃ and CH₃CN. Compounds **6-9** are more sensitive in solution to air and moisture than derivatives **1-5**. In solid state, the complexes **6-9** decompose slowly upon exposure to air, but are stable for months at room temperature under inert gas atmosphere.

2A.1.2.2 Molecular Structures

The molecular structures of compounds **1**, **2**, **4**, and **5** have been examined by single X-ray crystallography (a summary of the crystal and experimental data is reported in Table 1, **Appendix**). Two crystallographic independent molecules A and B in the unit cell were found for the compounds **1**·4(CH₃CN), **2**·2(CH₂Cl₂), and **2**·1/2(C₄H₁₀O, C₆H₁₄). Both A and B are located on a crystallographic centre of inversion in the midpoint of the Mo-Mo bond except **2**·1/2(C₄H₁₀O, C₆H₁₄), in which A performs the center of inversion approximately, whereas B resides on pseudo twofold axes which pass through the collinear C-C bonds of the acetate groups and the midpoint of the Mo-Mo bond.

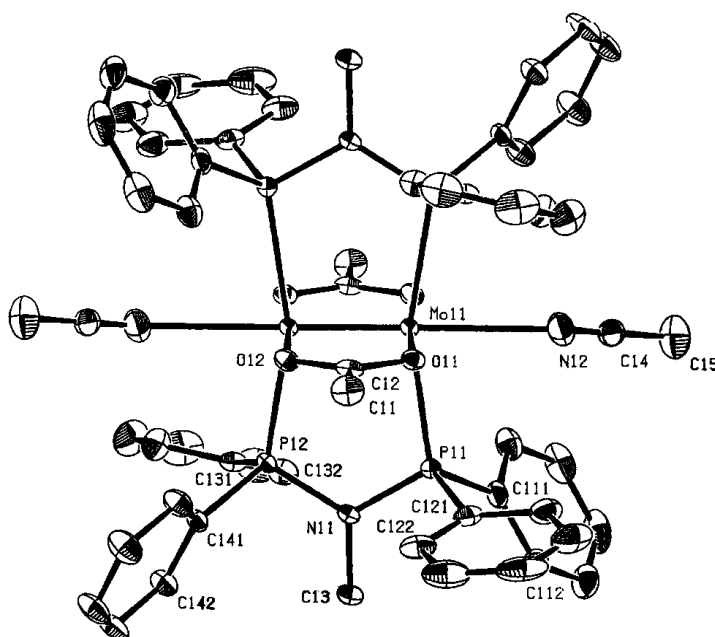


Figure 2A.1A. ORTEP drawing of the molecular structure of the dicationic part of $1 \cdot 4(\text{CH}_3\text{CN})$. Thermal ellipsoids are at the 50% probability level. Hydrogens are omitted for clarity.

The dimensions of eight molecules examined were collected and compared in Table 2 (see **Appendix**). Figure 2A.1A shows an ORTEP representation of compound **1**. The appropriate labeling scheme valid for all eight molecules described in Table 2 is given in Figure 2A.1B.

The Mo-Mo bond distances for all examined molecules are in the narrow interval of 211 - 213 pm. They seem not to be significantly affected by the axially coordinating nitrile ligands. The Mo-Mo distances in $2 \cdot 2(\text{CH}_2\text{Cl}_2)$ and $2 \cdot 1/2(\text{C}_4\text{H}_{10}\text{O}, \text{C}_6\text{H}_{14})$ are nearly identical even though in the first case the axial positions are unoccupied but in the second the counter ions are fixed by an $\text{F}_3\text{B}-\text{F} \cdots \text{Mo}$ interaction in the axial position. Obviously X-ray crystallography is not such a sensitive tool as Raman spectroscopy in this particular case (see below).

In general, the two bridging acetates and two dppma ligands are arranged *trans* to each other. Two BF_4^- anions or $\text{N}\equiv\text{C}-\text{R}$ ligands are forced to coordinate to the molybdenum atoms in the axial positions and the Mo-NCR/ FBF_3 bond is bent (Figure 2A.1C). Quadruply bonded molybdenum complexes with pairs of bridging dpppa (dpppa = bis(**d**iphenyl**p**hos**p**hino)**i**sop**p**ro**p**yl**a**mine), dppa, dppma and $(\text{O}_2\text{CCH}_3)^-$ ligands usually have

eclipsed conformation^[4]. Both steric (CH₃ instead of H on the bridging nitrogen atom) and electronic (CH₃ shows a stronger inductive effect than H) differences have been considered being responsible for the nearly two to three times higher torsion angles P-Mo-Mo-P of the dppma complexes compared to those observed in dppa derivatives (mean value 5.2°)^[2d]. However, the torsion angles are very similar in the case of compound **1** and its dppa congener, in the latter case the P-Mo-Mo-P angle is 9.75(8)° and 10.80(0)°, resp., for the two independent molecules within the unit cell^[2g].

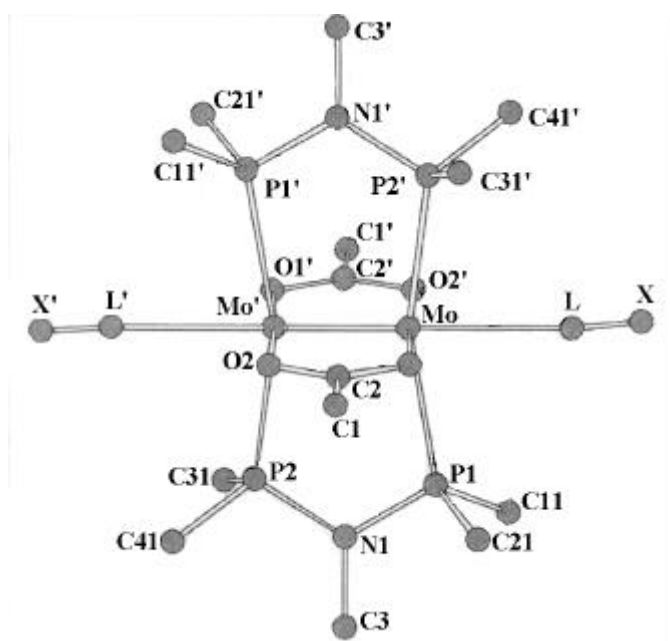


Figure 2A.1B. Schematic drawing with the appropriate labeling scheme for all eight molecules.

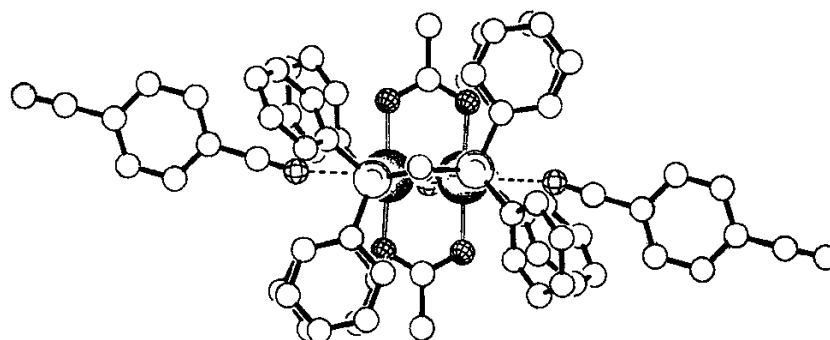


Figure 2A.1C. PLATON drawing of the molecular structure of the dicationic part of **5**, illustrating the bent bonding of the axial ligands.

The Mo-F/N bonds (from 250.5 pm to 265 pm) are comparatively long, indicating only very weak Mo-F/N interactions. However, the Mo-F/N distances are shorter than expected from the sum of the van der Waals radii (Mo-F: 374 pm; Mo-N: 382 pm) but longer than the sum of the covalent radii (Mo-F: 211 pm; Mo-N: 215 pm)^[5]..

2A.1.2.3 Spectroscopy

The ¹³C NMR resonances of the bridging nitrile carbons are listed in Table 2A.1A, the data for free ligands are also given for comparison. The signals appear in the region $\delta(^{13}\text{C}) = 119.5 - 128.5$ ppm for **1** and **3 - 5**, each of them is lower field shifted ca. 2 - 3 ppm in comparison to the free ligands. These slight shift changes reflect the weak bonding interactions between nitrile ligands and the MoMo core. Owing to the same reason, the IR vibrational frequencies of C \equiv N in **1** and **3 - 5** are nearly unchanged compared to the free ligands (Table 2A.1A). Although the significant difference of the C \equiv N vibrational frequencies in **6-8** compared to their precursor **1** (ca. 150 cm⁻¹) can be observed in the IR spectra, the FAB mass spectra show only signals for ions lacking the axial ligands, indicative of the existence of weak bonding between the axial ligands and the central metal atoms. However, the existence of an interaction between the MoMo core and the nitriles in complexes **1** and **3 - 5** is clearly expressed by the reduction in the Raman active $\nu(\text{MoMo})$ mode from 375 cm⁻¹ in **2** to 357 - 361 cm⁻¹ in **1** and **3-5**. The MoMo interaction in the case of the nitrile-free complex **2** is obviously stronger than in the cases of the nitrile-containing derivatives **1** and **3 - 5**.

Although no significant difference of the C \equiv N vibrational frequencies in **6 - 8** compared to their precursor **1** can be observed in the IR spectra, a strong chemical shift difference can be seen in the signal corresponding to the carbon atom of the bridging cyano group in the ¹³C NMR. This signal is shifted upfield ca. 15 - 25 ppm depending on the central metal of the axial ligand. Interestingly, the chemical shifts of the C \equiv N carbon atoms are very similar in the compounds **6 - 8**. This observation is in remarkable contrast to the Cr, Mo, W precursor molecules and has been also stated for the complexes $\text{Re}_2(\mathbf{m}\text{-O}_2\text{CCMe}_3)_4[\text{NCM}(\text{CO})_5]_2$ (M = Cr, Mo, W)^[3]. In the case of compound **9**, with its neutral Fe containing ligand, the $\delta(^{13}\text{C})$ of the nitrile carbon atom and the $\nu(\text{C}\equiv\text{N})$ and $\nu(\text{C}\equiv\text{O})$ IR vibrations remain virtually unchanged upon complexation (see Table 2.1A). However, the $\nu(\text{C}\equiv\text{O})$ vibrations of derivatives **6 - 8** are shifted to higher energies in

comparison to the starting materials. This implies a decrease in the back-bonding capability to the π^* CO ligand orbital from the M (Cr, Mo, W) center because part of the electron density at the M centers is shifted towards the MoMo core *via* the NC-unit.

Table 2A.1A. Selected spectroscopic data of compounds **1-9** and pure ligands

compound	axial ligand	$\nu(\text{C}\equiv\text{N})$ cm^{-1}	$\nu(\text{C}\equiv\text{O})$ cm^{-1}	$\delta(^{13}\text{C})\text{CN}/$ ppm	$\nu(\text{MoMo})/$ cm^{-1}	$\lambda_{\text{ab}/\text{max}} (\epsilon)/$ nm ($\text{M}^{-1} \text{cm}^{-1}$)
1	NCCH ₃	2250	—	119.5	361	513(1740) ^a
CH ₃ CN	—	2250	—	116.3	—	
2	FBF ₃ ⁻	—	—	—	375	514(3110) ^a
3	<i>t</i> -BuCN	2251	—	128.5	357	514 (1130) ^a
<i>t</i> -BuCN	—	2250	—	125.9	—	
4	NC C ₆ H ₅	2235	—	120.4	360	514(1220) ^a
C ₆ H ₅ CN	—	2230	—	118.8	—	
5	NC C ₆ H ₄ CCH	2235	—	119.9	360	513(3030) ^a
HCCC ₆ H ₄ CN	—	2228	—	118.2	—	
6	[NC-Cr(CO) ₅] ⁻	2101	2048 1972 1926 1902	127.2	334	546(2120) ^a
[NC-Cr(CO) ₅] ⁻	—	2111	2051 1996 1942 1919 1830	153.8	—	338(2230) ^b
7	[NC-Mo(CO) ₅] ⁻	2099	2055 1978 1928 1901	125.0	337	546(1043) ^a
[NC-Mo(CO) ₅] ⁻	—	2106	2058 1986 1935 1909 1831	149.2	—	355(2980) ^b

Table 2A.1A continued

compound	axial ligand	$\nu(\text{C}\equiv\text{N})$ cm^{-1}	$\nu(\text{C}\equiv\text{O})$ cm^{-1}	$\delta(^{13}\text{C})\text{CN}/$ ppm	$\nu(\text{MoMo})/$ cm^{-1}	$\lambda_{\text{ab/max}} (\epsilon)/$ $\text{nm} (\text{M}^{-1}\text{cm}^{-1})$
8	$[\text{NC-W}(\text{CO})_5]^-$	2101	2052 1967 1918 1896	125.2	334	546(1050) ^a
	$[\text{NC-W}(\text{CO})_5]^-$	2113	2056 1983 1934 1904 1815	140.0	—	359(2490) ^b
9	$\text{NC-Fe}(\text{CO})_2\text{Cp}$	2117	2056 2008	126.3	337	broad ^a
	$\text{NC-Fe}(\text{CO})_2\text{Cp}$	2117	2057 2007	125.9	—	347(1370) ^a

^a Measured in CH_2Cl_2 . ^b Measured in CH_3OH .

The strong Raman bands centered at 334, 337, 334 and 337 cm^{-1} for **6** - **9**, resp., can be unambiguously assigned to stretching frequencies of the quadruple bond between the Mo atoms, which are shifted to lower energies by ca. 40 cm^{-1} relative to **2**. This red shift suggests that coupling occur between the Mo-Mo stretching mode and the $\text{M-C}\equiv\text{N}$ stretching modes. It is also in accord with the occurrence of a less pronounced $\text{MoMo}\rightarrow\text{N}\equiv\text{CR}$ π back bonding than in the derivatives **1** and **3-5** which contain organic axial ligands. The MoMo interaction in complexes **6-9** is therefore somewhat weaker than in the derivatives **1** and **3-5**. However, a clear dependence of the MoMo bond strength on the ligand metal atom in the group Cr, Mo, W - as it has been observed for the above mentioned $\text{Re}(\text{II})_2$ complexes^[3] - can not be seen.

The weakly bonded organic axial nitriles in compounds **1** and **3-5** have no measurable effect on their electronic absorption spectra, all of them show the $\delta_{xy} \rightarrow \delta_{xy}^*$ transition at the same energy (514 nm) although changes in intensity occur (Table 2A.1A). The energy of this transition is comparable to other complexes containing both *trans* acetate and phosphine bridges^[3].

The electrochemical properties of complexes **1** - **4** have been investigated by cyclic voltammetry in 0.1 M TBAH/CH₂Cl₂ and the results are summarized in Table 2A.1B. The overall electrochemical behavior of these derivatives is quite complex. The general polarographic behavior of them is similar. An example is given in Figure 2A.1C. All derivatives display an irreversible oxidation in the potential range 1.23 to 1.31 V vs Fc/Fc⁺, [Mo₂]^{5+/4+} process. The cyclic voltammogram of Mo₂(O₂CCH₃)₄ in MeOH reveals a metal-based one-electron quasi-reversible oxidation with E_{1/2} = +0.24 V vs Ag/AgCl, being no reduction process observed [6]. In the cases examined here, four quasi-reversible or irreversible reductions have been detected: the first in the range of -1.14 to -1.33 V, the second in -1.48 to -1.62 V, the third in -1.74 to -1.90 V, and the fourth in -2.03 to -2.16 V. By comparison to the electrochemical behavior of mono- and binuclear molybdenum [7] and dimolybdenum thioxanthate complexes [8], the first reduction is considered to be metal centered. As shown in Figure 2A.1D, the first reduction couple is quasi-reversible when the potential sweep is extended to -2.0 V; *i*_{pa}/*i*_{pc} approaches a value of unity when the potential range scanned only covers the first reduction, suggesting a reversible process.

Table 2A.1B. Cyclovoltammetric data^a of complexes **1-4**

complex	oxidation process	reduction process			
1	+1.23(ir)	-1.33(100)	-1.62(90)	-1.90(qr, 50)	-2.18(ir)
2	+1.27(ir)	-1.23(90)	-1.61(70)	-1.87(ir)	-2.13(ir)
3	+1.31(ir)	-1.14(70)	-1.48(90)	-1.74(qr, 80)	-2.03(ir)
4	+1.30(ir)	-1.20(90)	-1.54(90)	-1.83(ir)	-2.09(ir)

^a Cyclic voltammograms were recorded in 0.1M TBAH/CH₂Cl₂ at a scan rate of 200 mV s⁻¹. Potentials are in V vs the ferrocene/ferrocenium couple, Fc/Fe⁺; error is ±0.2 V; peak-peak separations Δ*E*_p for reversible and quasi-reversible couples are given in parentheses.

The UV/Vis spectroscopy data for the complexes **6-9** together with their organometallic axial ligands are listed in Table 2A.1A. Figure 2A.1E presents a comparison between the products and their precursors. Each of the derivatives **6** - **8** contains a single broad peak centered at 546 nm which is lower in energy than both of the absorptions from **1** and [NCM(CO)₅]⁻ (M = Cr, Mo, W), and it is thus tentatively assigned as a MM'CT transition from M⁰ to Mo^{II}Mo^{II}. It is

surprising to observe this band of **6-8** to be located at the same energy, despite the different distinction coefficients. After the coordination of the $\text{Cp}(\text{CO})_2\text{Fe-CN}$ ligand to the Mo_2 moiety in compound **9**, the electronic spectrum alters significantly, with the appearance of a shoulder extending from 450 to 850 nm. This band can, in principle, be attributed to a charge transfer from the donor moiety, $\text{Cp}(\text{CO})_2\text{Fe-CN}$, to the acceptor, $[\text{Mo}_2(\mathbf{m}\text{-O}_2\text{CCH}_3)_2(\mathbf{m}\text{-dppma})_2]^{2+}$.

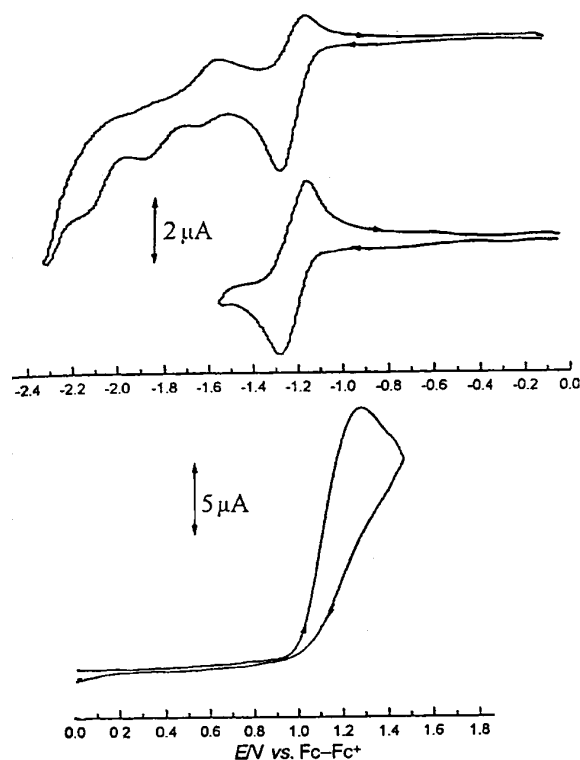


Fig.2A.1D Cyclic voltammogram of $\text{trans}[\text{Mo}_2(\mu\text{-O}_2\text{CCH}_3)_2(\mu\text{-dppma})_2(\text{CH}_3\text{CN})_2][\text{BF}_4]_2$ **1** in 0.1 M TBAH- CH_2Cl_2 . Scan rate is 200 mV s^{-1} ; potentials are vs. Fc/Fc^+ .

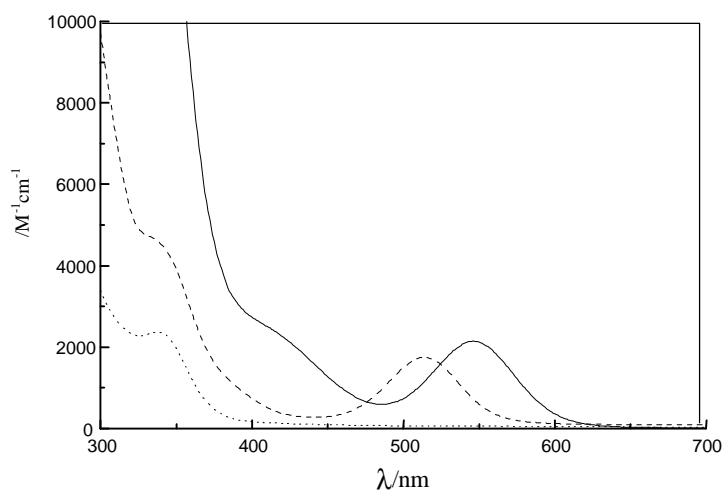


Fig. 2A.1E Comparison of the electronic spectra in CH_2Cl_2 (unless otherwise stated): 6(—), 1 (-----) and $\text{Na}[\text{NC-Cr}(\text{CO})_5]$ (.....).

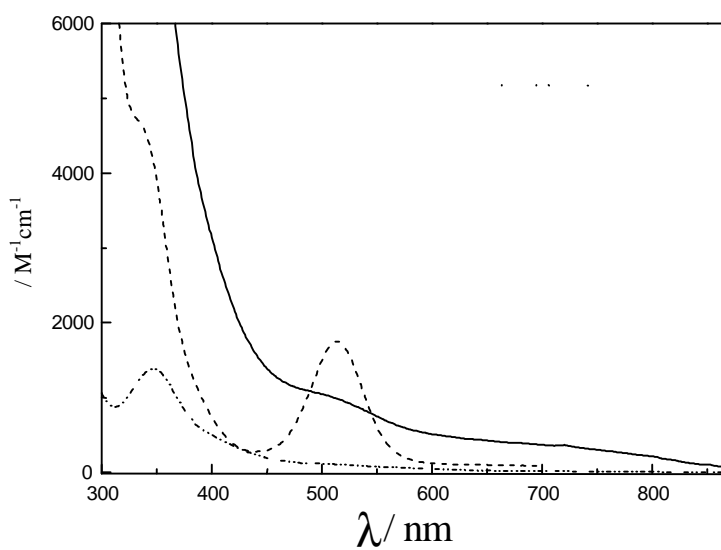


Fig. 2A.1F Comparison of the electronic spectra in CH_2Cl_2 (unless otherwise stated): 9(—), 1 (-----) and $\text{Na}[\text{NC-Fe}(\text{CO})_2\text{Cp}]$ (.....).

2A.2 Dimolybdenum(II) Complexes Linked by Pyridine and Its Derivatives

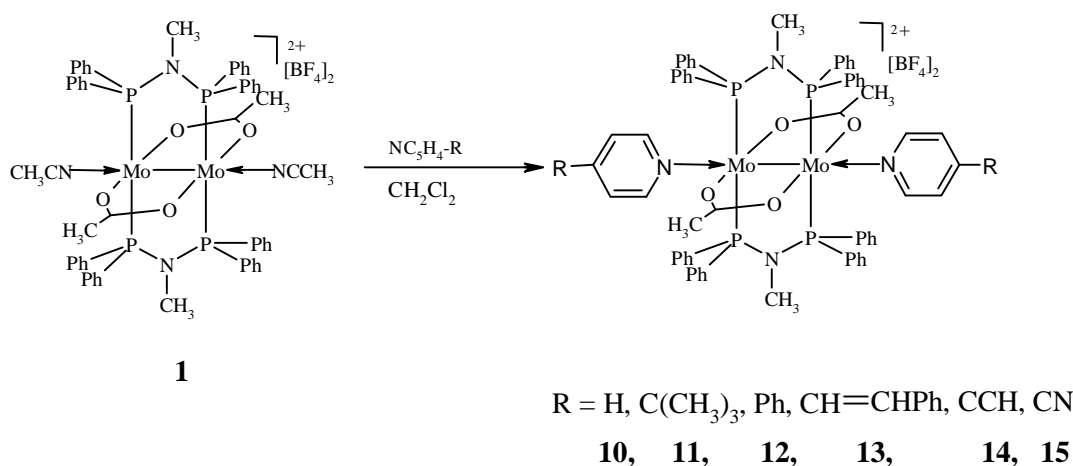
2A.2.1 Introduction

Recently supramolecular inorganic and organometallic materials have gained significant interest for their special electronic, magnetic, optical and other properties. Thus they may be applied in material science ^[1]. For preparing such materials, one of the most important tasks is to search for appropriate building blocks. It is well known that many metal-metal multiply bonded complexes bear axial ligands, some of which are polymers ^[2]. However, the Mo₂(O₂CR)₄ type complexes appear to be resistant to the attachment of axial ligands in several cases. Dirhenium compounds also display in general only a small tendency to bind axial ligands. Interestingly, however, the analogous Cr₂(O₂CR)₄ cannot be obtained in condensed phases without axial ligands ^[2] with only one exception reported by the Cotton's group recently ^[3]. In Chapter 2A.1 some compounds of the type *trans*-[Mo₂(*m*-O₂CCH₃)₂(*m*-dppma)₂(NCR)₂](BF₄)₂ where the axial ligands are nitrile derivatives were reported. Although the interaction between the MoMo core and the axial ligands is comparatively weak, the advantage of the easy substitution by other ligands at the axial position justifies the search for stronger ligands to get good building blocks for organometallic and inorganic polymers. In this chapter some pyridine derivatives are employed instead of nitriles as axial ligands for the propose mentioned above.

2A.2.2 Results and Discussion

2A.2.2.1 Synthesis

Reaction of *trans*-[Mo₂(*m*-O₂CCH₃)₂(*m*-dppma)₂(MeCN)₂](BF₄)₂ (**1**) with a two fold stoichiometric amount of the pyridine derivatives in methylene chloride at room temperature leads to complete replacement of the acetonitrile ligands by pyridines as represented in eqn. 2A.2. If the reaction is conducted in acetonitrile a mixture of nitrile and pyridine ligated complexes is obtained, due to the presence of the large acetonitrile excess.



eqn. 2A.2

Complexes **10-15** are soluble in CH₂Cl₂, CHCl₃, THF, and CH₃CN. In the latter solvent the axial ligands are partially exchanged by solvent molecules (see below), in the other solvents the molecules remain unchanged. Under inert gas atmosphere the complexes are stable for weeks in solution and for more than one year in solid state. However, when exposed to air they decompose within a few days in solid state and only within a couple of hours in solution.

2A.2.2.2 Structures

The molecular structure of the dication **10**·(CH₂Cl₂) is shown in Figure 2A.2. Selected inter atomic distances, angles and torsion angles are listed in Table 3 and selected crystallographic data in Table 4 (see **Appendix**). Complex **10** and all other 15 crystallographically characterized structures with a *trans*-[Mo₂(*m*-O₂CCH₃)₂(*m*-LL)₂]²⁺-type dication (LL = dppm, dppma)^[4a, b, c, d] exhibit a very similar [Mo₂(PNP)₂(OCO)₂] core geometry. The two bridging acetates and two dppma ligands are arranged *trans* to each other. Two pyridine ligands are forced to coordinate to the molybdenum atoms in the axial positions and are slightly bent bonded. Quadruply bonded molybdenum complexes with pairs of bridging, dppa/dppma and (O₂CCH₃)⁻ ligands, usually have eclipsed conformation and occupy in the solid state a crystallographic center of inversion except for four dications which either show a crystallographic two fold axis passing through the carbon atoms of the acetate ligands and the midpoint of the Mo-Mo bond or adapt the inversion center and the two fold axis^[2c-d]. The observed Mo-Mo bond distance in **10** (215.04(2) pm) is at

the upper part of the known range for Mo-Mo quadruple bonds. The Mo-O and Mo-P distances do not vary significantly for all known examples of this type. Similar as well are the P-N-P angles of the bridging dppma ligand. The P-N distances in the coordinated ligand are also very close to each other. The Mo-py bond is comparatively long (259.44(18) pm), indicating relatively weak Mo-N interaction.

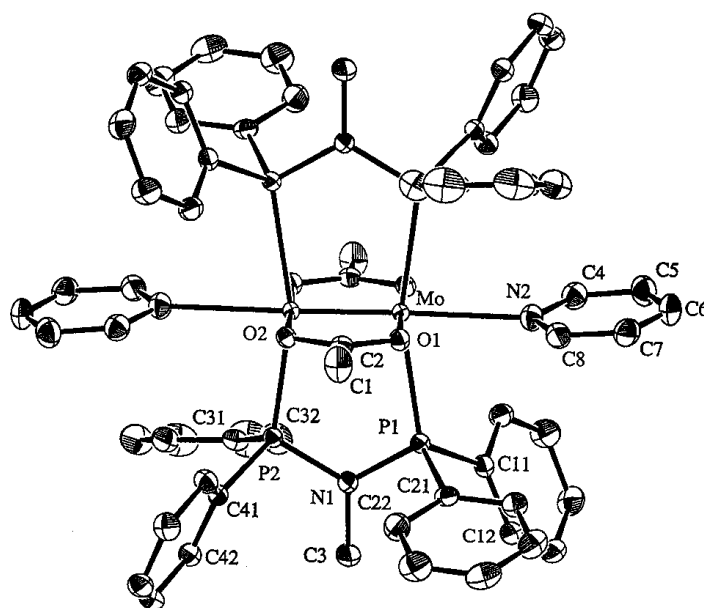


Fig. 2A.2. ORTEP drawing of the molecular structure of the dicationic salt of **10**·CH₂Cl₂. Thermal ellipsoids are at the 50% probability level. Hydrogens are omitted for clarity.

However, the Mo-N distance is significantly shorter than expected from the sum of the van der Waals radii (Mo-N: 382 pm) but longer than the sum of the covalent radii (Mo-N: 215 pm)^[5]. The Mo-N bond is in length between the Mo-N interactions of Mo₂(O₂CC(CH₃)₃)₄•bipy and Mo₂(O₂CC(CF₃)₃)₄•bipy^[9].

2A.2.2.3 Spectroscopy

The strong Raman bands centered around 348(±5 cm⁻¹) can be unambiguously assigned to stretching frequencies of the Mo-Mo quadruple bond. In comparison to the axial ligand free complex of formula [Mo₂(O₂CCH₃)₂(dppma)₂](BF₄)₂ [$\nu(\text{Mo-Mo}) = 375 \text{ cm}^{-1}$], **2**, the Mo-Mo vibration is shifted ca. 25-30 cm⁻¹ to lower energies, thus indicating a weakening of the metal-metal interaction. Nitrile ligands in axial positions cause low energy shifts of about 15 cm⁻¹ (see

Chapter 2A.1). These observations indicate that pyridine ligands are more strongly connected to the Mo(II) centers. However, compounds **10-15** display their Mo-Mo vibration in a narrow interval of only *ca.* 10 cm⁻¹, a clear dependence on the donor or acceptor capability of the axial ligands cannot be seen.

In the IR spectra of complexes **10 - 15**, the O-C-O vibrations appear as a set of distinctive two bands at $\nu_{\text{as}}(\text{OCO}) = 1483 \text{ cm}^{-1}$ and $\nu_{\text{s}}(\text{OCO}) = 1436 \text{ cm}^{-1}$. These vibrations are located at the same energies as those of the precursor compound **1**.

The axial ligand 4-cyanopyridine in compound **15** contains both heterocyclic N and nitrile N atoms. Therefore it is a good tool to find out whether a coordination of the py-N atom would be preferred to a coordination of the cyano-N atom. The coordination site can be determined by comparison of the C≡N, C-C and C-N(pyridine) stretching frequencies of the free ligand to the frequencies of complex **15**. No considerable change is observed in the C≡N stretching of compound **15** (2239 cm⁻¹) when compared to that of 4-cyanopyridine (2243 cm⁻¹). However, the principal pyridine bands at 1594 and 1498 cm⁻¹ in the free ligand are blue shifted to 1639 and 1508 cm⁻¹, respectively, in compound **15**. These features indicate the pyridine nitrogen being coordinated but the CN group being free. Mo-Mo bond being bridged by 4-cyanopyridine is therefore excluded. A similar complex which contains 4-cyanopyridine as axial ligand for a metal-metal bonded compound, namely [Rh₂(O₂CCH₃)₄(NC₅H₄CN)₂], was structurally characterized by Cotton and Felthouse^[51]. In this case the ligand is also bonded to the metal center by the pyridine N. Unfortunately, crystals of the complexes **14** and **15** could only be obtained from acetonitrile/diethyl ether/*n*-hexane mixtures. Due to partial exchange of the axial ligands by solvent molecules the crystals contain both **14** (or **15**, resp.) and **1** in an approximately 1:1 ratio[§]. However, it is clear from the obtained data that the Mo atoms are only coordinated by the pyridine N-atoms in both cases. There is also no evidence for the bridging of two MoMo

[§]Selected crystallographic data for the **14/1** mixture crystal: monoclinic crystals, P2₁/n, measurement temperature (153±1) K, a = 1386.42(9) pm, b = 1608.93(12) pm, c = 1471.96(11) pm, $\beta = 103.133(8)^\circ$. For the **15/1** mixture crystal: monoclinic crystals, P2₁/n, measurement temperature (143±1) K, a = 1382.91(15) pm, b = 1607.21(13) pm, c = 1471.83(15) pm, $\beta = 103.069(12)^\circ$.

cores by the ligands in the cases of both complexes **14** and **15**. When 4-ethynylpyridine is coordinated to the MoMo core (complex **14**), the C≡C vibration (2112 cm^{-1}) is shifted blue from the equivalent stretching of the free ligand (2099 cm^{-1}), suggesting electron transfer from C≡C to the pyridine ring. No evidence for bridging Mo₂ by 4-ethynylpyridine is observed in X-ray crystallography.

The proton NMR chemical shift of the CH₃CO₂ group is shifted down field from 2.09 ppm of **1** to ca. 2.30 ppm in the cases of **10** – **14** and 2.34 ppm of **15**. The chemical shift of the N-CH₃-protons of derivatives **10** - **15** is in the range of 2.37 - 2.63 ppm, which is located down field in comparison to the equivalent resonance of **1** ($\delta(^1\text{H}) = 2.34\text{ ppm}$). Among the examined complexes, 4-cyanopyridine, which contains the strongest electron-withdrawing CN group, has the strongest effect on the chemical shift of the acetate and dppma N-CH₃ protons. These facts suggest that the axial pyridine ligands are not only σ -donors but also π -acceptors. Electron transfer seems to take place from the acetate and dppma ligands through the MoMo core to the axial pyridine ligands.

Table 2A.2 gives a comparison of the chemical shifts of the pyridine protons (H_α and H_β) in compounds **10** - **15** to the free pyridines. When coordinated, the H_α resonance is up field shifted by 0.31 - 0.64 ppm in comparison to the free ligand. The only exception is derivative **15** which displays an up field shift of only 0.07 ppm. The reason for this observation might be the back bonding from the MoMo core to the pyridine ring because of the electron withdrawing effect of the cyano group. H_α is deshielded due to this strong electron-withdrawing effect so that only a rather small shift is observed. The shift effect on the H_β is not as considerable as on H_α in all examined cases, although H_β shows the overall tendency of being shifted to higher field after coordination, too. Temperature-dependent ^1H NMR measurement is performed on compound **15**. While the temperature is lowered from +40 to -90 °C, the resonances corresponding to H_α and H_β are shifted gradually to higher field from 8.74 and 7.30 ppm to 8.42 and 7.06 ppm, resp., and the doublets signals above room temperature turn to relatively broad singlets at lower temperature. However, a dynamic exchange of the cyanopyridine ligand especially with a coordination change between the cyano moiety and the pyridine-N atom seems not to take place.

Table 2A.2. Selected ^1H -NMR data (ppm) of the NC_5N_4 -R ligands in complexes **10 – **15**^a.**

complex	R	δ H (py)		$\Delta\delta$ H (py) ^b	δ H (py)		$\Delta\delta$ H (py) ^b
		Complex	Free ligand		Complex	Free ligand	
10	H	8.21(s)	8.52(m)	-0.31	7.20(t)	7.18(m)	+0.02
11	$\text{C}(\text{CH}_3)_3$	7.94(d)	8.48(q)	-0.54	7.24(d)	7.28(q)	-0.04
12	Ph	7.99(d)	8.63(q)	-0.64	7.46(d)	7.67(q)	-0.21
13	$\text{CH}=\text{CHPh}$	7.91(d)	8.55(q)	-0.64	7.24(d)	7.56(q)	-0.32
14	CCH	8.16(s)	8.56(q)	-0.40	7.15(s)	7.32(q)	-0.17
15	CN	8.71(d)	8.78(d)	-0.07	7.30(d)	7.50(d)	-0.20

^a The chemical shifts of the free ligands are given for comparison. The data were obtained in CD_2Cl_2 .

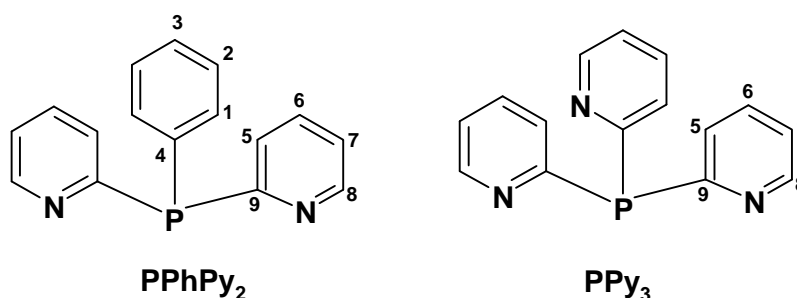
^b $\Delta\delta$, shift difference between complex and free ligand.

The $^{31}\text{P}\{^1\text{H}\}$ NMR spectra of **10**- **15** display a singlet in the range 95.6 - 98.9 ppm since all four phosphorous nuclei are chemically equivalent. This chemical shift is comparable to the precursor **1** (99.7 ppm) and is also similar to *trans*- $[\text{Mo}_2(\mathbf{m}\text{-O}_2\text{CCH}_3)_2(\mathbf{m}\text{-dppma})_2\text{Cl}_2]$ (100.3 ppm)^[4b], implying that the axial substitution (pyridines, nitriles, halogens) has little effect on the $^{31}\text{P}\{^1\text{H}\}$ NMR spectra.

2A.3 Synthesis and Characterization of Dimolybdenum and Dirhodium Complexes Bearing 2-pyridylphosphine Ligands, PPhPy₂ or PPy₃ (Ph = Phenyl, Py = 2-Pyridyl)

2A.3.1 Introduction

The coordination chemistry of 2-pyridylphosphine ligands [scheme 2A.3] has been studied in some detail during the recent years, mainly because of their ability to coordinate both with their phosphorus and their nitrogen atoms, which possess different coordination properties ^[1]. In addition to numerous mononuclear complexes ^[2], several binuclear species ^[3] as well as clusters ^[4] and oligomers ^[5], containing 2-pyridylphosphine ligands have been described.



Scheme 2A.3

For the coordination of complexes containing metal-metal multiple bonds, mainly diphenyl-2-pyridylphosphine, Ph₂PPy, has been used ^[3f-j, 6]. Complexes containing the ligands PhPPy₂ and PPy₃ are rare ^[7], even no X-ray crystal structures have been reported so far. However, some dimeric complexes of that type have claimed to be active catalysts for the reduction of alkenes ^[7b]. For the current examination of the polymerization of dienes and of the possibility of subsequent hydrogenation is being undertaken, it is of interest that these molecules might be useful model complexes for the initiator/catalyst systems. It is therefore also of interest, whether the nitrogen donor atoms of the ligands are strongly fixed to the metal centers or whether opening and closing of this bond can be observed especially in donor solvents. This could enable

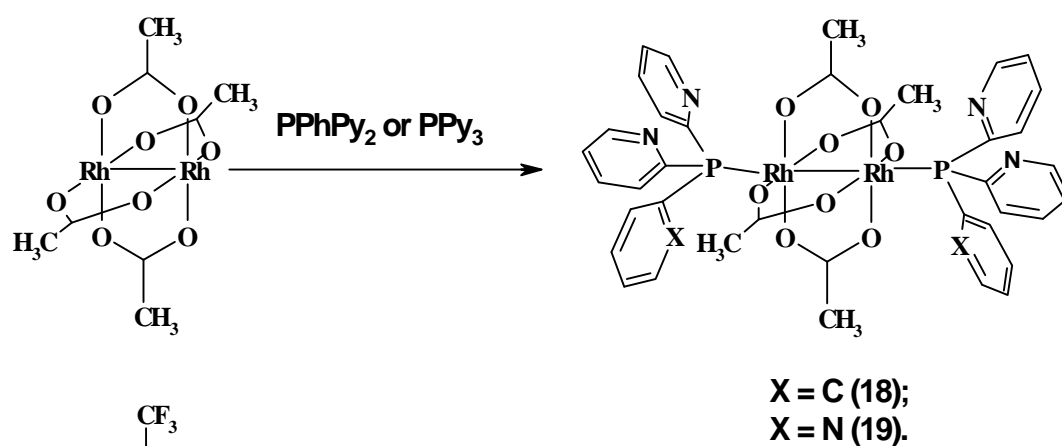
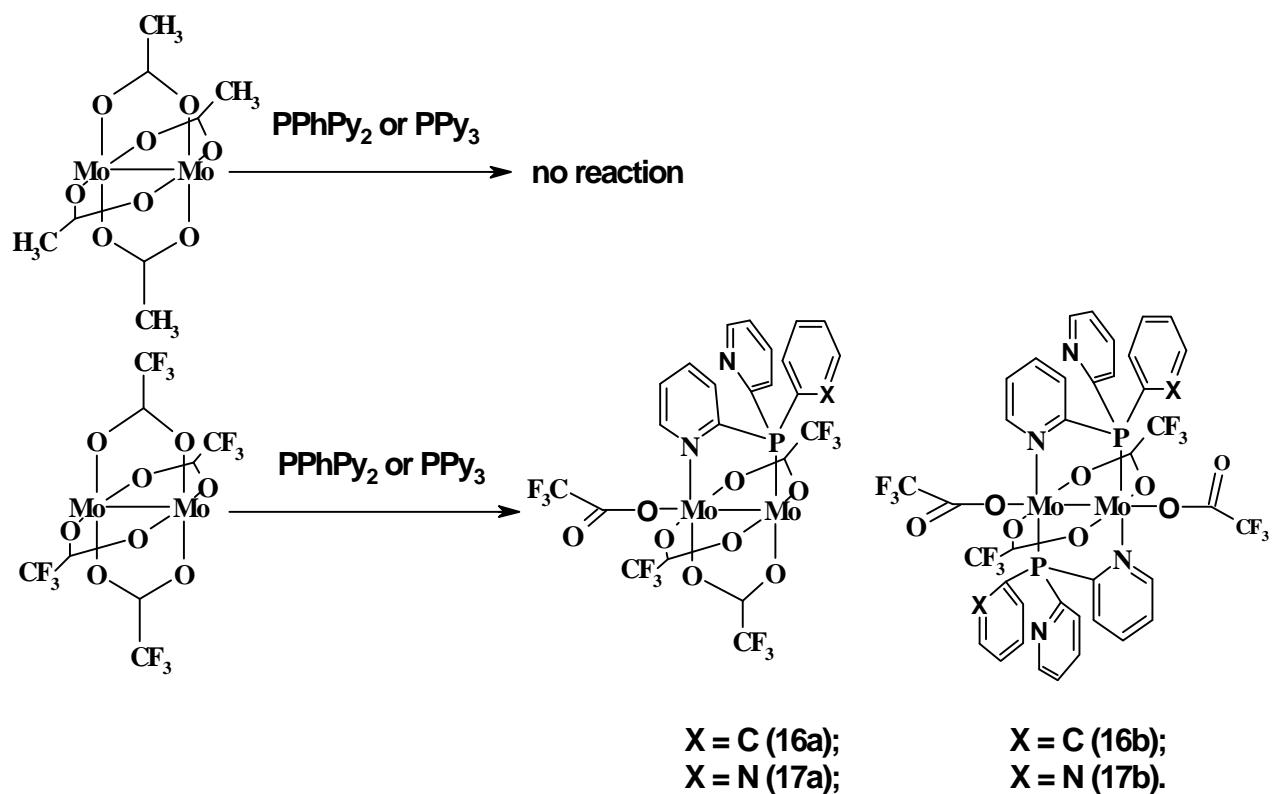
the (reversible) binding of substrate molecules to the metal center to initiate a polymerization process while the pyridine ligand would otherwise protect the potential coordination site, thus enhancing the initiator stability. In this work the syntheses and characterization of dimolybdenum and dirhodium compounds bridged and/or axially coordinated by PhPPy₂ and PPy₃ ligands were reported. The X-ray crystal structures of selected complexes are described as well.

2A.3.2 Results and Discussion

2A.3.2.1 Syntheses

The reactions of Mo₂(*m*-O₂CCF₃)₄ with two equivalents of the corresponding ligand at room temperature yield the complexes **16a** and **17a**, respectively, with only one CF₃CO₂⁻ group in the axial position according to eqn. 2A.3A. When excess of ligand (4-fold in these cases) is used at room temperature, complexes **16b** and **17b**(contaminated by **17a**), with two axial CF₃CO₂⁻ groups, are formed according also to eqn. 2A.3A. Even at reflux conditions attempting to prepare pure **17b**, still a mixture of **17a** and **17b** can be collected after 4 h, containing 73 % **17b**. Reaction of much more excess of PPy₃ with Mo₂(*m*-O₂CCF₃)₄ leads to a mixture of products as well. The reason for this behavior might be that a coordination of PPy₃ disfavors the coordination of a second complex of this type in *trans* position, due to the more pronounced *trans* effect of PPy₃ in comparison to PPhPy₂. The *cis* position is probably not available for a second PPy₃-ligand because of steric reasons. The compounds **16a**, **16b**, **17a**, and **17b** are insoluble in CH₂Cl₂, CH₃CN, diethyl ether, and decompose in methanol, DMF and DMSO. This behavior could be due to an opening of the pyridine-N bond to the metal center in the presence of polar solvents with subsequent cleavage of the metal-metal bond.

The orange-red complexes **18** and **19** can be prepared using excess of ligands to interact with Rh₂(μ-O₂CCH₃)₄ at room temperature. These two rhodium complexes are soluble in CH₂Cl₂, but insoluble in THF, acetone and CH₃CN. It is noteworthy in this context that Mo₂(μ-O₂CCH₃)₄ does not react with PPhPy₂ and PPy₃. And the interaction of Rh₂(μ-O₂CCF₃)₄ with two ligands is very complicate because the NMR, IR and Raman spectra of the products are unidentified. The reaction pathways are also shown in eqn. 2A.3A.



eqn. 2A.3A

2A.3.2.2 Structures

The molecular structures of compounds **16b** and **17b** have been determined by single crystal X-ray crystallography. The two compounds have similar crystal structure. A PLATON representation of compound **17b** was shown in Fig. 2A.3A. The crystal data are listed in Table 9 (**Appendix**). Selected bond distances and angles are listed in Table 10 (**Appendix**) for **16b** and for **17b**.

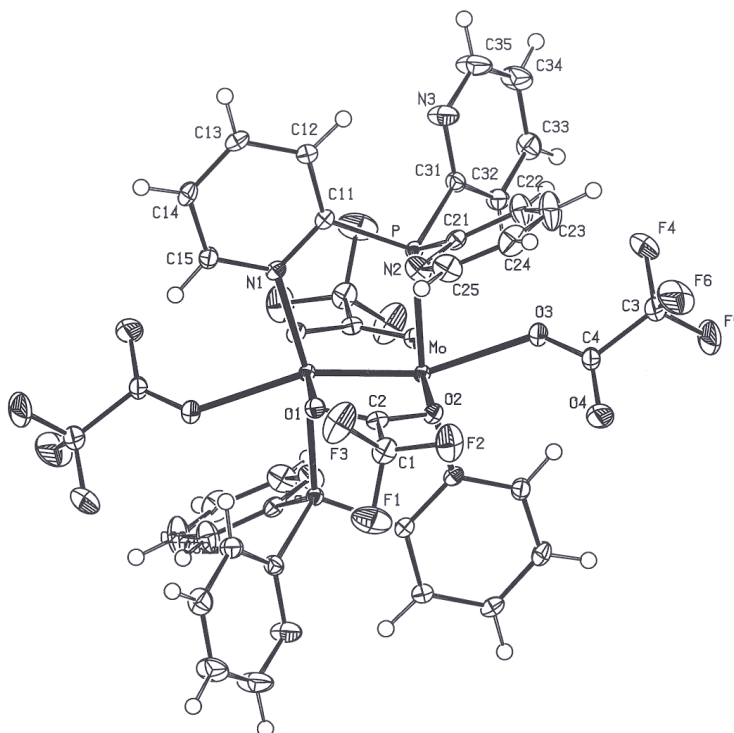


Fig. 2A.3A PLATON drawing of the molecular structure of $\text{Mo}_2(\mu\text{-O}_2\text{CCF}_3)_2(\text{O}_2\text{CCF}_3)_2(\text{PPy}_3)_2$ (**17b**). Thermal ellipsoids are given at the 50% probability level. Hydrogens are omitted for clarity.

The dimolybdenum centers are coordinated by two bridging CF_3COO^- ligands which are *trans* to each other, and resides on a crystallographic center of inversion. The other two CF_3COO^- groups each coordinates one metal center in the axial position. The two 2-pyridylphosphine ligands are in a head-to-tail relationship and are *trans* to each other. As can be seen in Fig. 2A.3A, the short Mo-N distance with C(15) close to the region of axial coordination, together with the long Mo-P distance and the other two uncoordinated pyridyl groups directed away from the axial region causes a displacement of the axial CF_3COO^- group away from the “linear” axial site by ca. 23.9° as have being encountered in the dimolybdenum compounds reported in

literature^[13h] and Chapter 2A.1. Due to the strong interaction of axial CF_3COO^- group with the Mo_2^{4+} moiety, the Mo-Mo distances, 219.01(3) pm for **16b** and 218.84(2) pm for **17b**, respectively, are longer by *ca.* 10 pm than their precursor $\text{Mo}_2(\mu\text{-O}_2\text{CCF}_3)_4$ (Mo-Mo: 209.0(4) pm)^[10], being in the upper end of normal Mo-Mo quadruple bond distances reported.^[9]

2A.3.2.3 Spectroscopy

□ IR and Raman

For dimolybdenum complexes, only the vibrations of **16b** and **17b** belonging to $\text{Mo}_2(\text{O}_2\text{CCF}_3)_4$ moiety are listed in Table 5 and Table 6, respectively (see **Appendix**). The solid-state IR spectra of complexes **16a** - **17b** show strong absorption bands in the range of 1650-1700 cm^{-1} , indicating the presence of monocoordinated carboxylate group(s)^[3f], of which 1690(**16b**) and 1684 cm^{-1} (**17b**) are assigned to two terminal carboxylate groups; 1654(**16a**) and 1647 cm^{-1} (**17a**) to one terminal carboxylate group. The vibrations located at *ca.*1600 cm^{-1} represent the asymmetric stretching vibration of the bridging trifluoroacetates. The Raman active (MoMo) mode shows that in the case of **16b** and **17b** the MoMo bond strength is greatly weakened by the incorporation of two phosphine ligands (comparison between **16b** (307 cm^{-1}), **17b** (308 cm^{-1}) and their precursor $\text{Mo}_2(\mu\text{-O}_2\text{CCF}_3)_4$ (397 cm^{-1})^[8]). Meanwhile, the MoMo stretching mode at 376 cm^{-1} (w) for **16b** and at 378 cm^{-1} (vs) for **17b** indicates that these two compounds are contaminated by **16a** and **17a**, respectively, being identical to the results of elemental analysis.

Selected IR and Raman spectra of **18** and **19** and their preliminary assignments are listed in Table 7 and Table 8, respectively (see **Appendix**). The stretching vibration of the bidentate acetato group located at 1596, 1434, 50, 542 cm^{-1} for **18** and at 1594, 1422, 695, 561, 525 cm^{-1} for **19**, respectively, indicate that only one type of carboxylate structure is existing; the strong Raman band at 337 cm^{-1} (**18**) and 338 cm^{-1} (**19**) refers to the complete symmetric Rh-O_4 vibrations of RhO_4 square-planar fragments. Its asymmetric vibrations can appear as IR active mode. In addition, very intensive Raman band at 287 cm^{-1} (**18**) and 289 cm^{-1} (**19**) can be assigned to the Rh-Rh stretching mode. Thus, unlike equatorial coordination patterns of these pyridylphosphine ligands to $\text{Mo}_2(\mu\text{-O}_2\text{CCF}_3)_4$ moiety, these ligands prefer axial interaction with $\text{Rh}_2(\mu\text{-O}_2\text{CCH}_3)_4$. The compounds $\text{Rh}_2(\mu\text{-O}_2\text{CR})_4\text{L}_n$ ($n = 1$ or 2) are the largest class of dirhodium(II) compounds known to date^[9].

□ NMR Spectroscopy

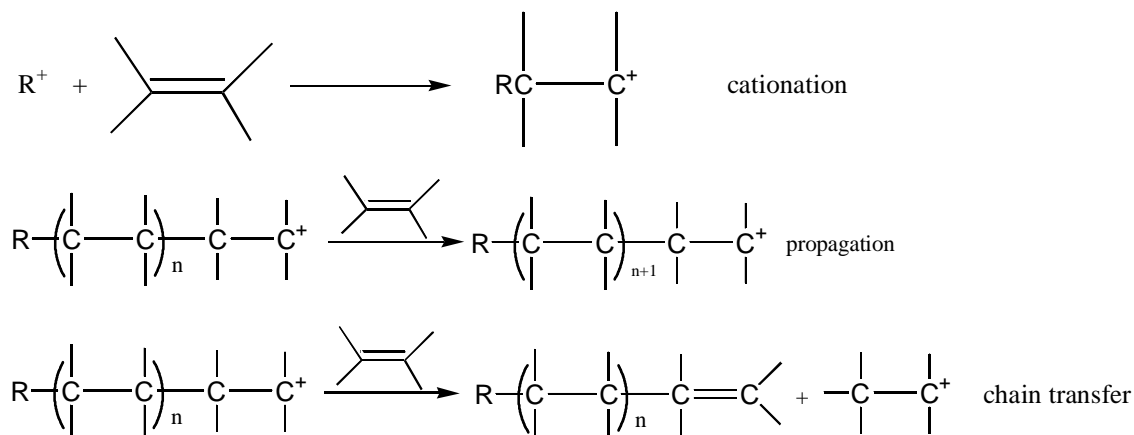
The proton NMR spectra of the pyridyl groups in complexes **18** and **19** display a downfield shift and a little more splitting patterns compared to the free ligand. Before IR and Raman spectra were carefully studied, it was assumed that structures of **18** and **19** were identical to those of molybdenum analogues and that the singlets of hydrogen atoms of acetates at room temperature should be explained as the presence of quick exchange reactions of bridging acetates at equatorial position with axially terminal acetates ^[3f]. Temperature-dependent ¹H NMR spectroscopy was therefore performed to examine fluxionality of the acetates. The results, however, showed that there was no broadening or splitting in the range of -90°C to 30°C. Their IR and Raman spectra were examined again in more detail and found that the Rh₂(μ-O₂CCH₃)₄ moiety is maintained. The ³¹P{¹H}-NMR signals, located at -8.99 (complex **18**) and -2.64 ppm (complex **19**), are singlets in both cases. The ligand signals are shifted 5.75 ppm more upfield in complex **18**, compared to free ligand. The shift change in the case of complex **19** is smaller, only ca. 1.30 ppm. These observations indicate that the additional pyridine moiety in the ligand PPy₃ shifts significantly more electron density to the phosphorus center than the Ph-ligand in PhPPy₃. Therefore, the effect of the metal coordination on the chemical shift of the phosphorus atom is not so strong as in complex **18**.

□ Electronic absorption spectroscopy

The electronic absorption spectra of the complexes **18** and **19** were measured in methylene chloride at room temperature. The lowest energy absorptions centered at 496 nm ($\epsilon = 600 \text{ M}^{-1} \text{ cm}^{-1}$) for compound **18** and at 568 nm ($\epsilon = 250 \text{ M}^{-1} \text{ cm}^{-1}$) for compound **19**, are tentatively assigned to $\pi^*(\text{Rh}_2) \rightarrow \sigma^*(\text{Rh}_2)$ transitions ^[9].

Part B. Cationic Polymerization of Olefins

The cationic polymerization of an alkene (or diene) can be envisaged to involve the reactions shown in Scheme 2B^[1]. The first step is nucleophilic attack of the carbon-carbon double bonds of the alkene (or diene); then the resulting monomer cations add additional monomer molecules for propagation of chains; the last step is the termination of the polymerization by chain transfer to form relatively stable carbocations which are no longer capable of adding monomer.



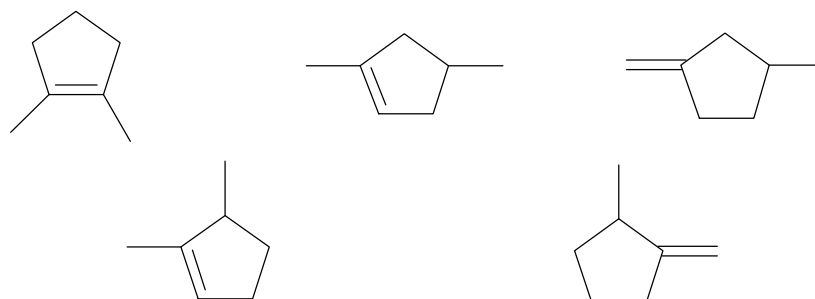
Scheme 2B

Initiators for cationic polymerization of olefins include primarily four classes^[1, 24]: (a) Lewis acids such as AlCl_3 , BF_3 , I_2 , RAlCl_2 , etc.; (b) Brønsted acids including HClO_4 , CF_3COOH and others; (c) carbenium salts like $(\text{C}_6\text{H}_5)_3\text{C}^\oplus$, formed by the dissociation of $(\text{C}_6\text{H}_5)_3\text{CCl}$; (d) high-energy radiation through high-energy electrons and Co^{60} radiation. In addition to these four classes, cationic polymerization can also be initiated electrochemically, photochemically and *via* charge transfer complexes^[1, 24].

Despite a great number of monomers are suitable for cationic polymerization, few cationic polymerizations are performed industrially. The main reason is the inherent instability (high activity) of many macrocations which undergo termination and transfer reactions much frequently, thereby forming oligomers.

Isobutene has been polymerized cationically on a large industrial scale (with 4% isoprene as comonomer) for preparation of elastomers, adhesives, viscosity improvers, etc., employing $\text{BF}_3 + \text{H}_2\text{O}$ as initiator.

Cyclopentadiene and dicyclopentadiene provide olefinic sites in terpolymers with ethylene and propylene, and are also employed in blends with other olefins and diolefins which are then polymerized to hydrocarbon resins. These copolymers have many commercial applications, e.g. tackifiers' resins, hot-melt and pressure-sensitive adhesives ^[2]. In 1985, Hercules established a production unit using dicyclopentadiene in a metathesis reaction injection moulding (RIM) process ^[3]. The thermoset polymer, which has a high modulus and impact strength, is sold under the name Metton. Heating dicyclopentadiene alone at *ca.* 200°C yields oligomers up to the pentamers ^[4]. Nevertheless, cyclopentadiene, one of the most active monomers with respect to cationic polymerization, has limited commercial applications, despite a variety of studies on this monomer has been undertaken. The most obvious reason for this is the existence of a double bond in its product that easily subjects to oxidation ^[5]; it is also partly because the polymer could undergo partial crosslinking using traditional Friedel-Crafts initiating systems for polymerization and double bonds may migrate to form isomerized units of the type shown below:



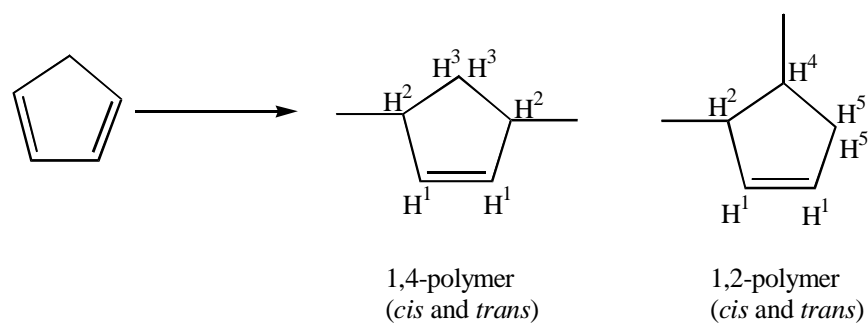
2B.1 Solvent Stabilized Transition Metal Cations as Initiators for Cyclopentadiene Polymerization

2B.1.1 Introduction

Since in 1926 Staudinger and Bruso ^[1] introduced inorganic halides, such as SnCl_4 , AlBr_3 and TiCl_4 , to initiate the cationic polymerization of cyclopentadiene, various catalytic systems have been examined. For instance, Wassermann ^[2] reported the formation of deeply colored

conjugated polycyclopentadiene possessing electrical conductance properties when trichloroacetic acid was used as catalyst. Yen et al. [3] employed Ziegler-type catalysts, like $(i\text{Bu})_3\text{Al}$ mixed with TiCl_4 , for the homogenous polymerization of cyclopentadiene. Interestingly, the initiation of a cyclopentadiene polymerization by either HClO_4 , or AcClO_4 leads to a very rapid but incomplete polymerization [4] and these authors give no explanation of this phenomenon, but one explanation might be that a cyclization reaction is more favorable for an ester-terminated chain than for an ionically growing chain. In addition, the radiation induced stereospecific and asymmetric inclusion polymerization of cyclopentadiene has been carried out in crystal canals of thiourea [5] and deoxycholic acid [6], respectively.

More recently, McCann and his coworker [7] used quadruply bonded dimolybdenum(II, II) catalysts, namely, $[\text{Mo}_2(\text{MeCN})_8][\text{BF}_4]_4$ and $[\text{Mo}_2(\mu\text{-O}_2\text{CCH}_3)_2(\text{MeCN})_8][\text{BF}_4]_2$, for the cationic polymerization either of neat cyclopentadiene or for solutions of the monomer in dichloromethane and found that these two complexes are extremely efficient initiators for polymerization of cyclopentadiene (Scheme 2B.1A). In addition, the homogeneous polymerization of cyclopentadiene is effected by the dimolybdenum(II, II) salts in acetonitrile [7]. However, when dichloromethane was as a monomer solvent with the latter catalysts, $[\text{Mo}_2(\mu\text{-O}_2\text{CCH}_3)_2(\text{MeCN})_8][\text{BF}_4]_2\text{-SiO}_2$, the polymer yield increased significantly. In most cases there were approximately equal amounts of the 1,2- and 1,4-structures present in the polymers.



Scheme 2B.1A

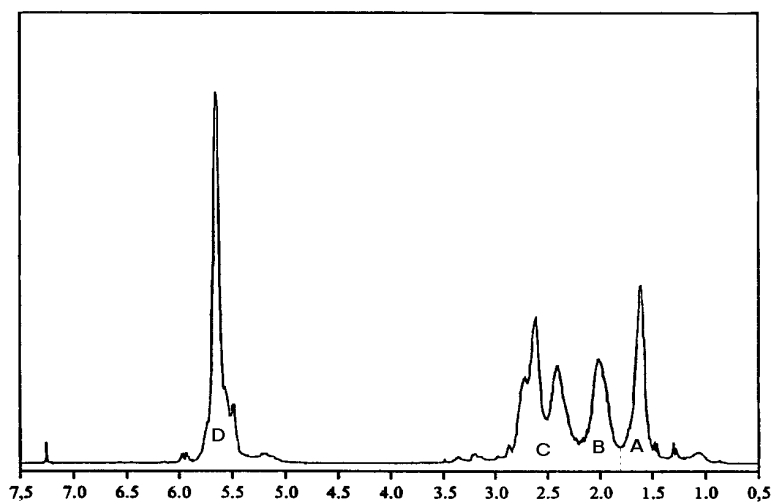
Solubility of the polycyclopentadiene products was dependent on reaction conditions and the catalysts used. Furthermore, when dichloromethane solutions of cyclopentadiene were polymerized with $[\text{Mo}_2(\mu\text{-O}_2\text{CCH}_3)_2(\text{MeCN})_8][\text{BF}_4]_2$, black conducting plastics precipitated. Catalysts could be reused many times to polymerize successive batches of monomer. In this chapter it is demonstrated that these two complexes are not isolated cases concerning their

catalytic applications. A broad variety of easily accessible Cr-, Mo-, and Rh-complexes show excellent activity as initiators in the cationic polymerization, as exemplified on the polymerization of cyclopentadiene^[8].

2B.1.2 Results and Discussion

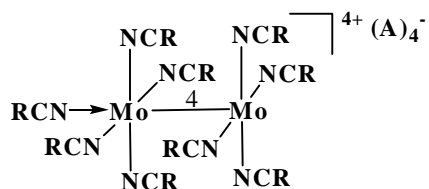
As shown in Scheme 2.B.1A, the unit ring contained in polycyclopentadiene can have the 1,4- and/or 1,2-structure when side reactions such as branching and double bond migration (isomerization) are excluded.

The ¹H NMR spectrum of chloroform-soluble polycyclopentadiene (see Fig. 2B.2A) contains a fairly sharp peak (D) at $\delta = 5.6$ ppm (olefinic protons H¹), and three broad and partially overlapping peaks (A, B, C) ranging from $\delta = 1.5 - 3.0$ ppm (methine and methylene protons (H² - H⁵)).

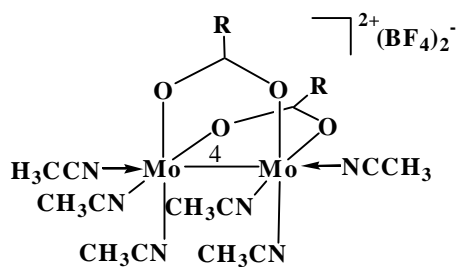
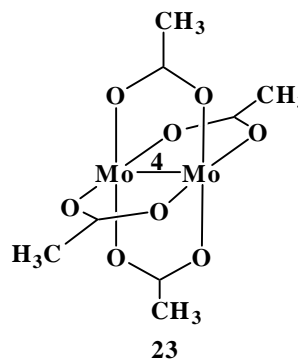
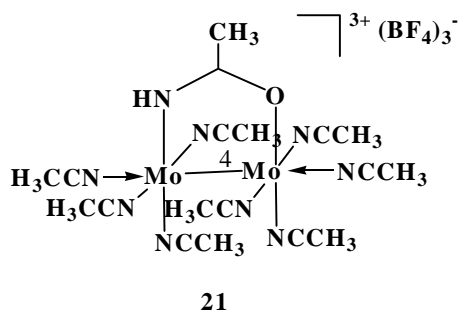


Scheme 2B.2A

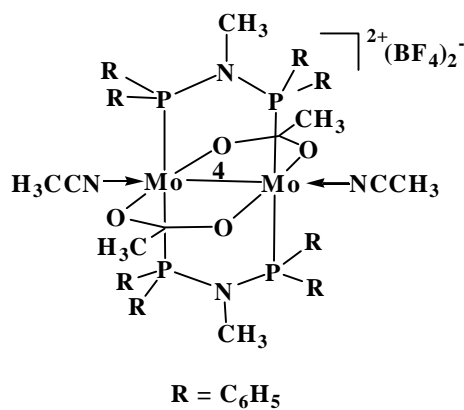
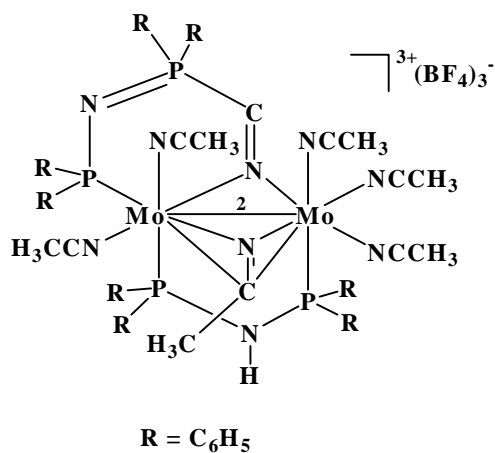
Comparison of the polymer spectrum with those of model compounds suggests that peak A is probably due to β -methylene proton (H³) in the 1,4- structure. Peak B and C appear to be due to α -methylene (H⁵) and α -, β -methine protons (H² and H⁴) and are unable to be assigned separately. Thus the content of the 1,2-structure in the polymer can be calculated from the relative peak areas as follows:

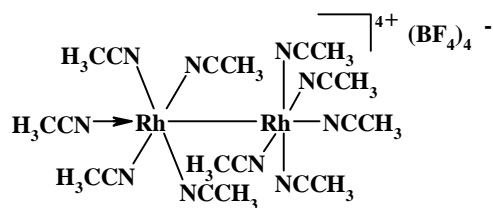


$R = \text{CH}_3$, $A = \text{BF}_4^-$ (20); $R = \text{C}_6\text{H}_5$, $A = \text{BF}_4^-$ (20a); $R = \text{C}(\text{CH}_3)_3$, $A = \text{BF}_4^-$ (20b), $R = \text{CH}_3$, $A = \text{O}_3\text{SCF}_3^-$ (20c).

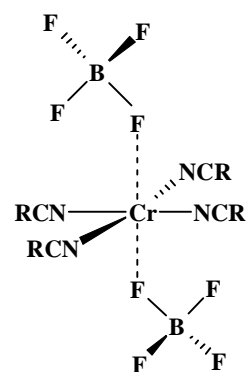


$R = \text{CH}_3$, (22);
 $R = \text{CH}_2\text{Cl}$ (24); $R = \text{CHCl}_2$ (25); $R = \text{CCl}_3$ (26).





29



R = CH₃ (30); R = C₆H₅ (30a);
R = C(CH₃)₃ (30b)

Scheme 2B.1B Catalysts for polymerization of cyclopentadiene

$$1,2\text{-structure (\%)} = \frac{\{(B + C) - A\}}{\{A + (B + C)\}} \times 100$$

The error in the calculated content of the 1,2-structure (%), arising from overlapping peaks, is likely to be a few percent. The aliphatic: olefinic proton ratio (a / o) is simply calculated as (A + B + C) / D and should be equal to 2 for a polymer containing only 1,4- and/or 1,2-units in the chain. This value can change if the polymer undergoes cross linking, or if double-bond migration occurs to give isomerized units, as described above.

The polymerization of cyclopentadiene initiated by the complexes **20-30** (Scheme 2B.1B) at room temperature with an initiator: monomer ratio of 1:1000 led to quantitative monomer conversion after 16 h in several cases. [Mo₂(NCCH₃)₉][BF₄]₂ (**20**) was selected as an example to examine the reaction conditions in detail. These results were compared with data already available from the literature ^[7].

2B.1.2.1 Effect of Reaction Time

The polymer yield increases with the reaction time in an approximately linear manner (Fig. 2B.1C). An induction period can be assumed because the initiator is not dissolved immediately but only within about one hour in the solvent, CH₂Cl₂. Meanwhile it was found that during the reaction time the number average of the molecular weight (M_n) of the product polymer decreases from about 20000 after 2 h to ca. 8000 after 16 h. Accordingly, the polydispersity index decreases from 3.0 after 2 h to 1.6 after 6 h. After this time it remains nearly unchanged.

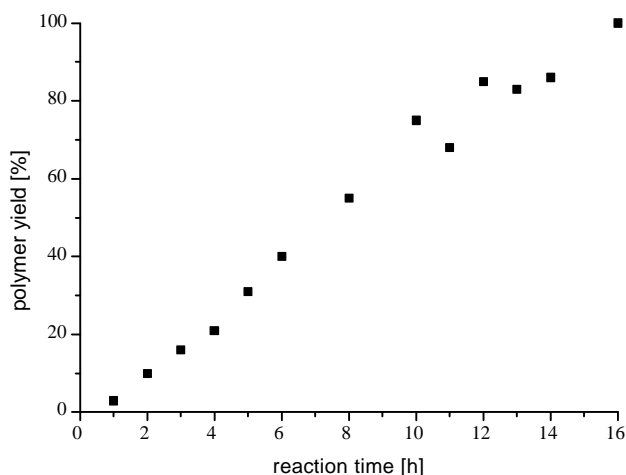


Fig.2B.1C Dependence of the polymer yield on the reaction time (initiator: $[\text{Mo}_2(\text{NCCH}_3)_9][\text{BF}_4]_4$; $T = 20^\circ\text{C}$; $V(\text{CH}_2\text{Cl}_2) = 40 \text{ mL}$; $c(\text{Cp}) = 2.27 \text{ mol/L}$; $c(\text{initiator}) = 2.5 \text{ mmol/L}$).

2B.1.2.2 Effect of Concentration of the Initiator

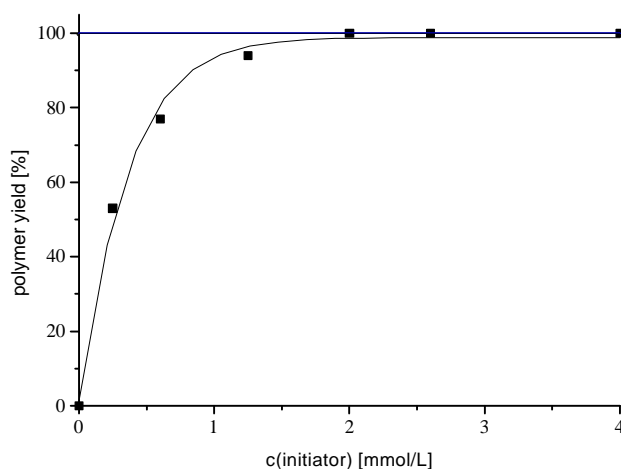


Fig. 2B.1D Dependence of the polymer yield after 16 h on the initiator concentration (initiator: $[\text{Mo}_2(\text{NCCH}_3)_9][\text{BF}_4]_4$; $t = 16 \text{ h}$; $T = 20^\circ\text{C}$; $V(\text{CH}_2\text{Cl}_2) = 40 \text{ mL}$; $c(\text{Cp}) = 2.27 \text{ mol/L}$; Catalyst aging time: 10 d).

The product yield increases quickly with increasing amount of catalyst (Fig. 2B.1D). For instance, when the concentration of the initiator is 0.25 mmol/L, the polymer yield is 53%; if the concentration of the catalyst is increased to 1.25 mmol/L, the conversion of the monomer

amounts to 93%. The polymer yield reaches 100% after 16 h at a catalyst: substrate ratio of ca. 1:1500. This corresponds to a catalyst activity (turn over frequency TOF) of ca. $3 \cdot 10^{-2}$ Mol monomer per Mol catalyst per second.

2B.1.2.3 Effect of Solvents

The solvent has a strong influence on the reaction. In nonpolar, noncoordinating solvents (e. g. *n*-hexane, toluene) the yield is low (< 10 % after 16 h); in polar, noncoordinating solvents it is high, with all other conditions unchanged (e. g. quantitative in CH₂Cl₂). However, in polar, coordinating solvents (e. g. acetonitrile) the yield is below the 10 % level. Possible reasons for this observation are the competition of substrate and solvent for the coordination sites at the Mo(II) centers, thus leading to less opportunity for the substrate to occupy active sites at the metal centers, and the more pronounced ion pair separation in polar solvents, which has opposite influence on the product yield, too.

2B.1.2.4 Effect of Aging Time

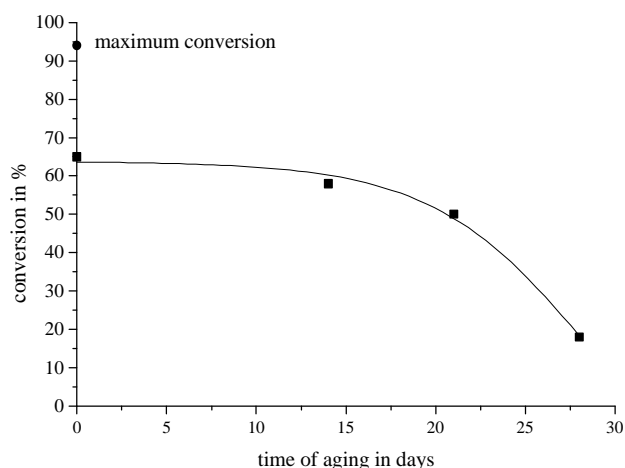


Fig. 2B.1E Effect of catalyst aging on conversion of monomer with [Mo₂(NCCH₃)₉][BF₄]₄ as initiator (t = 16 h; T = 20°C; V(CH₂Cl₂) = 40 mL; c(Cp) = 2.27 mol/L; c(initiator) = 1.25 mmol/L).

Another observation worth mentioning for complex **20** is the aging effect. Although the freshly prepared initiator can converse the substrate to polymer in 94% yield, the catalyst that polymerize the monomer in 65% yield is arbitrarily selected here as reference to investigate its

aging effect. Fig. 2B.1E shows clearly that the activity of the catalyst reduces considerably with increase of storage time. After storage of four weeks the activity of the catalyst drops to less than one third of that of a freshly prepared catalyst. For this behavior the reaction of complex **20** with traces of moisture could be responsible. It is known that complex **20** forms a complex of composition $[\text{Mo}_2(\text{N}(\text{H})\text{C}(\text{CH}_3)\text{O})(\text{NCCH}_3)_8][\text{BF}_4]_3$ (**21**) with one equivalent of water, with two equivalents of water $[\text{Mo}_2(\text{N}(\text{H})\text{C}(\text{CH}_3)\text{O})_2(\text{NCCH}_3)_6][\text{BF}_4]_2$ is formed^[6]. Complexes of this type are less active than compound **20** (see Table 2.1A). Higher amounts of water lead to total decomposition of **20** with the formation of molybdenum oxides and hydroxides (EA and IR evidence).

2B.1.2.5. Other Effects

The influences of charge, electronic and steric effects of the ligands, the counter ion and the central metal have been examined, too (see table 2B.1A). With complex **20** 94% of the substrate is transformed into a polymer after 16 h if a catalyst: substrate ratio of 1:2000 is applied. After the replacement of two equatorial nitrile ligands by a bridging acetamido ligand (compound **21**) the product yield goes down to 74 %. The substitution of four of the equatorial nitrile ligands by two acetates (complex **22**) leads to a further decline of the product yield to 70%. The cation charge changes from +IV in the case of molecule **20** to +III in the case of complex **21** to +II in derivative **22**. The activity of the catalyst is therefore coupled with the charge of the cation, as would be expected in the case of a coordinative cationic reaction as postulated by McCann^[7b]. This conclusion is supported by the result obtained with the neutral derivative **23**. In this case no polymer formation can be observed.

Not only the total charge of the cations is of importance for the product yield but also the effective charge at the metal centers. Formal replacement of the CH_3 -protons in compound **22** (70 % yield) by electron withdrawing chlorine atoms (derivative **26**) leads to a yield increase to 97 %. The introduction of only two chlorines per acetate ligand (compound **25**) already increases the polymer yield to more than 90 %. Remarkably low is the product yield in the case of the monochlorinated derivative **24** (54 %). This result, ranging even below the unsubstituted bisacetate complex **22**, might be due to a steric effect, over-compensating the comparatively weak electronic effect in the case of one chlorine atom per acetate ligand.

Steric effects should be of significant impact on the postulated coordinative cationic mechanism, too. However, the substitution of all the acetonitrile ligands in the case of complexes **20** or **22** by pivalonitrile (compounds **20a** and **22a**) or benzonitrile (derivatives **20b** and **22b**) does not change the product yield after 16 h significantly. Obviously the steric bulk of those weakly coordinated ligands is of no concern for the reaction mechanism. NMR experiments show the rapid exchange of these nitrile ligands in polar solvents ^[12]. If the acetonitrile ligands are replaced by more strongly coordinating, bulky but neutral ligands e. g. bis(diphenylphosphino)amine (dppa) or bis(diphenylphosphino)methylamine (dppma) the product yield decreases significantly, even if the initiator concentration is doubled. Using the complex **27**, with the charge 3+, only a polymer yield of 10 % is reached after 16 h. Compound **28** containing no equatorial acetonitrile ligands does not initiate any polymerization, despite its 2+ charge. This means weakly coordinated equatorial ligands are crucial for activity of these catalysts.

To examine the influence of the counter ion, the very weakly coordinating BF_4^- counter ion was replaced by the somewhat stronger coordinating triflate (CF_3SO_3^-) counter ion (compound **20c**). The less pronounced ion pair separation is reflected in a polymer yield decrease from 94 % (complex **20**) to 82 % (complex **20c**).

Additionally, the influence of the central atom has to be taken into account. A formal replacement of the Mo central atoms in **20** by Rh atoms (compound **29**) leads to a significantly lower polymer yield despite unchanged charge and sterical bulk of the ligands. In solution ¹H-NMR, while complex **20** displays only one singlet for the nitrile protons, derivative **29** exhibits two signals in a 4:1 ratio. In solid-state ¹H-NMR complexes **20** and **29** display two singlets (in an 8:1 and a 4:1 ratio, resp.). In both cases the bigger signal is much more low field shifted, due to the more pronounced electron deficiency of the corresponding protons. This result shows the stronger interaction of the equatorial nitrile ligands with the metal center in the case of the Rh(II) compound, which is also responsible for the diminished polymer yield. Probably the amount of free coordination sites for the substrate molecules is reduced due to the stronger metal-nitrile interaction. The monomeric Chromium(II) complexes **30**, **30a**, **30b**, however, are of a comparable activity to compound **20**. As in the case of the latter complex the equatorial nitrile ligands are only weakly coordinated ^[9]. The presence of a metal-metal quadruple bond in the

molecule seems therefore not to be an important feature, especially when the solvent coordinated metal center is of high reactivity as in the Cr (II) case.

A comparison of the products derived by the classical cationic polymerization pathway ($\text{Et}_2\text{AlCl}/\text{H}_3\text{C}-\text{C}_6\text{H}_4-\text{CH}_2\text{Cl}$, *n*-hexane, $-80\text{ }^\circ\text{C}$) to the polymers derived by polymerization with transition metal complex cations shows that the latter cases display a significantly higher percentage of 1,2- cyclopentadiene units ($^1\text{H-NMR}$). This can be due to the stronger ion pair separation at the active chain end ^[8a - c]. In the examined case the weaker ion pair separation is due to the weaker coordination capability of the BF_4^- in comparison to $\text{AlEt}_2\text{Cl}_2^-$, the stronger solvent polarity and especially the higher reaction temperature.

Table 2B.1A: Overview on the catalytic results gained by utilizing complexes **20-30** as initiators for the cyclopentadiene polymerization. (Reaction time = 16 h, temperature = 25 °C, solvent: CH₂Cl₂, reaction volume = 40 mL)

No.	complex ^a	C(Init.) [mol/L]	C ₀ (Cp) [mol/L]	Yield [%]	M _n (GPC) ^a	M _w (GPC) ^a	1,2-prod. [%] ^b	TOF ^c [10 ⁻² s ⁻¹]
20	[Mo ₂ (AN) ₉][BF ₄] ₄	0.00125	2.27	94	8500	21300	45	3.0
20a	[Mo ₂ (BN) ₉][BF ₄] ₄	0.00125	2.27	96	13800	33800	44	3.0
20b	[Mo ₂ (PN) ₉][BF ₄] ₄	0.00125	2.27	93	13100	33800	44	2.9
20c	[Mo ₂ (AN) ₉][O ₃ SCF ₃] ₄	0.00125	2.27	82	6300	19500	38	2.6
21	[Mo ₂ (AA)(AN) ₈][BF ₄] ₃	0.00125	2.24	74	11000	22200	39	2.3
22	[Mo ₂ (Ac) ₂ (AN) ₆][BF ₄] ₂	0.00125	2.27	70	9300	16600	42	2.2
23	Mo ₂ (Ac) ₄	0.00125	2.24	0	0	0	-	0
24	[Mo ₂ (ClAc) ₂ (AN) ₆][BF ₄] ₂	0.00125	2.27	54	7800	16600	43	1.7
25	[Mo ₂ (Cl ₂ Ac) ₂ (AN) ₆][BF ₄] ₂	0.00125	2.24	92	9500	18900	43	2.9
26	[Mo ₂ (Cl ₃ Ac) ₂ (AN) ₆][BF ₄] ₂	0.00125	2.27	97	9800	20600	44	3.1
27	[Mo ₂ (dppa) ₂ (AN) ₇][BF ₄] ₃	0.0025	1.42	10	32700	61700	38	0.1
28	[Mo ₂ (dppma) ₂ (Ac) ₂][BF ₄] ₂	0.0025	1.42	0	0	0	-	0

Table 2B.1A *continued*

No.	complex ^a	C(Init.) [mol/L]	C ₀ (Cp) [mol/L]	Yield [%]	M _n (GPC) ^a	M _w (GPC) ^a	1,2-prod. [%] ^b	TOF ^c [10 ⁻² s ⁻¹]
29	[Rh ₂ (AN) ₁₀][BF ₄] ₄	0.00125	2.24	47	12300	25200	40	1.5
30	[Cr(AN) ₄][BF ₄] ₂	0.00125	2.27	92	14800	33400	44	2.9

^adetermined by RI-detector, calibration standard polystyrene.

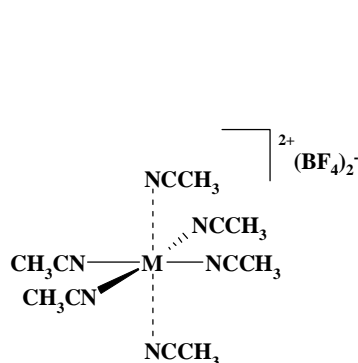
^bthe remaining amount is 1,4-product.

^cMol monomer per Mol catalyst per sec

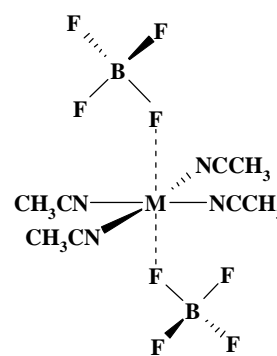
2B.2 Monometallic Solvent Stabilized Transition Metal Cations as Initiators for Cyclopentadiene Polymerization

2B.2.1 Introduction

In chapter 2B.1 we have shown that these catalytic applications are not limited to $[\text{Mo}_2]^{2+}$ complexes coordinated by acetonitrile and acetato ligands. Several other dimeric systems containing molybdenum and rhodium central atoms are also active initiators for the polymerization of cyclopentadiene at room temperature. Crucial for the catalytic activity is the coordination sites at equatorial positions occupied by very weakly coordinating solvent molecules, e.g. acetonitrile. It has also been found that at least two monomeric complexes, namely $[\text{Cr}(\text{NCCH}_3)_4][\text{BF}_4]_2$ (see Chapter 2B.1) and $[\text{Pd}(\text{NCCH}_3)_4][\text{BF}_4]_2$ ^[1] are also active as initiators in the diene polymerization.



M = V(II) (31)



M = Cr(II) (30); Mn(II) (32); Fe(II) (33); Co(II) (34);
Ni(II) (35); Pd(II) (36); Cu(II) (38); Zn(II) (39).

Complexes 30-39

Then the scope was extended to other divalent monomeric acetonitrile stabilized compounds shown above as well as a Cu^{I} salt, $[\text{Cu}(\text{CH}_3\text{CN})_4][\text{BF}_4]$ and found that many of these compounds are excellent initiators in the cationic polymerization, taking the polymerization of cyclopentadiene as example.

2B.2.2 Results and Discussion

The polymerization of cyclopentadiene initiated by the complexes **31-39** at room temperature with an initiator:monomer ratio of usually *ca.* 1:1800 or 1:3600, respectively, has been examined. $[\text{Co}(\text{NCCH}_3)_4][\text{BF}_4]_2$ (**34**) was selected as an example to examine the reaction conditions in more detail. The obtained results were compared with data already available from the chapter 2B.1 and are summarized in Table 2B.2A, Figure 2B.2A and Figure 2B.2B.

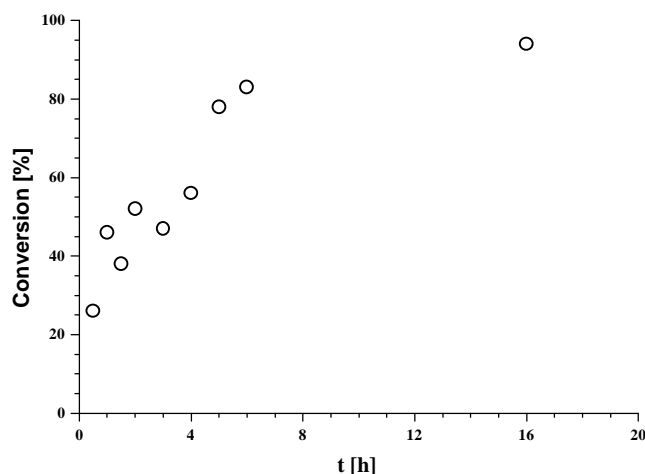


Figure 2B.2A: Dependence of the conversion of cyclopentadiene ($c_{o(\text{Cp})} = 2.27 \text{ mol/L}^{-3}$) on the reaction time (initiator: $[\text{Co}(\text{NCCH}_3)_4][\text{BF}_4]_2$ (**34**), $c_{\text{I}} = 0.000625 \text{ mol/L}$; $T = 25 \text{ }^\circ\text{C}$; solvent: CH_2Cl_2).

The preparation of the initiators has been performed according to modified literature procedures as described in the experimental part. It can be assumed that the examined complexes exist as $[\text{M}(\text{NCCH}_3)_6]^{2+}$ cations in solution ^[2, 3-9]. In most of the cases two of the acetonitrile ligands can be removed very easily in oil pump vacuum according to elemental analyses and thermogravimetry (TG)^[8] examinations. However, even upon prolonged drying (days) in oil pump vacuum the removal of more than two acetonitrile ligands is nearly impossible. The elemental analyses that are obtained after drying the samples in oil pump vacuum for several hours usually show complexes of the composition $[\text{M}(\text{NCCH}_3)_4](\text{BF}_4)_2$. Only in the case of the vanadium complex **31** the composition $[\text{M}(\text{NCCH}_3)_6](\text{BF}_4)_2$ remained unchanged even after prolonged drying in oil pump vacuum at room temperature.

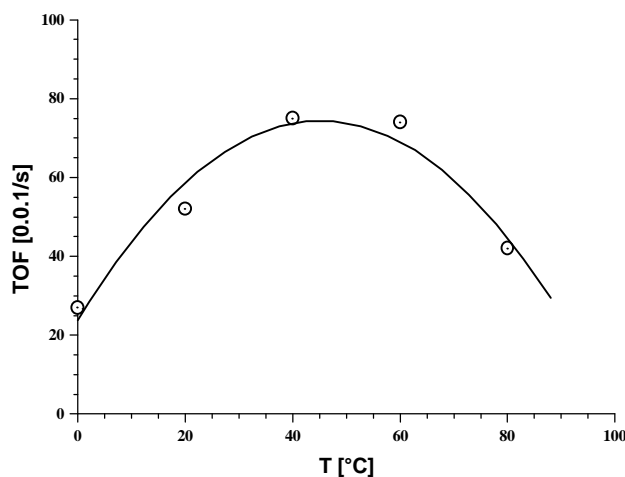


Figure 2B.2B: Polymerization of cyclopentadiene – dependence of the turnover frequencies (TOFs, calculated after 16 h reaction time) on the reaction temperature (initiator: $[\text{Co}(\text{NCCH}_3)_4][\text{BF}_4]_2$ (**34**)). Exp. Conditions: see Table 2B.2A.

The solvent- and initiator concentration dependence of the yield is in the case of the compounds **30-39** very similar to those of the bimetallic solvent stabilized transition metal compounds that have been examined in chapter 2B.1. Polar non-coordinating solvents e.g. CH_2Cl_2 are the most useful solvents in order to obtain good product yields. The steric bulk of the coordinating nitrile ligands seem to have no significant influence on the polymerization, as it was observed in the case of the bimetallic complexes which have been explored in chapter 2B.1. Acetonitrile, pivalonitrile, and benzonitrile ligands coordinated to a $\text{M}(\text{II})^{2+}$ center do not change the product yield significantly. The initiator:substrate ratio was kept on a level (usually *ca.* 1:1800) on which only the most active systems reached 100 % conversion. In order to get a closer insight into their activity differences the most active systems (Mn^{2+} , Fe^{2+} , Co^{2+}) were examined with initiator:substrate ratios in the range of *ca.* 1:3600 – 1:36000 (Table 2B.2A).

While $[\text{V}(\text{NCCH}_3)_6][\text{BF}_4]_2$ is completely inactive as initiator in the cyclopentadiene polymerization and $[\text{Ni}(\text{NCCH}_3)_4][\text{BF}_4]_2$ shows only very little activity, most of the other $[\text{M}(\text{NCCH}_3)_4][\text{BF}_4]_2$ complexes are of comparable or even higher activity than the dimeric $[\text{M}_2(\text{NCCH}_3)_{10}][\text{BF}_4]_4$ compounds ($\text{M} = \text{Mo}, \text{Rh}$) which were examined in the last chapter.

The activity of the monomeric complexes, described by the TOFs (TOF = Turn Over Frequency) correlates very well with the predicted ligand field stabilization energy of octahedral cations (Figure 2B.2C) ^[10, 11]. Low ligand field stabilization energy indicates a weak metal-ligand interaction and therefore allows an easy exchange of the original ligands.

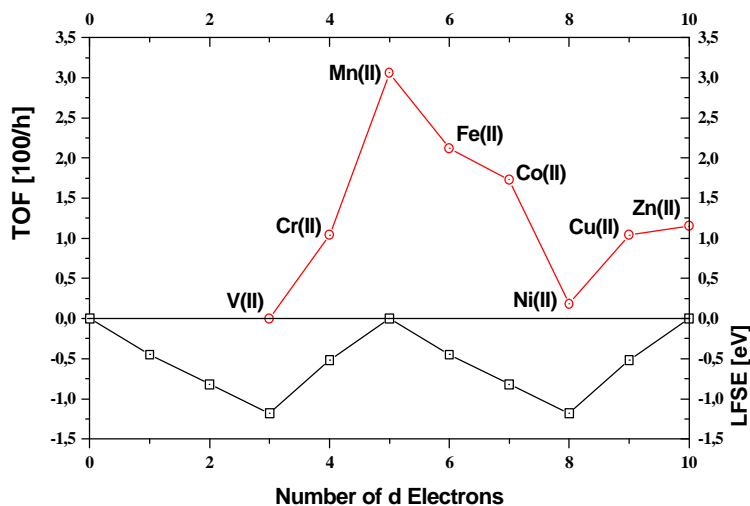


Figure 2B.2C: Polymerization of cyclopentadiene – turnover frequencies (TOFs) and predicted ligand field stabilization energies (LFSEs) ^[11] as a function of the number of d electrons for octahedrally coordinated transition metal cations.

This stabilization energy should be highest for the V^{2+} and Ni^{2+} complexes and smallest for the Mn^{2+} and Zn^{2+} -complexes (no stabilization). Consistently the Mn^{2+} -complexes **32** and **32b** are the most active ones (depending also on the coordination ability of the counter anion, see below), the Ni^{2+} -complex **35** and the V^{2+} -complex **31** show (nearly) no initiator activity. This correlation shows that the complexes with the weakest metal-nitrile interaction are the most active initiators. The easier it is to replace the acetonitrile-ligands by substrate molecules the faster the reaction can proceed. Therefore the rate-determining step of the reaction seems likely to be the replacement of a nitrile ligand by a cyclopentadiene molecule.

The initiator activity is also in good accord with the thermal stability regarding nitrile ligand loss of the initiator complexes. $Ni(II)^{2+}$ and $V(II)^{2+}$ -complexes have been found to be the most

(thermally) stable complexes^[8]. Despite the observed differences are rather small (only ca. 15 K between the thermal decomposition onset of the most and the least stable complex), the readiness of the M^{2+} -complexes for exchanging ligands surely has a crucial influence on the catalytic performance. It is therefore assumed that the replacement of one of the original ligands by a cyclopentadiene molecule is probably the initial step for the cyclopentadiene polymerization.

This view is supported by the influence of the counter ion on the reaction rate. While more strongly coordinating counter ions e. g. BPh_4^- in complex **32a** clearly hamper the polymerization, non coordinating counter ions such as $TFPB^-$ ($TFPB^-$ = tetrakis[3,5-bis(trifluoromethyl)phenyl]borate) in **32b** accelerate the reaction significantly. Despite all TOFs summarized in Table 2B.2A refer to 16 h reaction time it has been observed the reaction to be virtually complete after significantly less than 1 h using derivative **32b** as initiator. This raises the “real TOF” by at least one order of magnitude in comparison to the TOF given in table 2B.2A. The TOF of complex **32b** is therefore at least two orders of magnitude higher than that of complex **32**, containing BF_4^- as the counter ion and three orders of magnitude in comparison to the BPh_4^- compound **32a**.

A more detailed examination of the reaction behavior of the Co^{2+} -complex **34** shows no obvious induction period (see Figure 2B.2A). The conversion is very quick within the first hours and then slows down as most of the substrate is consumed. The TOFs given in table 2B.2A can therefore be regarded as lower limits for the real turnover frequencies, which must be considerably higher.

The initiator activity is also dependent on the reaction temperature. At 0°C the activity is low. An optimum is reached above room temperature at ca. 40 °C. At this temperature the ligand exchange velocity in solution is very high as NMR-measurements of closely related diamagnetic complexes indicate^[2,12,13]. Below room temperature the ligand-metal interaction is increasingly stronger and exchange reactions are being hindered. Above 50 °C the activity starts already to decline, possibly due to beginning initiator decomposition (Figure 2B.2B). An additional explanation for the lower activity can be a competition between substrate and dicyclopentadiene for free coordination sites. Dicyclopentadiene is formed by a Diels-Alder reaction at higher temperatures. Experiments have shown that dicyclopentadiene acts as efficient inhibitor for the polymerization of cyclopentadiene.

Polymerization of cyclopentadiene initiated by low concentrations of less active transition metal complex leads to white air sensitive plastics that are soluble in THF. Higher concentrations of the same initiator compounds or the use of compounds of higher activity as initiators usually leads to crosslinking and accordingly to insoluble products. A comparison of the products derived by the classical cationic polymerization pathway ($\text{Et}_2\text{AlCl}/\text{H}_3\text{C}-\text{C}_6\text{H}_4-\text{CH}_2\text{Cl}_2$, *n*-hexane, $-80\text{ }^\circ\text{C}$) to the polymers derived by polymerization with transition metal complex cations shows that the latter cases produce a significantly higher percentage of 1,2- cyclopentadiene units in comparison to 1,4 units ($^1\text{H-NMR}$). Indications for the appearance of 1,3-cyclopentadiene units or other byproducts have not been found. This can be due to the stronger ion pair separation at the active chain end ^[14a-c]. In the examined case the weaker ion pair separation is due to the weaker coordination capability of the BF_4^- in comparison to $\text{AlEt}_2\text{Cl}_2^-$, the stronger solvent polarity of methylene chloride in comparison to *n*-hexane, and especially the higher reaction temperature.

Table 2B.2A: Overview on the catalytic results gained by utilizing complexes **30-39** as initiators for the cyclopentadiene polymerization. (Reaction time = 16 h, temperature = 25 °C, solvent = CH₂Cl₂, reaction volume = 40 mL)

No.	Complex ^a	c(Init.) [mol/L]	c ₀ (Cp) [mol/L]	C ₁ /C _{Cp}	Yield [%]	M _n (GPC) ^b	M _w (GPC) ^b	M _w /M _n	1,2-prod. [%] ^c	TOF ^d [10 ⁻² s ⁻¹]
30	[Cr(AN) ₄][BF ₄] ₂	0.00125	2.27	1:1816	92	14800	33400	2.25	44	
31	[V(AN) ₆][BF ₄] ₂	0.00125	2.27	1:1816	0	0	0	-	-	0
32	[Mn(AN) ₄][BF ₄] ₂	0.000625	2.27	1:3632	100	24800	67000	2.70	43	6.3
32	[Mn(AN) ₄][BF ₄] ₂	0.000313	2.27	1:7264	67	_e	_e	-	_e	8.5
32a	[Mn(AN) ₄][BPh ₄] ₂	0.000625	2.27	1:3632	10	_f	_f	-	_e	0.6
32b	[Mn(AN) ₆][TFPB] ₂	0.000063	2.27	1:36320	100	_e	_e	-	_e	63
33	[Fe(AN) ₄][BF ₄] ₂	0.000625	2.27	1:3632	94	4600	11200	2.43	42	5.9
33a	[Fe(AN) ₄][BPh ₄] ₂	0.000625	2.27	1:3632	< 5	_f	_f	-	_e	< 0.3
34	[Co(AN) ₄][BF ₄] ₂	0.000625	2.27	1:3632	76	36800	170000	4.62	45	4.8
35	[Ni(AN) ₄][BF ₄] ₂	0.00125	2.27	1:1816	15	_f	_f	-	_e	0.5
36	[Pd(AN) ₄][BF ₄] ₂	0.00125	2.27	1:1816	66	G	g	-	_e	2.1
37	[Cu(AN) ₄][BF ₄]	0.00125	2.27	1:1816	0	0	0	-	-	0

Table 2B.2A *continued*

No.	Complex ^a	c(Init.) [mol/L]	c _o (Cp) [mol/L]	C _l /C _{Cp}	Yield [%]	M _n (GPC) ^b	M _w (GPC) ^b	M _w /M _n	1,2-prod. [%] ^c	TOF ^d [10 ⁻² s ⁻¹]
38	[Cu(AN) ₄][BF ₄] ₂	0.00125	2.27	1:1816	91	18800	41900	2.23	38	2.9
39	[Zn(AN) ₄][BF ₄] ₂	0.00125	2.27	1:1816	100	29900	73500	2.46	43	3.2

^a AN = acetonitrile; ^b determined by RI-detector, calibration standard polystyrene; ^c the remaining amount is 1,4-product; ^d Mol monomer per Mol catalyst per sec; ^e not determined; ^f oily, oligomeric products were obtained;

^g high gelation.

2B.3 Synthesis and Characterization of MCM-41-Supported Dimolybdenum Complexes

2B.3.1 Introduction

A broader variety of quadruply bonded dimolybdenum(II,II) $[\text{Mo-Mo}]^{4+}$ complexes as initiators for cationic polymerization of cyclopentadiene were explored and it was shown that some of them exhibit excellent activity. Fixing of such dimolybdenum catalysts on carrier materials to get defined heterogeneous catalysts and to examine the catalytic activity of the resulting catalysts was performed ever since the beginning of exploration of such type of complexes as catalysts or catalytic precursors for organic transformations.^[1] For instance, McCann and his coworkers^[1, 2] have anchored *cis*- $[\text{Mo}_2(\text{Ac})_2(\text{MeCN})_6][\text{BF}_4]_2$ and $[\text{Mo}_2(\text{MeCN})_{10}][\text{BF}_4]_4$ on the surface of amorphous silica and have explored the activity of the formed heterogeneous complexes for cationic polymerization of cyclopentadiene and dicyclopentadiene. However, these materials were not well characterized and there was no direct physical evidence for the exact nature of the final dimolybdenum species on the surface, that is, whether the Mo–Mo bond was retained (as observed for $[\text{Mo}_2(\text{Ac})_4]-\text{SiO}_2$ ^[3]) or broken to give mononuclear species (as reported for $[\text{Mo}_2(\eta\text{-C}_3\text{H}_5)_4]-\text{SiO}_2$ ^[4]).

There is now considerable interest in the application of the new generation of mesoporous siliceous and nonsiliceous oxides as catalyst support materials^[5]. MCM-41 is one member of this family^[6]. A generally accepted structural model for MCM-41 materials consists of a hexagonal arrangement of cylindrical pores embedded in a matrix of amorphous silica. The pore diameters are tunable in the range 20–100 Å and the best materials have high surface areas ($1000 \text{ m}^2 \cdot \text{g}^{-1}$), high pore volumes ($1 \text{ cm}^3 \cdot \text{g}^{-1}$) and very narrow pore size distributions. They therefore have properties intermediate between those of amorphous refractory oxides and microporous crystalline molecular sieves. Like the commonly used silica and alumina supports, the inner surfaces of MCM-41 are covered with nucleophilic silanol groups which enable the immobilization of transition metal catalysts by direct grafting with organometallic and transition metal complexes.

In this chapter the heterogenization of the dimolybdenum complexes $[\text{Mo}_2(\text{MeCN})_{10}][\text{BF}_4]_4$, $[\text{Mo}_2(\text{Ac})_2(\text{MeCN})_6][\text{BF}_4]_2$ and $[\text{Mo}_2(\text{Ac})_2(\text{dppa})_2(\text{MeCN})_2][\text{BF}_4]_2$ on the surface of purely siliceous MCM-41 was performed and the supported materials have been characterized by

elemental analysis, powder X-ray diffraction (XRD), N₂ adsorption studies, FTIR and solid-state magic angle spinning (MAS) NMR (¹³C, ²⁹Si, ³¹P) spectroscopy.

2B.3.2 Results and Discussion

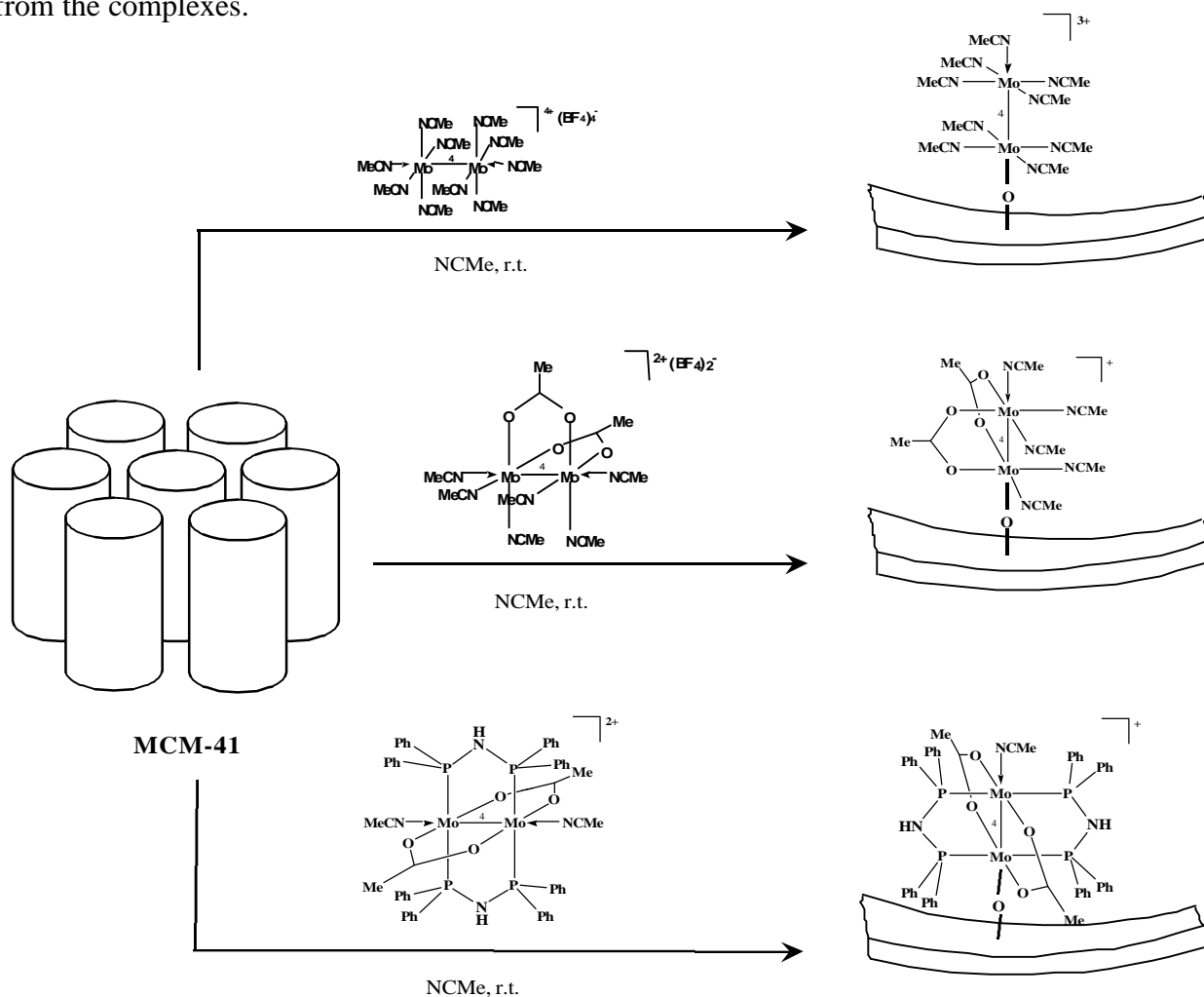
2B.3.2.1 Synthesis and Textural Characterization

The supported materials, [Mo₂(MeCN)₁₀][BF₄]₄-MCM-41 (**20**/MCM-41), [Mo₂(Ac)₂(MeCN)₆][BF₄]₂-MCM-41 (**22**/MCM-41) and [Mo₂(Ac)₂(dppa)₂(MeCN)₂][BF₄]₂-MCM-41 (**40**/MCM-41), were prepared by diffusion of an excess of the complex salts [Mo₂(MeCN)₁₀][BF₄]₄ (**20**), [Mo₂(Ac)₂(MeCN)₆][BF₄]₂ (**22**), and [Mo₂(Ac)₂(dppa)₂(MeCN)₂][BF₄]₂ (**40**)^[7], into calcined and dehydrated MCM-41 in dry acetonitrile at room temperature. The powders were washed repeatedly with acetonitrile to remove unreacted **20** (deep blue), **22** (red) and **40** (red-purple).

When isolated and dried in vacuum at ambient temperature, **20**/MCM-41 is light blue but the color slowly changes to blue-violet over a period of several days to a few weeks storage under a nitrogen atmosphere at room temperature. Material **22**/MCM-41 is initially dark pink-purple and this color is maintained with storage under a nitrogen atmosphere. In contrast, McCann and co-workers obtained purple and brown products after reacting **20** and **22** respectively with silica in acetonitrile for 7–10 days^[8]. Both **20**/MCM-41 and **22**/MCM-41 are very unstable and exposure to air results in transformation to brown-grey powders within several minutes. This parallels the behavior of the precursor complexes **20** and **22** which decompose to brownish residues when exposed to air^[7, 9]. When isolated, **22**/MCM-41 is pink but the color gradually changes to pink–light brown over a period of several days to weeks storage under nitrogen at ambient temperature. At any stage the powder is sensitive and when exposed to air becomes grey within a few hours. This is in marked contrast to the precursor complex **40**, which is relatively air and moisture insensitive.

Elemental analysis indicated that **20**/MCM-41, **22**/MCM-41 and **40**/MCM-41 contained 2.36, 3.62 and 2.21 mass% Mo respectively. It follows that the surface coverage of Mo atoms in these materials is approximately in the range 2.9×10^{-25} mol/nm² (0.17 Mo atoms per nm²) to 4.7×10^{-25} mol/nm² (0.28 Mo atoms per nm²) respectively. With the molybdenum-molybdenum bond intact, the high end of this range corresponds to a surface coverage of one dimolybdenum species per 700 Å². The surface-fixed species are therefore isolated and well dispersed on the silica

surface, a distinct advantage as far as supported catalysts are concerned. McCann *et al.* did not report loadings or any structural characterization for their SiO₂-fixed Mo-Mo complexes **20** and **22**^[2]. It was however inferred from catalytic results that substantial structural and electronic changes had occurred upon binding the salts to the support material. The authors proposed that the surface fixation occurred at pendant silanol groups upon removal of labile NCCH₃ ligands from the complexes.



The colors of complexes **20**, **22**, **40** get lighter when the complexes are supported on MCM-41. This moderate color change shows that the structures of the compounds do not undergo significant changes during the fixation process, as the colors of (Mo₂)⁴⁺-derivatives are very sensitive to changes of the ligand environment^[10]. The replacement of two equatorial acetonitrile ligands by one acetamido substituent in the case of compound **20**, for example,

changes the color from deep blue to red-violet^[11]. However, exchanges of axial ligands are of less importance for the colors of the complexes (see Chapter 2A). This implies that the reaction of the complexes with surface OH groups of MCM-41 either involves only the replacement of axial nitrile ligands or not of more than one equatorial nitrile molecule. This would suggest a relatively weak coordination of the complexes to the MCM-41 surface (Scheme 2B.3A).

2B.3.2.2 Powder XRD

The XRD pattern of the parent calcined (pristine) MCM-41 contains the characteristic and intense low angle peak at $d = 35.74 \text{ \AA}$ which can be indexed as the d_{100} reflection on a hexagonal unit cell ($a = 2d_{100}/\sqrt{3} = 41.27 \text{ \AA}$, Figure 2B.3A). The pattern also displays a broad secondary feature at about $4.6^\circ 2\theta$ where (110) and (200) reflections would be expected for a hexagonally ordered material such as MCM-41. The absence of resolved peaks indicates that any structural order of the material did not extend over a long range. A very similar result was obtained by Schmidt *et al.* for a purely siliceous MCM-41 prepared as in this work using the surfactant $[(C_{14}H_{29})NMe_3]Br$ ^[12].

The (100) reflection practically disappears on derivatization with the complex $[Mo_2(MeCN)_{10}][BF_4]_4$ (**20**) (Figure 2B.3A). Identical results were obtained with the other two complexes, $[Mo_2(Ac)_2(MeCN)_6][BF_4]_2$ (**22**) and $[Mo_2(Ac)_2(dppa)_2(MeCN)_2][BF_4]_2$ (**40**). It has been shown that the intensity of the X-ray peaks in derivatized mesoporous solids decreases with decreasing ‘scattering contrast’ and is zero when the scattering power of the silica wall and the pore filling material are similar^[13]. This reduction in X-ray contrast might erroneously be interpreted as a severe loss of crystallinity. A qualitative indication that the pore structure in the [Mo–Mo]-derivatized materials was still intact was obtained after calcination of a sample of MCM-41 derivatized with **20** (air: 540 °C, 24 h) resulted in restoration of the d_{100} peak to almost the same position and intensity as observed for the pristine MCM-41 ($d = 33.57 \text{ \AA}$, $a = 38.76 \text{ \AA}$, Figure 2B.3A). The decrease in the unit cell parameter suggests a strong interaction between the mesoporous walls and the molybdenum centers. A similar observation was reported when hexane solutions of $(O^iPr)_3V=O$ were reacted with a mesoporous, cubic MCM-48 support^[14]. It was suggested that oxovanadium functional groups, multiply coordinated via (Si–O–V) bridges to the walls, could tend to curve the silica walls. In calcined **20**, a pore-size shrinkage could be caused by the generation of isolated MoO_4 and/or polymeric oxomolybdenum species on the

surface. Such species have been structurally characterized previously on the surface of calcined molybdocene-grafted MCM-41^[15]. The formation of these species may also have caused a slight decrease in the long-range order of the material and therefore explain why calcination of compound **20** did not fully restore the intensity of the d_{100} reflection to that observed for pristine MCM-41.

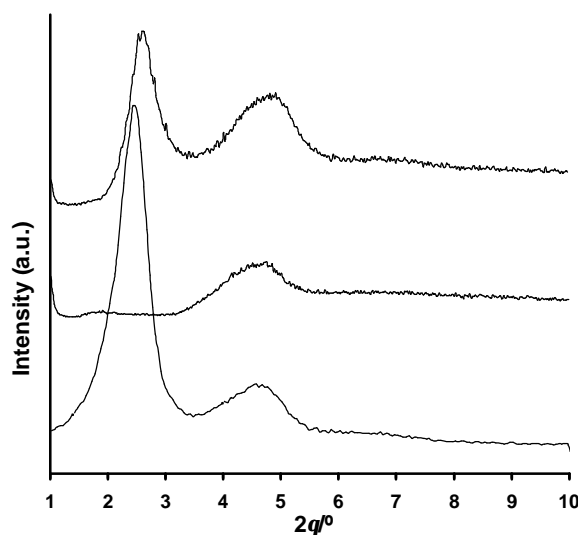


Figure 2B.3A. Powder XRD of MCM-41: (A) as synthesized; (B) functionalized with **20**; (C) **20**/MCM-41 calcined at 540 °C, 24h.

2B.3.2.3 N₂ Adsorption Studies

The N₂ adsorption-desorption isotherm for the pristine MCM-41 at 77K is similar to that reported previously for MCM-41-type mesoporous solids [Figure 2B.3B(a)]. It is defined as a reversible Type IV isotherm in the IUPAC classification^[16], and until now has only been encountered for MCM-41 materials^[12,17]. At low relative pressures ($P/P_0 \leq 0.3$) the adsorbed volume increases linearly with increasing pressure – this region corresponds to a monolayer-multilayer adsorption on the pore walls. Between $P/P_0 = 0.3$ and 0.4 there is a sharp increase in the adsorbed volume, attributed to capillary condensation. At higher relative pressures multilayer adsorption takes place on the external surface, resulting in a gradual linear increase of the adsorbed volume. The BET specific surface area was calculated as 1035 m²·g⁻¹, with the cross-sectional area of a N₂ molecule taken as 16.2 Å².

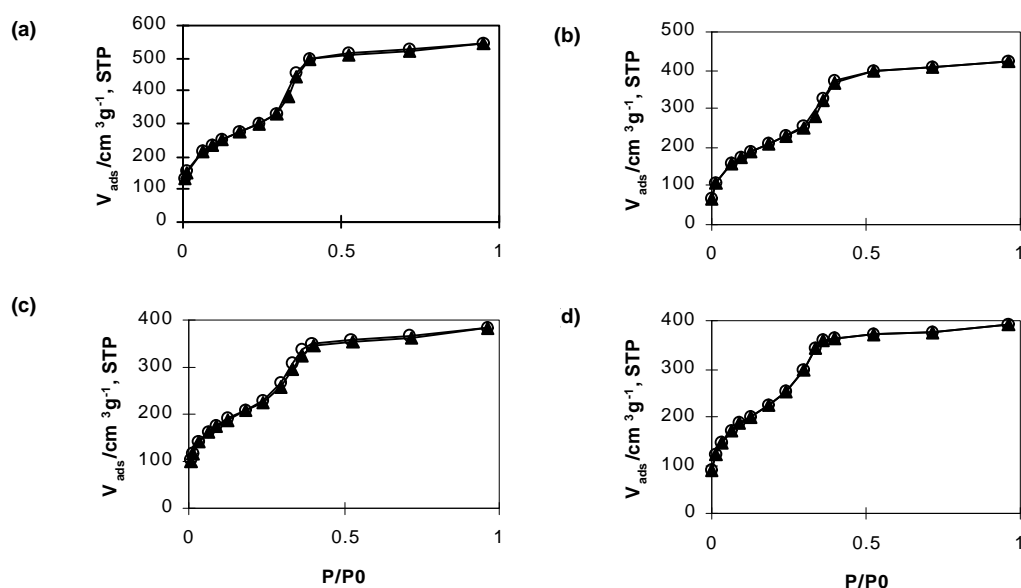


Figure 2B.3B. N_2 adsorption-desorption isotherms recorded at 77K of MCM-41 samples: (a) as synthesized; (b) functionalized with $[Mo_2(MeCN)_{10}][BF_4]_4$; (c) functionalized with $[Mo_2(Ac)_2(MeCN)_6][BF_4]_2$; (d) functionalized with $[Mo_2(Ac)_2(dppa)_2(MeCN)_2][BF_4]_2$. Triangles denote adsorption and circles correspond to desorption.

Reversible Type IV isotherms similar to the pristine MCM-41 were obtained for the three functionalized solids, providing strong evidence that the mesoporous structure of the silica support was retained throughout the grafting process and that the channels remained accessible [Figure 2B.3B(b–d)]. The BET specific surface areas were calculated as $795 \text{ m}^2 \cdot \text{g}^{-1}$, $780 \text{ m}^2 \cdot \text{g}^{-1}$ and $880 \text{ m}^2 \cdot \text{g}^{-1}$ for **20**/MCM-41, **22**/MCM-41 and **40**/MCM-41 respectively. The main difference between these isotherms and that of the starting material is in the limiting uptake at high P/P_0 . For example, the total volumes of adsorbed N_2 at 77 K and $P/P_0 = 0.6$ are 0.74, 0.57, 0.51 and $0.53 \text{ cm}^3 \cdot \text{g}^{-1}$ for parent calcined MCM-41, **20**/MCM-41, **22**/MCM-41 and **40**/MCM-41, respectively. This approximate 30% decrease in the total volume of adsorbed N_2 can be attributed to successful grafting of the molybdenum complex fragments on the internal surfaces of the silica support.

To investigate how the dimolybdenum complexes react and bind with the mesoporous silica, the materials have been studied using solid-state MAS NMR (^{13}C , ^{29}Si , ^{31}P) and FTIR spectroscopy.

2B.3.2.4 Solid-State NMR and FTIR Spectroscopy

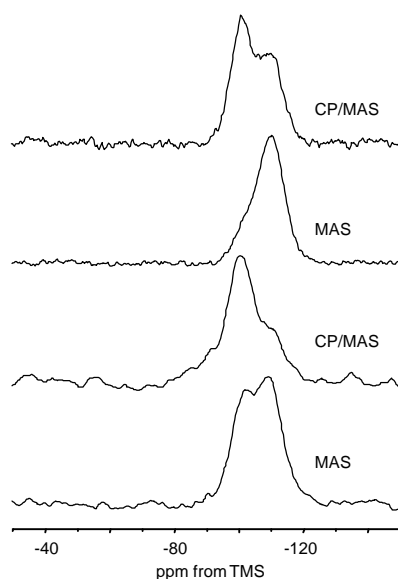


Figure 2B.3C. ^{29}Si CP MAS and MAS NMR of MCM-41 at room temperature. From bottom to top: the first two for MCM-41 as synthesized; the other two for MCM-41 functionalized with $[\text{Mo}_2(\text{MeCN})_{10}][\text{BF}_4]_4$.

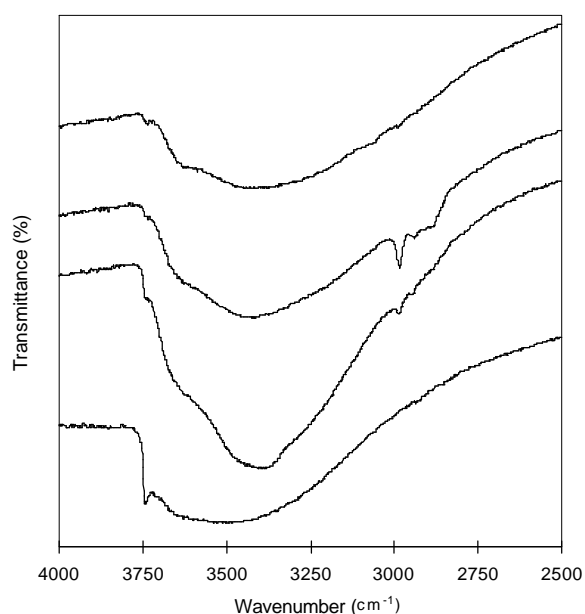


Figure 2B.3D. FTIR spectra in the range $4000\text{--}2500\text{ cm}^{-1}$ of the samples. From bottom to top: (1) Pure calcined MCM-41 (dehydrated at $160\text{ }^\circ\text{C}$ in vacuum for 3 h); (2) MCM-41 functionalized with $[\text{Mo}_2(\text{MeCN})_{10}][\text{BF}_4]_4$; (3) MCM-41 functionalized with $[\text{Mo}_2(\text{Ac})_2(\text{MeCN})_6][\text{BF}_4]_2$; (4) MCM-41 functionalized with $[\text{Mo}_2(\text{Ac})_2(\text{dppa})_2(\text{MeCN})_2][\text{BF}_4]_2$.

Figure 2B.3C shows the ^{29}Si MAS and CP MAS NMR spectra of pristine MCM-41 and $[\text{Mo}_2(\text{MeCN})_{10}][\text{BF}_4]_4\text{-MCM-41}$ (**20**/MCM-41). The ^{29}Si MAS spectrum of the starting material exhibits two broad overlapping peaks at $\delta = -101.3$ and -109.8 , assigned to, respectively, Q_3 and Q_4 units of the silica framework [$\text{Q}_3/\text{Q}_4 = 1.0$, $\text{Q}_n = \text{Si}(\text{OSi})_n(\text{OH})_{4-n}$]. Even given the ca. 8% error inherent in spectral deconvolution, the Q_3/Q_4 population ratio reflects the extent of silanol condensation, indicating the large number of OH groups present at the surface ^[18]. A small amount of Q_2 , faint peak at approximately $\delta = -92$, is also present. The ^{29}Si CP MAS NMR spectrum shows a marked increase in the relative intensity of the Q_2 and Q_3 lines in comparison with the ^{29}Si MAS spectrum, confirming that these silicones are attached to hydroxyl groups. The successful anchoring of the complex **20** at the channel surface is demonstrated by Figure 2B.3C(B). Both ^{29}Si MAS ($\text{Q}_3/\text{Q}_4 = 0.26$) and CP MAS NMR spectra clearly show the diminished relative intensity of the Q_2 and Q_3 peaks, indicating the esterification of the free hydroxyl groups by substitution of the NCCH_3 ligands in the complexes. A decrease in the population of isolated OH groups was further confirmed qualitatively by a decrease in the relative intensity of the sharp IR absorption band at 3742 cm^{-1} associated with free OH groups on the silica surface (Figure 2B.3D) ^[19]. In the OH stretching region a very broad absorption band is also observed at ca. 3600 cm^{-1} , assigned to water and/or hydrogen-bonded SiOH groups. Similar results were obtained for **22**/MCM-41 and **40**/MCM-41.

The ^{29}Si CP MAS NMR spectrum of **20**/MCM-41 shows that there are still a large number of unreacted Q_3 silicon atoms in the composite material. Similar results were obtained with ferrocenyl-modified MCM-41 and MCM-48, prepared *via* ring-opening reaction of the strained [1]ferrocenophane $[\text{Fe}\{(\eta\text{-C}_5\text{H}_4)_2\text{SiMe}_2\}]$ ^[20]. These silanol groups may be contained within the wall framework and sequestered from electrophilic attack. In addition, there may be a large number of hydrogen bonded Q_3 silanols present at the surface, $(\text{SiO})_3\text{Si-OH-OH-Si}(\text{SiO})_3$, which are unreactive to the dimolybdenum complexes. These types of silanols have previously been shown to be inert to silylating agents, for example ^[19]. In a detailed study of the surface chemistry of MCM-41, Zhao *et al.* determined the number of silanol groups/ nm^2 to be 2.5 for a material which was prepared and treated in a similar way to ours (as-synthesized sample calcined at $540\text{ }^\circ\text{C}$ for 24 h in air, then dried at $110\text{ }^\circ\text{C}$ for 24 h in vacuum) ^[19]. Our sample was calcined at the same temperature for 6 h in air, then dehydrated and outgassed at $160\text{ }^\circ\text{C}$ for 3 h in vacuum prior to solvent impregnation of the complexes **20**, **22**, **40**. Zhao *et al.* estimated that 0.7 of the

silanol groups were isolated single hydroxyls and the remainders were hydrogen-bonded silanols with a small contribution from geminal silanols. Furthermore, an FTIR study showed that outgassing temperatures of 200°C or higher were required before dehydroxylation of hydrogen-bonded and geminal SiOH groups took place significantly, to form siloxane bonds and simultaneously more free SiOH groups. Dehydroxylation of single SiOH groups is impossible since they are too far apart (0.5 nm) and such a process would necessarily involve the unfavorable formation of highly strained linked structures.

In the derivatized materials, the surface coverage of Mo atoms is in the range 0.15 to 0.3/nm², somewhat lower than the above value for the concentration of free hydroxyls on the surface of pristine MCM-41. The low loading could be due to steric crowding of the guest complexes which may prevent reaction with a large fraction of surface silanol sites. In general it has been estimated that 8–27% of the silicon atoms in MCM-41 have pendant OH groups and that the average separation of these groups is in the range 5 to 10 Å. It seems unlikely therefore that the dimolybdenum complexes could undergo bipodal anchoring to the silica surface, as suggested by McCann *et al.* for silica-fixed **20** and **22** [2]. Monopodal anchoring, as depicted in Scheme 2B.3A, seems more plausible as the dominant mechanism for surface attachment. A similar conclusion was reached for MCM-41 and MCM-48 modified with the *ansa*-bridged titanocene [SiMe₂{(η⁵-C₅H₄)₂}]TiCl₂ [21]. However, it is worth noting that tripodal anchoring of organometallic fragments to the surface of MCM-41 has been reported, for example with Cp₂TiCl₂-grafted MCM-41 [22].

The ¹³C CP MAS NMR spectrum of [Mo₂(MeCN)₁₀][BF₄]₄-MCM-41 (**20**/MCM-41) exhibits two broad peaks at δ ca. 140 and 120 attributed to NCCH₃ and two peaks at δ = 1.6 and -1.5 attributed to equatorial and axial NCCH₃, respectively [Figure 2B.3E(B)]. Material **20**/MCM-41 is very air and moisture sensitive and on several occasions the sample began to decompose during packing of the NMR rotor and spectrum acquisition, resulting in many broad peaks in the region δ = 3.0 to 0.5. Compared to the ¹³C CP MAS NMR spectrum of the complex [Mo₂(MeCN)₁₀][BF₄]₄ (**20**), these peaks are shifted further upfield. The isotropic chemical shifts of **20** are at δ = 149.5 and 148.0 (NCCH₃, equatorial), around δ = 123.6 (NCCH₃, axial), and δ = 3.5 and 0.8 attributed to the equatorial and axial NCCH₃, respectively [Figure 2B.3E(A)]. The IR spectrum of **20** contains in the nitrile region three stretches at 2322, 2298 and 2266 cm⁻¹ [Figure

2B.3F(A), Table 2B.3A]. These are shifted to significantly lower wavenumbers compared to the corresponding bands for **20** (2359, 2322, 2293 cm^{-1}), indicating a weakening of the bond.

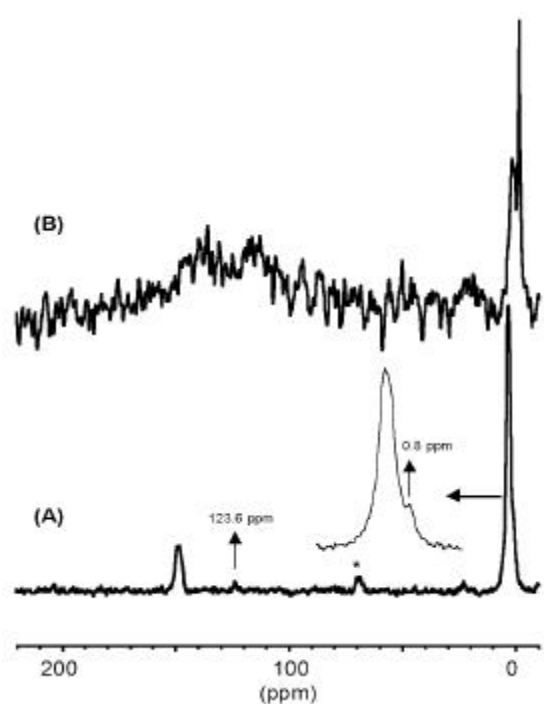


Figure 2B.3E. ^{13}C CP MAS NMR at room temperature: (A) $[\text{Mo}_2(\text{MeCN})_{10}][\text{BF}_4]_4$, 1450 transients; (B) $[\text{Mo}_2(\text{MeCN})_{10}][\text{BF}_4]_4$ -MCM-41, 22352 transients. * denotes spinning sidebands.

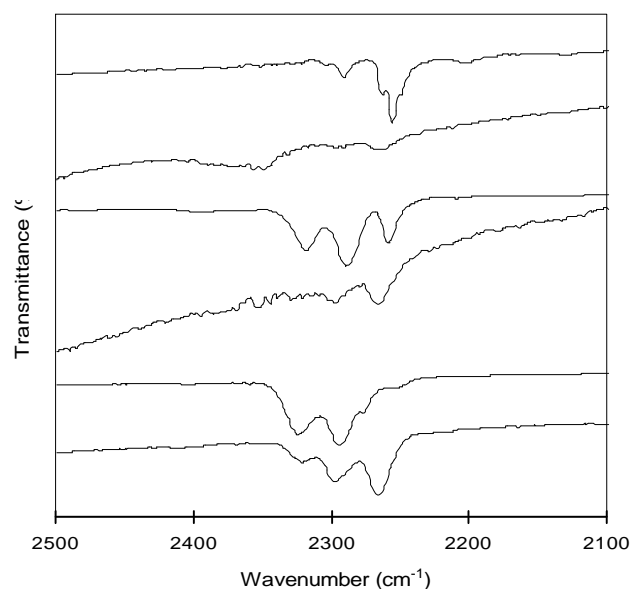


Figure 2B.3F. FTIR spectra in the range 2400–2200 cm^{-1} of the samples. From bottom to top: (1) MCM-41 functionalized with **20**; (2) $[\text{Mo}_2(\text{MeCN})_{10}][\text{BF}_4]_4$ (**20**); (3) MCM-41 functionalized

with **22** (4); $[\text{Mo}_2(\text{Ac})_2(\text{MeCN})_6][\text{BF}_4]_2$ (**22**); (5) MCM-41 functionalized with **40**; (6) $[\text{Mo}_2(\text{Ac})_2(\text{dppa})_2(\text{MeCN})_2][\text{BF}_4]_2$ (**40**).

The room-temperature solid state ^{13}C CP MAS NMR spectrum of $[\text{Mo}_2(\text{Ac})_2(\text{MeCN})_6][\text{BF}_4]_2$ -MCM-41 (**22**/MCM-41) is shown in Figure 2B.3G. Five broad resonances are observed at δ ca. 186, 146, 129, 19 and 2 attributed to C-O, NCCH_3 , O_2CCH_3 and NCCH_3 , respectively. All these signals are broader than those of the related crystalline compound $[\text{Mo}_2(\text{Ac})_2(\text{MeCN})_6][\text{BF}_4]_2$ (**22**). The broadness is due to the range of chemically different environments in which the molecule is located. A large number of scans were required to obtain these spectra. In the ^{13}C CP MAS NMR spectrum of the complex **22** five peaks are observed at $\delta = 187.6$, 148 (doublet), 121 (doublet), 22.7 and 2.1 (multiplet) attributed to C-O, NCCH_3 (equatorial and axial), O_2CCH_3 and NCCH_3 (equatorial and axial), respectively. The IR spectrum of the solid **22**/MCM-41 (KBr matrix) contains the carboxylate for the material $[\text{Mo}_2(\text{Ac})_2(\text{dppa})_2(\text{MeCN})_2][\text{BF}_4]_2$ -MCM-41 (**40**/MCM-41) the bridging acetato complex is clearly identified by $\nu_{\text{asym}}(\text{OCO})$ at 1483 cm^{-1} and the very strong $\nu_{\text{sym}}(\text{OCO})$ at 1440 cm^{-1} in the IR spectrum (Table 2B.3A).

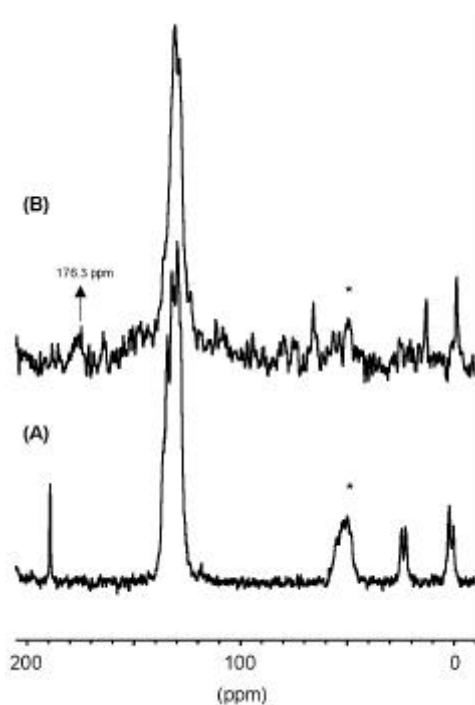
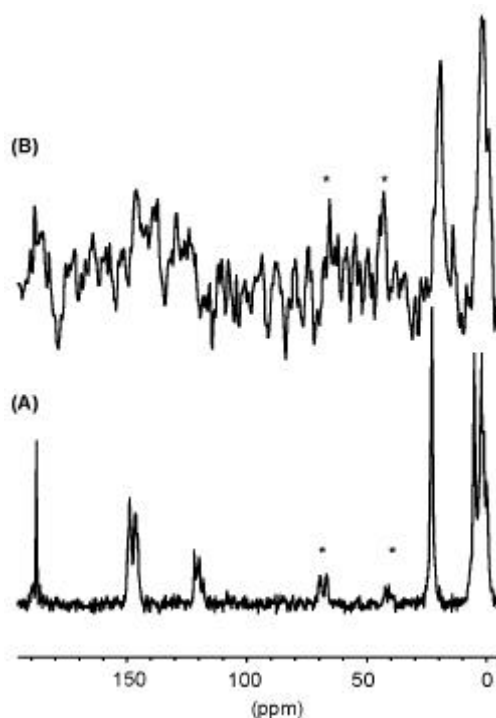


Figure 2B.3G. ^{13}C CP MAS NMR at room temperature: (A) $[\text{Mo}_2(\text{Ac})_2(\text{MeCN})_6][\text{BF}_4]_2$, 14889 transients; (B) $[\text{Mo}_2(\text{Ac})_2(\text{MeCN})_6][\text{BF}_4]_2$ -MCM-41, 16680 transients. * denotes spinning sidebands.

Table 2B.3A. Selected IR data for the complexes **20**, **22**, **40** and corresponding MCM-41-supported derivatives (KBr discs, ν_{\max} in cm^{-1})

	$\nu(\text{C}\equiv\text{N})$	$\nu_{\text{asym}}(\text{CO}_2)$	$\nu_{\text{sym}}(\text{CO}_2)$
$[\text{Mo}_2(\text{MeCN})_{10}][\text{BF}_4]_4$ 20	2359, 2322, 2293, 2276sh, 2253	—	—
$[\text{Mo}_2(\text{MeCN})_{10}][\text{BF}_4]_4$ -MCM-41 20/MCM-41	2322, 2298, 2266	—	—
$[\text{Mo}_2(\text{Ac})_2(\text{MeCN})_6][\text{BF}_4]_2$ 22	2288, 2259, 2319	1501	1444
$[\text{Mo}_2(\text{Ac})_2(\text{MeCN})_6][\text{BF}_4]_2$ -MCM-41 20/MCM-41	2298, 2266	1489	1440
$[\text{Mo}_2(\text{Ac})_2(\text{dppa})_2(\text{MeCN})_2][\text{BF}_4]_2$ 40	2291, 2262sh, 2255, 2249sh	1482	1436
$[\text{Mo}_2(\text{Ac})_2(\text{dppa})_2(\text{MeCN})_2][\text{BF}_4]_2$ -MCM-41 40/MCM-41	2264	1483	1440

**Figure 2B.3H.** ^{13}C CP MAS NMR at room temperature: (A) $[\text{Mo}_2(\text{Ac})_2(\text{dppa})_2(\text{MeCN})_2][\text{BF}_4]_2$ (**40**), 1055 transients; (B) $[\text{Mo}_2(\text{Ac})_2(\text{dppa})_2(\text{MeCN})_2][\text{BF}_4]_2$ -MCM-41 (**40/MCM-41**), 21174 transients. * denotes spinning sidebands.

The presence of the bridging acetates is a clear indication that the molybdenum-molybdenum bond is intact. Weak bands attributable to the NCCH_3 ligands are present at 2298 and 2266 cm^{-1} . Complex **22** exhibits two nitrile vibrations in similar positions (2288 , 2259 cm^{-1}) and a third one at 2319 cm^{-1} , not observed in the spectrum of **22/MCM-41**.

The C–C and C–H vibrations attributed to the dppa ligand are very similar to the initial complex. Only one nitrile vibration was observed in the IR spectrum, at 2264 cm^{-1} . Complex **40** has one main band in this region (2255 cm^{-1}). The ^{31}P MAS spectrum of **40**/MCM-41 (not shown) exhibits a broad singlet for the coordinated dppa ligand at $\delta = 87.3$, shifted downfield slightly from that observed for the free complex $[\text{Mo}_2(\text{Ac})_2(\text{dppa})_2(\text{MeCN})_2][\text{BF}_4]_2$ ($\delta = 82.6$, free dppa exhibits a chemical shift of $\delta = 42.0\text{ ppm}$ ^[23]). The difference between these shifts is small and this suggests that the interaction between the complex **22** and MCM-41 has only a minor effect on the shielding of the phosphorous nuclei. It may be inferred therefore that binding of the complex to the silica surface occurs by substitution of a surface silanol group for an axial acetonitrile molecule in the complex, as depicted in Scheme 2B.3A. It is known that in complexes of the type $\text{Mo}_2(\text{Ac})_2(\text{dppa})_2\text{X}_2$ ($\text{X} = \text{Cl}, \text{Br}, \text{I}$) the nature of the axially coordinated halo ligands has little influence on the ^{31}P MAS chemical shifts (the Mo–X distances are comparatively long, indicating only weak Mo–halo interactions) ^[24]. Similarly, in complex **40**, a long axial Mo–N distance indicates that the acetonitrile molecules might very easily be replaced by stronger donors. ^{31}P MAS NMR studies of **40**/MCM-41 also suggested that one phosphorus-containing by-product is formed ($\delta = 29.3$) possibly attributing to a decomposition product (e.g. phosphine oxide).

The ^{13}C CP MAS NMR spectrum of **40**/MCM-41 exhibits a weak broad peak at 176.2 (C–O), two sharp resonances at 130.9 and 128.7 (phenyl groups) and two well-defined singlets at 13.0 (CH_3COO) and -1.4 (NCCH_3).

2B.4 XAFS Analysis and Catalytic Activity of MCM-41-supported Dimolybdenum Complexes Containing Metal-Metal Bonds

2B.4.1 Introduction

In the last chapter, three dimolybdenum compounds, $[\text{Mo}_2(\text{AN})_{10}](\text{BF}_4)_4$, $[\text{Mo}_2(\text{Ac})_2(\text{AN})_6](\text{BF}_4)_2$, and $[\text{Mo}_2(\text{Ac})_2(\text{dppa})_2(\text{AN})_2](\text{BF}_4)_2$, immobilized in the micelle-templated silica MCM-41, was characterized by MAS NMR (^{13}C , ^{29}Si), FTIR, X-ray diffraction and N_2 adsorption. These studies indicated that the quadruply bonded Mo_2 complexes were attached to the surface largely unchanged by a mechanism involving the displacement of labile acetonitrile ligands, probably in the axially coordinated position, from the complexes by reaction with pendant silanol groups.

In this chapter, the MCM-41-supported dimolybdenum complexes were further analyzed by molybdenum K-edge X-ray absorption fine structure (XAFS) spectroscopy. This technique has been used successfully to study related systems such as oxide-grafted molybdenum catalysts derived from $\text{Mo}_2(\text{Ac})_4$.^[1, 2] In addition, the derivatized materials have been tested as initiators for the polymerization of methylcyclopentadiene.

2B.4.2 Results and Discussion

In addition to the three immobilized dimolybdenum complexes, the acetamidato analogue $[\text{Mo}_2(\mu\text{-CH}_3\text{CONH})_2(\text{AN})_4](\text{BF}_4)_2/\text{MCM-41}$ (**21**/MCM-41), prepared using the same general method, was also analyzed.

2B.4.2.1 XAFS Analysis

Mo K-edge X-ray absorption spectra were recorded for $\text{Na}_2\text{MoO}_4 \cdot 2\text{H}_2\text{O}$, $\text{Mo}_2(\text{Ac})_4$, model complexes, and the four grafted MCM materials. After the last spectrum was recorded for each grafted material, the sample was removed and exposed to air at room temperature for 2 hours. EXAFS measurements were then continued for these samples, designated as **20-22**/MCM-41/air and **40**/MCM-41/air, respectively. These experiments were carried out in order to be certain that

the four air-sensitive grafted materials had not undergone decomposition during acquisition of the data.

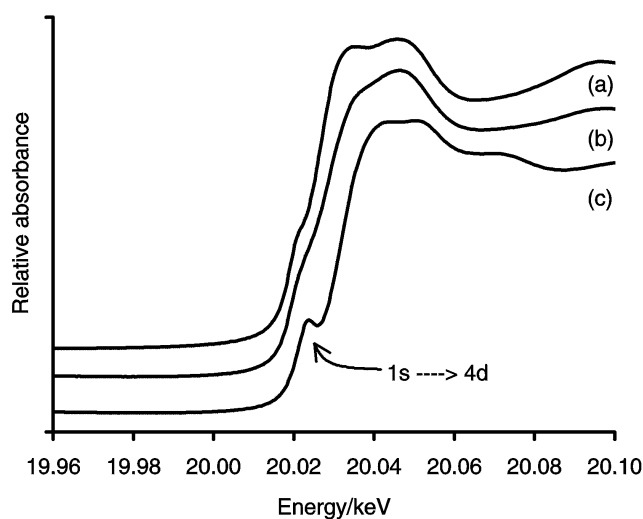


Fig. 2B.4.1 the X-ray absorption near-edge (XANES) data for (a) $[\text{Mo}_2(\text{Ac})_2(\text{AN})_6](\text{BF}_4)_2$ (**22**); (b) **22**/MCM-41; (c) **22**/MCM-41/air.

Fig. 2B.4.1 shows the X-ray absorption near-edge (XANES) data for $[\text{Mo}_2(\text{Ac})_2(\text{AN})_6](\text{BF}_4)_2$ (**22**) and the corresponding grafted material **22**/MCM-41. The two samples show little differences in both amplitude and frequency of the EXAFS oscillations, indicating that the grafting process imposed minor changes in the local structural order around the molybdenum centers. Substantial changes are however evident upon exposure of the grafted material to air. A resolved pre-edge peak is observed that is attributed to a bound state transition ($1s \rightarrow 4d$). Enhancement of this transition has been associated with an increasing number of Mo=O bonds.^[3] The same pre-edge feature is also observed for sodium molybdate, though the absorption is much more intense.

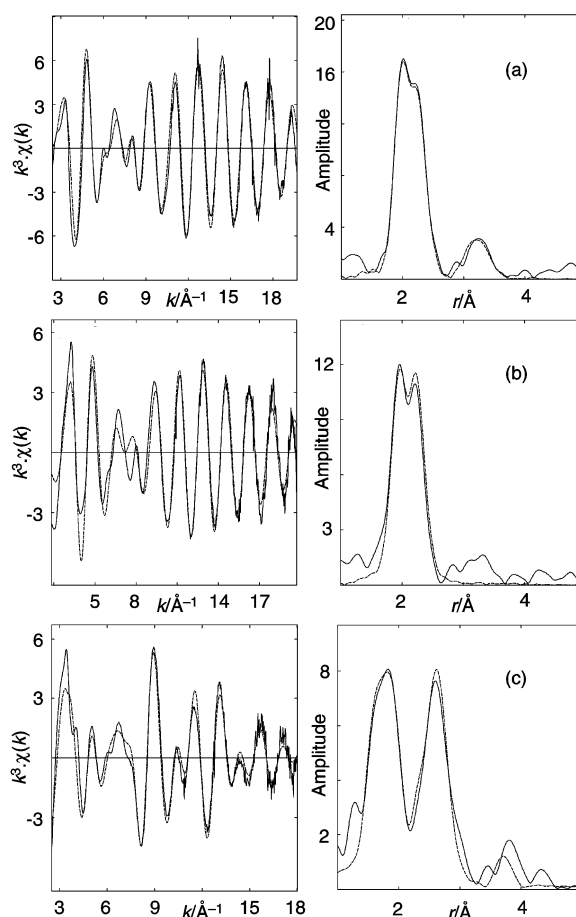


Fig. 2B.4.2 The Mo K-edge EXAFS data for (a) $[\text{Mo}_2(\text{Ac})_2(\text{AN})_6](\text{BF}_4)_2$ (**22**); (b) **22**/MCM-41; (c) **22**/MCM-41/air.

The best fit to the Mo K-edge EXAFS of the tetrafluoroborate salt **22** was obtained with four atomic shells [Table 2B.4.1, Fig. 2B.4.2(a)]. Multiple scattering was included for the Mo–N–C (acetonitrile) unit with the Mo–N–C bond angle set at 180° . The Debye-Waller factor and interatomic distance for the nitrogen shell were fixed and not included in the final refinement, due to high correlations with the corresponding parameters for the shell of two oxygens at 2.07 Å. The refined distances are in agreement with crystallographic values to within 0.01 Å.^[4] On grafting of compound **22** into MCM-41, a simplified model was required for a reasonable fit to the Mo K-edge EXAFS, comprising three oxygens at 2.07 Å and one molybdenum at 2.11 Å [Fig. 2B.4.2(b)]. No acceptable fit could be obtained for a carbon shell corresponding to N-coordinated CH_3CN , and therefore no nitrogen shell was included. The Mo–Mo distance is similar to that for the starting complex **22** and clearly indicates that the Mo–Mo quadrupole bond is retained in the grafted species. The results support the conclusion in chapter 2B.3 that the

complex is attached to the surface largely unchanged by a mechanism involving the displacement of labile acetonitrile ligands, probably in the axially coordinated position, from the complexes by reaction with pendant silanol groups.

Table 2B.4.1: Mo K-edge EXAFS-derived structural parameters for $[\text{Mo}_2(\text{Ac})_2(\text{AN})_6](\text{BF}_4)_2$ (**22**) and grafted **22**/MCM-41

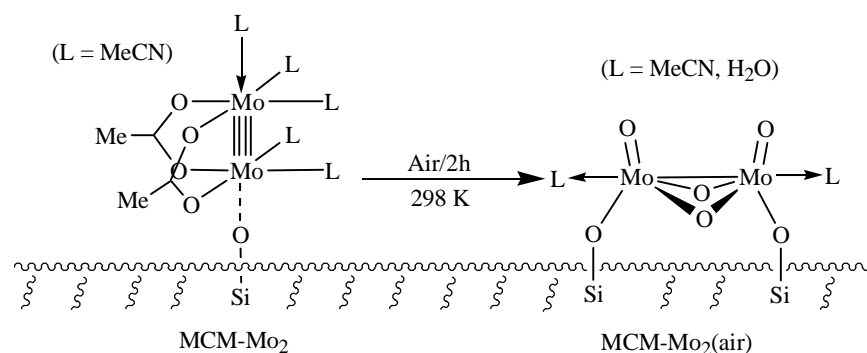
Sample	Atom	CN ^a	$r/\text{\AA}$	$2s^{2b}/\text{\AA}^2$	E_f^c/eV	$R(\%)^d$
22 (3 ^e)	O	2.0(2)	2.069(8)	0.0060(16)	-2.4(5)	22.5
	Mo	1.0(1)	2.131(2)	0.0039(2)		
	N	2	2.12	0.007		
	C	2	3.224(10)	0.0120(19)		
22 /MCM-41 (7)	O	3.0(2)	2.067(6)	0.0046(11)	-12.1(6)	31.0
	Mo	1.0(1)	2.109(4)	0.0050(3)		
22 /MCM-41/air (3)	O	1.5(1)	1.680(3)	0.0061(5)	1.7(5)	31.2
	O	3.0(3)	1.963(4)	0.0121(8)		
	O	1.0(1)	2.134(11)	0.0099(24)		
	Mo	1.0(2)	2.582(2)	0.0088(4)		
	Si	1.0(4)	3.722(22)	0.0111(43)		

^a CN = Coordination number. Values in parentheses are statistical errors generated in EXCURVE. The true errors in coordination numbers are likely to be of the order of 20%; those for the interatomic distances *ca.* 1.5%.^[2a] ^b Debye-Waller factor; s = root-mean-square internuclear separation. ^c E_f = edge position (fermi energy), relative to calculated vacuum zero.

^d $R = (\int[\Sigma^{\text{theory}} - \Sigma^{\text{exptl}}]k^3 dk / \int[\Sigma^{\text{exptl}}]k^3 dk) \times 100\%$. ^e Number of summed scans in parentheses.

As noted above, the grafted material $[\text{Mo}_2(\text{Ac})_2(\text{AN})_6](\text{BF}_4)_2/\text{MCM-41}$ (**22**/MCM-41) is very air-sensitive. Analysis of the Mo K-edge EXAFS of the grafted dimolybdenum species exposed to air revealed that the Mo···Mo distance had increased to 2.58 Å [Fig. 2B.4.2(c)]. This obviously suggests considerable disruption to the Mo–Mo quadruple bond, although the longer distance still allows Mo–Mo bonding. Four other components were included in the final fit: 1.68 Å, 1.96

Å and 2.13 Å Mo–O, and 3.72 Å Mo···Si distances. The Mo–O and Mo–Mo distances point strongly towards the presence of a dioxo-bridged binuclear Mo^V complex, most likely with a single bond between the metal atoms.^[5] For example, the distances are comparable with those for the cysteine complex Na₂[Mo₂O₄(cys)₂]·5H₂O (Mo–O_t = 1.71; Mo–O_b = 1.95, 1.91; Mo–Mo = 2.57 Å).^[6] It is therefore proposed that the mean site can be described as a surface-fixed [Mo₂O₄]²⁺ species (Scheme 2B.4). There is some doubt about the validity of the silicon shell (high statistical errors in the refined structural parameters). However, the Mo···Si distance seems reasonable for Mo–O–Si bonding, and in this case the longer Mo–O interaction at 2.13 Å is assigned to a Si–O oxygen that is trans to the Mo=O bond. In the model the terminal oxo groups on the two Mo atoms bend back away from each other. If they were not bent back, their distance would equal 2.58 Å, which is considerably shorter than the van der Waals contact distance of 2.80 Å. It is interesting to note that a similar binuclear molybdenum species has been generated and characterized on a Al₂O₃ support, but only after a complex series of high temperature reductive and oxidative treatments of a [Mo₂(η³-C₃H₅)₄]-grafted precursor.^[7] The alumina-supported catalyst was highly active for propene metathesis.



Scheme 2B.4

Further experiments will be required to ascertain whether the final dioxo-bridged dimolybdenum surface species represented in Scheme 2B.4 is stable to long-term exposure to air. Interestingly, the results obtained for [Mo₂(Ac)₂(AN)₆](BF₄)₂/MCM-41(**22**/MCM-41) have been confirmed also for the acetamidato analogue [Mo₂(μ-CH₃CONH)₂(AN)₄](BF₄)₂/MCM-41(**42**/MCM-41), prepared in exactly the same way. The EXAFS analysis results for the latter material, including those for the material exposed to air, were remarkably similar to those

obtained for the acetato derivative and point to the presence of the same surface species in the two materials.

The Mo K-edge EXAFS of the tetrafluoroborate salt $[\text{Mo}_2(\text{AN})_{10}](\text{BF}_4)_4$ (**20**) was fitted by a model comprising one molybdenum atom at 2.17 Å, four nitrogen atoms at 2.10 Å, four carbon atoms at 3.21 Å and four carbon atoms at 4.80 Å (Table 2B.4.2). Multiple scattering was included for the Mo–N–C–C unit (equatorially coordinated CH_3CN) with the Mo–N–C bond angle set at 175° and the N–C–C bond angle set at 180°. The EXAFS-derived bond distances are in agreement with the mean crystallographic values (Mo–Mo = 2.18 Å, Mo–N = 2.13 Å).^[8] It was not possible to fit a shell for nitrogen atoms corresponding to axially coordinated CH_3CN (expected at ca. 2.6 Å).

The EXAFS results for $[\text{Mo}_2(\text{AN})_{10}](\text{BF}_4)_4/\text{MCM-41}$ (**20/MCM-41**) are also shown in Table 2B.4.2. It proved to be difficult to obtain a good fit to the data.

Table 2B.4.2: Mo K-edge EXAFS-derived structural parameters for $[\text{Mo}_2(\text{AN})_{10}](\text{BF}_4)_4$ (**20**) and grafted **20/MCM-41**

Sample	Atom	CN	$r/\text{Å}$	$2s^2/\text{Å}^2$	E_f/eV	R (%)
20 (4)	Mo	1.0(1)	2.171(3)	0.0052(3)	0.4(4)	18.6
	N	4	2.104(3)	0.0047(10)		
	C	4	3.206(6)	0.0125(10)		
	C	4	4.801(15)	0.0208(37)		
20/MCM-41	O	4.0(4)	2.113(7)	0.0145(16)	-6.7(7)	33.7
	Mo	1.0(1)	2.174(5)	0.0105(6)		
	Si	1.0(4)	3.241(11)	0.0052(20)		
20/MCM-41/air (6)	O	1.0(1)	1.663(4)	0.0058(8)	2.0(9)	29.0
	O	5.0(4)	2.002(6)	0.0250(11)		
	Mo	1.0(2)	2.542(4)	0.0108(5)		
	Si	1.0(4)	3.719(20)	0.0103(41)		

Air-oxidation of **20**/MCM-41 produced marked changes in the XANES and EXAFS data, comparable to those observed for $[\text{Mo}_2(\text{Ac})_2(\text{AN})_6](\text{BF}_4)_2/\text{MCM-41/air}$ (**22**/MCM-41/air). Thus, a resolved pre-edge feature became apparent, attributed to the formation of Mo=O bonds. The presence of a short Mo–O_t interaction was confirmed by analysis of the Mo K-edge EXAFS (Table 2B.4.2), which also revealed only one Mo–Mo interaction at 2.54 Å. There was some evidence for the presence of a Mo...Si interaction at 3.7 Å. The conclusion from these results is that, as found for the acetato and acetamidato systems, air-oxidation of **20**/MCM-41 results in the formation of a surface-fixed $[\text{Mo}_2\text{O}_4]^{2+}$ species.

2B.4.2.2 Heterogeneous Polymerization of Methylcyclopentadiene

The dimolybdenum complex salts $[\text{Mo}_2(\text{AN})_{10}](\text{BF}_4)_4$ (**20**), $[\text{Mo}_2(\text{Ac})_2(\text{AN})_6](\text{BF}_4)_2$ (**22**) and $[\text{Mo}_2(\text{Ac})_2(\text{dppa})_2(\text{AN})_2](\text{BF}_4)_2$ (**40**) act as initiators for the polymerization of cyclopentadiene and methylcyclopentadiene in homogeneous phase. The activity of the compounds **20** and **22** is significantly higher than that of compound **40**. The reason for this is that, according to the earlier examinations in chapter 2B.1, weakly coordinating equatorial ligands must be present, which can be easily replaced by the substrate, if the latter is applied in significant excess.

It has been shown by McCann *et al.* that systems comprising silica-fixed **20** and **22** are also active under special conditions as initiators in heterogeneous phase.^[9] However, it was completely unclear how the initiator complexes were fixed to the surface and whether or not they changed significantly during the heterogenization process. Since it is now known that how the complexes **20**, **22** and **40** are fixed on the surfaces of MCM materials the consequent step was of course the examination of the activity of the defined hybrid materials as initiators for diene polymerization reactions.

The concentration of the initiators used in the experiments was only 1/300 of the amounts previously used for catalysis in homogeneous phase (initiator:monomer ratio ca. 1:300000) in chapter 2B.1. Methylcyclopentadiene was used due to its higher polymerization reactivity compared to cyclopentadiene.^[10] After 16 hours reaction time with species $[\text{Mo}_2(\text{AN})_{10}](\text{BF}_4)_4/\text{MCM-41}$ (**20**/MCM-41) as the initiator, polymethylcyclopentadiene was obtained with a molecular mass of 95,968 g/mol and a PDI (polydispersity index) of 1.93 (Table 2B.4.3). Considering the low amount of initiator used, the catalyst activity, as reflected in the TOF, is of a comparable order of magnitude as would be expected for the same monomer in homogeneous phase.

As has been observed in homogeneous phase, an increased amount of initiator led to an increased amount of product. However, increasing the initiator amount also led to a higher polydispersity index and a lower molecular mass of polymethylcyclopentadiene. This is in good accord with the expectations: if more initiator molecules are present more polymer chains start growing at the same time, and the reactions are terminated more easily, due to the lower amount of substrate available per initiator molecule. Therefore, the polymer chains are shorter in average and the polydispersity index is higher. Anyway, in comparison with the results obtained in homogeneous phase, the picture is quite similar. Obviously, the initiator activity is not significantly reduced by the heterogenization process.

Table 2B.4.3 Catalytic results with MCM-41-supported $[\text{Mo}_2(\text{AN})_{10}](\text{BF}_4)_4$ (**20**), $[\text{Mo}_2(\text{Ac})_2(\text{AN})_6](\text{BF}_4)_2$ (**22**) and $[\text{Mo}_2(\text{Ac})_2(\text{dppa})_2(\text{AN})_2](\text{BF}_4)_2$ (**40**) as initiators for methylcyclopentadiene polymerization (reaction time = 16 h, temperature = 25 °C, solvent = CH_2Cl_2).

Material	Yield (%)	M_w (GPC)	PDI	TOF/h ⁻¹
20 /MCM-41	7.7	95970	1.93	1450
22 /MCM-41	7.2	55830	3.03	1350
40 /MCM-41	0.5	8485	1.97	100

The results obtained for **20**/MCM-41 have been confirmed with the supported catalysts **22**/MCM-41 and **40**/MCM-41 (Table 2B.4.3). Paralleling the results in homogeneous phase, **22**/MCM-41 is less active than **20**/MCM-41, and **40**/MCM-41 shows very little activity.

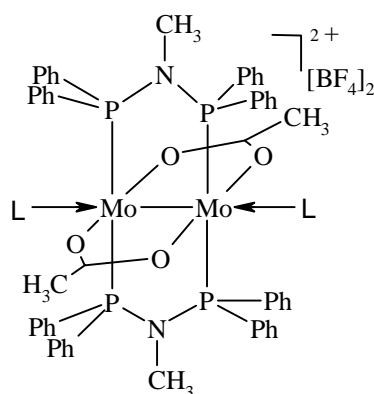
Some additional experiments were performed with $[\text{Mo}_2(\text{AN})_{10}](\text{BF}_4)_4$ /MCM-41(**20**/MCM-41) and $[\text{Mo}_2(\text{Ac})_2(\text{AN})_6](\text{BF}_4)_2$ /MCM-41(**22**/MCM-41) in order to ascertain whether leaching plays a role in the examined cases. Under the usual reaction conditions but without any substrate the supported catalysts were stirred for 16 h. After this time the liquid phase was removed and substrate (methylcyclopentadiene) added, in the excess usually applied for the catalytic reactions. This mixture was stirred for 72 h and then the solvent was removed under vacuum. The remaining white solid was examined with ¹H- and ¹³C-NMR spectroscopy. No polymer was found. The white precipitate consisted of dimers and trimers, which are formed due to Diels-

Alder reactions from the substrate under the conditions applied (no stabilizer was present). It can therefore be concluded that no or at least no significant amounts of **20** or **22** were present in the reaction mixtures. The MCM-41-supported complexes are accordingly stable against leaching under the conditions applied.

In addition to the examinations of these solvent stabilized transition mono- and bimetallic complexes as initiators for polymerization of olefins, some of them have also been tested as catalytic precursors for hydroamination of alkynes, using 6-aminohex-1-yne as a standard substrate. The results showed that no activity of the tested complexes was found with exception of Cu^I salt, **37**, with ca. 80% conversion of 6-aminohex-1-yne to 2-methyl-1, 2-dehydropiperidine.

Chapter 3. Summary

Since the first recognition of the M-M quadruple bond in 1964 by the group of Cotton, the field of multiple bonds between metal atoms has been one of the active areas of modern coordination chemistry ^[1] and, indeed, continues to draw attention from those interested in reactivity, structure, and bonding, as can be seen from the recent discourse on the Ga-Ga triple bond. ^[2] Molecules of the type $[\text{Mo}_2(\mu\text{-O}_2\text{CCR})_2(\text{LL})_2(\text{S})_2][\text{BF}_4]_2$ (R = H, F; LL = a diphosphine; S = acetonitrile) can act as good building blocks for syntheses of other complexes or even polymers since the acetonitriles at the axial positions can be readily displaced by other inorganic or organometallic donor ligands.



L = NCCH₃, **1**; No L, **2**; NC(CH₃)₃, **3**; NCC₆H₅, **4**;

NCC₆H₄-CCH, **5**; NCFe(CO)₂Cp, **9**; Py, **10**;

Py-C(CH₃)₃, **11**; Py-Ph, **12**; Py-CH=CHPh, **13**;

Py-CCH, **14**; Py-CN, **15** (Py = Pyridyl).

L = NCM(CO)₅, M = Cr **6**, Mo **7**, W **8** (no BF₄).

Chart 3.1

In the first part of this work, *trans*-[Mo₂(*m*-O₂CCH₃)₂(dppma)₂(NCCH₃)₂](BF₄)₂, **1**, was employed as a starting material. A variety of ligands with nitrile-functionality and of pyridine derivatives can therefore be introduced by replacing axial acetonitriles, as presented in chart 3.1. While the nitrile ligands act as electron donors, the pyridine derivatives are not only σ -donors but also π -acceptors. The MoMo interaction is slightly weakened, dependent on the donor capabilities of the axial ligands, but the overall influence on the MoMo moiety and the equatorial ligands is comparatively weak in all examined cases. Raman spectroscopy proves to be the most sensitive tool to establish the influence of the axial ligands on the metal-metal interaction. In

comparison with the molecules with Mo-nitrile interactions, the Mo-pyridine associations appear to be unequivocally stronger as can be concluded from the Raman spectra. The ligands 4-ethynylbenzenonitrile ($\text{NCC}_6\text{H}_4\text{C}\equiv\text{CH}$), 4-styrylpyridine ($4\text{-NCC}_5\text{H}_4\text{N}$) and 4-ethynylpyridine ($4\text{-CH}\equiv\text{CC}_5\text{H}_4\text{N}$) seem to be potential good building blocks for organometallic and inorganic polymers.

The species $\text{M}_2(\text{O}_2\text{CCR}_3)_n(\text{PPh}_m\text{Py}_{3-m})_x$ ($\text{M} = \text{Mo}$ or Rh ; $\text{R} = \text{H}$ or F ; $n = 2$ or 3 ; $m = 1$ or 0 ; $x = 1$, or 2) have also been synthesized. *trans*- $\text{Mo}_2(\mu\text{-O}_2\text{CCF}_3)_2(\text{O}_2\text{CCF}_3)_2(\text{PPhPy}_2)_2$ and *trans*- $\text{Mo}_2(\mu\text{-O}_2\text{CCF}_3)_2(\text{O}_2\text{CCF}_3)_2(\text{PPy}_3)_2$ are the first two complexes of this type characterized by X-ray crystallography. Although they have no activity as initiators for polymerization of olefins, this new type of M-M multiple bond complexes is undoubtedly an interesting member of the family of bimetallic multiple-bonded compounds.

Although the applications of Mo-Mo quadruple-bonded complexes as initiators for polymerization and ring-opening metathesis polymerization (ROMP) of olefins have been explored already before^[4], many problems were still completely unclear.

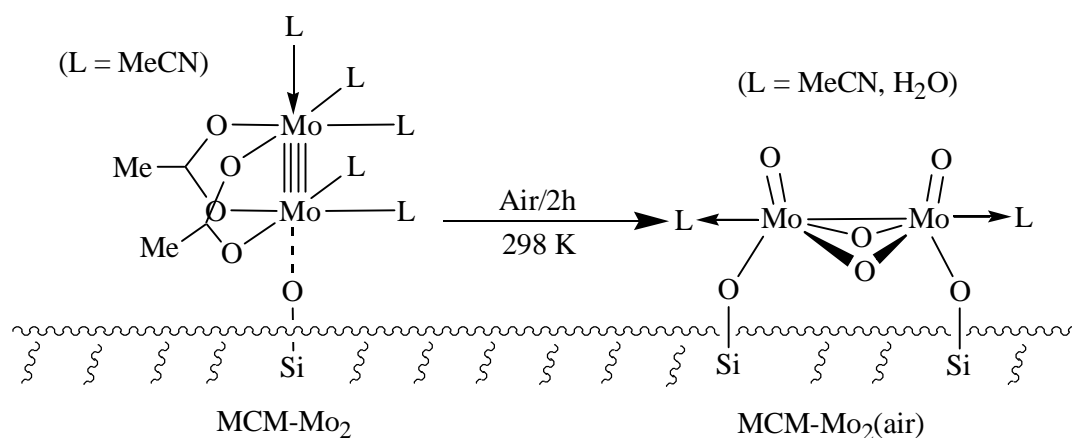
In the second part of this work, in addition to the two dimolybdenum salts, $[\text{Mo}_2(\text{NCCH}_3)_{8-10}][\text{BF}_4]_4$ and $[\text{Mo}_2(\mu\text{-O}_2\text{CCH}_3)_2(\text{NCCH}_3)_6][\text{BF}_4]_2$, many other dimolybdenum salts and $[\text{Rh}_2(\text{NCCH}_3)_{10}][\text{BF}_4]_4$ as well as a mononuclear complex, $[\text{Cr}(\text{NCCH}_3)_4][\text{BF}_4]_2$, were exploited firstly. It was found that the cation charge and the effective charge at the metal center, resp., play a crucial role for the initiator activity. Electron withdrawing ligands improve the activity, whereas electron-donating ligands reduce the catalytic efficiency, if all other parameters are kept unchanged. The yield increases nearly linear with the reaction time, the number average of the molecular weight (M_n) decreases during reaction time. Sterical hindrance by strongly coordinating ligands such as diphosphine ligands strongly reduces the initiator activity. The presence of labile equatorial ligands is of significant importance, too. Axially coordinated nitrile ligands are obviously not sufficient to guarantee catalytic activity. In addition to dimolybdenum complexes, the corresponding dirhodium salt is also active for polymerization of cyclopentadiene. For the polymerization reaction a coordinative cationic reaction mechanism is likely based on the obtained results. The first step of the reaction cannot include an interaction of a cyclopentadiene with the metal-metal multiple bond. It is more likely that an interaction of the substrate with the metal center starts by an attack of the substrate on a free equatorial coordination site at the metal center or by replacement of one of the weakly coordinated nitrile

ligands. The presence of a metal-metal multiple bond, however, seems not to be of importance for the polymerization of cyclopentadiene, since the mononuclear chromium compound, $[\text{Cr}(\text{NCCH}_3)_4][\text{BF}_4]_2$, is as active as the most active one among the explored bimetallic complexes.

The research was therefore extended to other solvent stabilized monometallic complexes of the general molecular formula $[\text{M}(\text{NCCH}_3)_{4-6}][\text{A}]_2$ ($\text{A} = \text{BF}_4^-$; $\text{M} =$ first row transition metal). The results demonstrate that mononuclear transition metal cations in the oxidation state +II can act as efficient initiators of the cyclopentadiene polymerization. The activity of these complexes is in good correlation to their predicted ligand field stabilization energy as a function of the number of d electrons available. Non-coordinating anions such as TFPB^- ($\text{TFPB}^- =$ tetrakis[3,5-bis(trifluoromethyl)phenyl]borate) can significantly improve the TOFs of the polymerization reaction. The results obtained with these monometallic complexes further prove that the initiation of the polymerization reaction is not dependent on the presence of a metal-metal multiple bond interaction. The polymerization process could also involve the nucleophilic attack of a substance on a free coordination site at the metal center or by replacement of one of the weakly coordinated ligands.

No exact structure of quadruply bonded dimolybdenum salts on the silica surfaces has been reported so far. Therefore, the structure of dimolybdenum complexes on the surface of MCM-41 was examined using a variety of physical techniques. $[\text{Mo}_2(\text{NCCH}_3)_{8-10}][\text{BF}_4]_4$, $[\text{Mo}_2(\mu\text{-O}_2\text{CCH}_3)_2(\text{NCCH}_3)_6][\text{BF}_4]_2$, $[\text{Mo}_2(\mu\text{-O}_2\text{CCH}_3)_2(\text{dppa})_2(\text{NCCH}_3)_2][\text{BF}_4]_2$ and $[\text{Mo}_2(\mu\text{-CH}_3\text{CONH}_2)_2(\text{NCCH}_3)_6][\text{BF}_4]_2$ were employed as model compounds. These compounds react with purely siliceous MCM-41 in acetonitrile to give unstable composite materials in which solvent-stabilized cationic molybdenum fragments are isolated and well dispersed on the silica surface. Powder XRD and N_2 adsorption studies confirm that the textural properties of the high surface area mesoporous host are retained throughout the grafting process. Solid-state MAS NMR and IR spectroscopy indicate that the mechanism of surface attachment involves the displacement of labile acetonitrile ligands, most likely in the axially coordinated positions, from the complexes by combination with isolated nucleophilic silanol groups at the silica surface. It can be inferred from the spectral data that the molybdenum-molybdenum bond is intact in all the functionalized solids and that the complexes undergo only a weak interaction with the surface. The further analysis of the derivatized materials by Mo K-edge X-ray absorption fine structure

(XAFS) spectroscopy revealed that the Mo-Mo distances are similar to those of their corresponding starting complexes, unequivocally indicating that the Mo-Mo quadruple bond is retained in the grafted species. The EXAFS data of the fixed materials exposed to air revealed the significant prolonging of the Mo-Mo bond length. This obviously suggests considerable disruption to the Mo-Mo quadruple bond, most likely a single bond between the molybdenum atoms. Combining all spectroscopic data of the grafted species and the air-oxidized derivatives, the structure of the MCM-41-supported dimolybdenum complexes and of the air-oxidized derivatives could be described as in scheme 1, being exemplified by $[\text{Mo}_2(\text{NCCH}_3)_{10}][\text{BF}_4]_4$.



Scheme 1

Additionally, the catalytic activity of the fixed species for polymerization of methylcyclopentadiene was examined. The results showed that the initiator activity is not significantly reduced by the heterogeneous process. A leaching test demonstrated that the grafted materials are stable against leaching under the conditions applied.

4 Experimental Part

4.1 General

□ Inert Gas Atmosphere

Due to significant air- and moisture-sensitivity of the metal-metal bound complexes, all preparations and manipulations were carried out under an oxygen- and water-free argon (ScheiBargon 4.6) or nitrogen atmosphere using standard Schlenk techniques. The nitrogen was previously purified with a CuCrO_2 catalyst, and dried over phosphorous pentoxide (Granusic[®], Baker) and molecular sieves (4 Å). Every commercial substance and organic ligands should be degassed using vacuum line. All glassware and magnet stirring bar must be dried for 2 hours in drying cabinet at 130 °C before use.

□ Glove Box Technique

All polymerization reactions should be performed in a glove box. Similarly, the preparation of samples of the air- and moisture-sensitive compounds for IR spectroscopy analysis is accomplished in a glove box.

□ Solvents

Diethyl ether, toluene, benzene, and hexane were distilled under nitrogen atmosphere from sodium benzophenone, CH_2Cl_2 from calcium hydride, methanol from magnesium powder, acetonitrile from P_2O_5 , and kept over 4 Å molecular sieves, except for acetonitrile and methanol over 3 Å molecular sieves. Anhydrous tetrahydrofuran (thf) was purchased from Aldrich. Deuterated solvents CDCl_3 , CD_2Cl_2 were stored over 4 Å molecular sieves, CD_3CN , CD_3OD over 3 Å molecular sieves, under argon atmosphere.

4.2 Characterization and Analysis of the Complexes

□ IR Spectroscopy

IR spectra were obtained on a Perkin-Elmer FT-IR spectrometer (resolution 4 cm^{-1}) using KBr pellets as IR matrix or on a Unicam Mattson Mod 7000 FTIR spectrophotometer employing KBr pellets and/or solutions. The KBr should be dried under vacuum and filled with argon and then put in the glove box. The absorption bands are described in the form of wave number ν (cm^{-1}). The representations of the intensities of the absorption bands are abbreviated as following: w, weak; vw, very weak; m, middle; s, strong; vs, very strong; vvs, very very strong; sh, shoulder.

□ UV/Vis Spectroscopy

Electronic absorption spectra were performed on a Perkin-Elmer Lambda 2 UV/VIS spectrometer and. The measurements were carried out using quartz cuvettes (10-mm light path and 3 ml volume). Dr. Wen-Mei Xue performed part of this measurement.

□ Cyclic Voltammetry

Cyclic voltammograms were recorded with a computer-controlled D 6734 Lambrecht Potentiostat Galvanostat (HEKA elektronik) in argon-saturated and dried methylene chloride solution with tetrabutylammonium hexafluorophosphate (TBAH, 0.1 M) as supporting electrolyte. The working electrode was platinum and the reference electrode was silver-coated with AgCl. Potentials are quoted vs. the ferrocene-ferrocenium couple as an internal standard. Dr. Wen-Mei Xue carried out this work.

□ Raman Spectroscopy

Raman spectra were measured by back scattering at room temperature with a S. A: (Riber Jobin Yvon) Model S3000 instrument equipped with a Coherent Innova 301 Kr ion laser (647.1 nm) (performed by Dr. Gabriele Raudaschl-Sieber).

□ NMR Spectroscopy

NMR spectra were recorded using Bruker Avarice DPX-400 (^1H , 400.13 MHz; ^{13}C , 100.85 MHz; ^{31}P , 160.80 MHz) as well as a (9.4T) Bruker MSL 400P spectrometer (^{29}Si , 79.49 MHz; ^{13}C , 100.62 MHz). The chemical shifts are quoted as δ value in parts per million (ppm). The deuterated solvents are used as internal standard for measurement of ^1H , ^{13}C NMR spectra. The representations of multiplicities of the signals are abbreviated in the following: s, singlet; d, doublet; t, triplet; q, quartet; dd, doublet of doublet; tt, triplet of triplet; m, multiplet; etc..

^{29}Si MAS NMR spectra were recorded with 40° pulses, spinning rates of 5.0-5.5 kHz and 60 s recycle delays. ^{29}Si CP MAS NMR spectra were obtained with 5.5 μs pulses, a spinning rate of 5.0 kHz and 4 s recycle delays. ^{13}C CP MAS NMR spectra were recorded with 4.5 μs pulses, a spinning rate of 8 kHz and 4 s recycle delays. Chemical shifts are quoted in parts per million from TMS. ^{31}P MAS NMR spectra were obtained at 162 MHz, using 45° pulses with recycle delays of 60 s and a spinning rate of 14 kHz. Chemical shifts are quoted in parts per million from H_3PO_4 (85%). The group of Prof. Dr. Isabel S. Gonçalves performed this work.

□ Elemental Analysis

Elemental analyses were performed in the microanalytical laboratory of our institute under the leadership of Mr. M. Barth.

□ X-ray Structure Analysis

The single crystal X-ray structure analyses were performed by Dr. E. Herdtweck.. X-ray crystallographic data were obtained on a Nonius CAD 4 or Nonius Mach 3 four-circle Diffractometer with graphite monochromator. Data were corrected for Lorentz and polarization effects ^[1a]. Neutral atom scattering factors for all atoms and anomalous dispersion corrections for the non-hydrogen atoms were taken from the *International Tables for X-Ray Crystallography*^[1b]. All calculations were performed on a DEC 3000 AXP workstation and an Intel Pentium II PC 'with the **STRUX-V**^[1c] system, including the programs **PLATON**^[1d], **SIR92**^[1e] and **SHELXL-97**^[1f].

□ Nitrogen Adsorption Analysis

Nitrogen adsorption isotherms were recorded using a CI electronics MK2-M5 microbalance connected to a vacuum manifold line. The pristine MCM-41 starting material was dehydrated overnight at 723 K to an ultimate pressure of 10^{-4} mbar and then cooled to room temperature prior to adsorption. Extra care with the functionalized materials was necessary due to the possibility of aerial oxidation, therefore transfer to the balance and outgassing of the system was rapid. A lower dehydration temperature (413 K) was used with these samples to further minimize destruction of the functionalities. Nitrogen isotherms were then recorded at 77 K. Equilibration of each data point was monitored using CI electronics' Labweigh software and the pressure monitored using an Edwards Barocel pressure sensor. Specific surface areas were determined from the linear part of the BET plot ($P/P_0 = 0.05-0.3$) using forum 1. This work was performed by the group of Prof. Dr. Isabel S. Gonçalves.

□ XAFS measurements and analysis.

Mo K-edge X-ray absorption spectra were measured at room temperature in transmission mode on beamline BM29 at the ESRF (Grenoble), operating at 6 GeV in 2/3 filling mode with typical currents of 170–200 mA. Typically, scans were recorded in the range 19.8–21.5 keV and set up to record the pre-edge at 5 eV steps and the post-edge region in $0.025-0.05 \text{ \AA}^{-1}$ steps, giving a total acquisition time of ca. 40 min per scan. The order-sorting double Si(311) crystal monochromator was detuned to give 40% harmonic rejection. Solid samples were diluted with BN and pressed into 13 mm pellets. Air-sensitive samples were handled under inert atmosphere. Ionisation chamber detectors were filled with Kr to give 30% absorbing I_o (incidence) and 80% absorbing I_t (transmission).

The programs EXCALIB and EXBACK (SRS Daresbury Laboratory, UK) were used in the usual manner for calibration, summing and background subtraction of the raw data. EXAFS curve-fitting analyses, by least-squares refinement of the non-Fourier filtered k^3 -weighted EXAFS data, were carried out using the program EXCURVE (version EXCURV98^[2]) using fast curved wave theory.^[3] Phase shifts were obtained within this program using *ab initio* calculations based on the Hedin Lundqvist/von Barth scheme. All added atomic shells in this thesis were found to have at least 99% probability of being significant according to the Joyner test. The more rigorous reduced χ^2 test was also used to check the statistical validity of shells.^[4] Thus, unless otherwise stated, addition of each shell detailed in this thesis resulted in a decrease in the calculated value of reduced χ^2 .

□ **Ligands synthesized according to the literature**

4-Styrylpyridine^[5]

4-Ethynylpyridine^[6]

Phenylbis(2-pyridyl)phosphine^[7]

Tri(2-pyridyl)phosphine^[8]

4.3 Syntheses and Characterization of the Compounds

4.3.1 Dimolybdenum (II) Complexes Linked by Cyano Bridges to Organic and Organometallic Ligands

□ *trans*-[Mo₂(μ-O₂CCH₃)₂(μ-dppma)₂(CH₃CN)₂][BF₄]₂ **1** and *trans*-[Mo₂(μ-O₂CCH₃)₂(μ-dppma)₂][BF₄]₂ **2**

0.23 g (0.32 mmol) of *cis*-[Mo₂(μ-O₂CCH₃)₂(CH₃CN)₆][BF₄]₂^[9] and 0.27 g (0.67 mmol) of dppma were dissolved in 20 cm³ of acetonitrile. The purple solution was stirred at room temperature for 4 h and then the solvent was reduced to ca. 5 cm³. Diffusion of diethyl ether through a layer of *n*-hexane into this solution led to red-colored crystals of **1** suitable for X-ray analysis. Yield: 0.26 g, 83% based on *cis*-[Mo₂(μ-O₂CCH₃)₂(CH₃CN)₆][BF₄]₂. Drying the solid of **1** at room temperature in vacuum (1 mmHg) until the ν(C≡N) vibration disappeared from the IR spectrum gave complex **2**. The crystals of **2** for X-ray analysis were obtained by diffusion of diethyl ether into a methylene chloride solution of the compound.

1: EA: C₅₈H₅₈B₂F₈Mo₂N₄O₄P₄ (1364.5)

Calcd.: C, 51.01; H, 4.25; N, 4.10.

Found: C, 50.47; H, 4.22; N, 3.41.

IR (KBr, cm⁻¹): 3056 m, 2968 m, 2934 m, 2852 m, 2250 m (ν(C≡N)), 1636 w, 1482 m, 1436 vs, 1190 m, 1098 vs, 1059 vs, 885 s, 748 s, 698 s, 670 m, 644 m, 526 s, 498 m, 472 m, 429 w.

¹H NMR (ppm, CD₂Cl₂): δ 1.95 (s, 6, CC₃N), 2.09 (s, 6, CH₃C), 2.34 (s, 6, CH₃N), 7.42 – 7.72 (m, 40, Ph-H).

¹³C NMR (ppm, CD₂Cl₂): δ 1.9 (CH₃CN), 23.7 (CH₃C), 33.9 (CH₃N), 119.5 (CN), 129.6, 132.7, 133.4 (Ph-C), 189.1 (CO₂).

³¹P{¹H} NMR (ppm, CD₂Cl₂): δ 99.7 (s).

2: EA: C₅₄H₅₂B₂F₈Mo₂N₂O₄P₄ (1281.5)

Calcd: C, 50.57; H, 4.06; N, 2.18.

Found: C, 50.68; H, 4.21; N, 2.07.

IR (KBr, cm⁻¹): 3056 w, 2938 w, 1633 w, 1483 m, 1436 vs, 1184 m, 1098 vs, 1083 vs, 1000 m, 962 m, 879 s, 748 s, 695 s, 668 m, 641 m, 527 s, 500 m, 470 m.

¹H NMR (ppm, CDCl₃): δ 2.10 (s, 6, CH₃C), 2.34 (s, 6, CH₃N), 7.49 (m, 40, Ph-H).

¹³C NMR (ppm, CDCl₃): δ 23.3 (CH₃C), 34.0 (CH₃N), 128.3, 129.0, 131.8, 133.1, 133.3 (Ph-C), 188.0 (CO₂).

³¹P{¹H} NMR (ppm, CDCl₃): δ 99.7 (s).

□ ***trans*-[Mo₂(μ-O₂CCH₃)₂(μ-dppma)₂(NCR)₂][BF₄]₂** (**R** = C(CH₃)₃, **3**; C₆H₅, **4**; C₆H₄C≡CH, **5**).

To a methylene chloride solution of **1** (0.23 g, 0.32 mmol) was added 0.26 cm³ (1.28 mmol) of benzonitrile or 0.14 cm³ (1.28 mmol) of *tert*-butylnitrile or 0.41 g (3.2 mmol) of *p*-nitriethynylbenzene, resp. The reaction mixture was then stirred at room temperature for 24 h. After being concentrated to ca. 5 cm³, the solution was layered with a mixture of diethyl ether and *n*-hexane. Red crystals were obtained for each compound. Yield: 0.21 g, 80% for **3**; 0.23 g, 89% for **4** and 0.45 g, 92% for **5** based on **1**.

3: EA: C₆₄H₇₀B₂F₈Mo₂N₂O₄P₄ (1448.7)

Calcd: C, 53.06; H, 4.87; N, 3.87.

Found: C, 52.63; H, 4.85; N, 3.69.

IR (KBr, cm⁻¹): 3052 w, 2977 w, 2933 w, 2251 m, (ν(C≡N)), 1481 m, 1435 vs, 1123 m, 1098 vs, 1083 vs, 1056 vs, 1036 m, 881 s, 748 s, 697 s, 526 s, 500 m, 479 m.

^1H NMR (ppm, CD_2Cl_2): δ 1.34 (s, 18, $(\text{CH}_3)_3\text{C}$), 2.09 (s, 6, CH_3C), 2.34 (s, 6, CH_3N), 7.48 – 7.55 (m, 40, Ph-H).

^{13}C NMR (ppm, CD_2Cl_2): δ 23.4 (CH_3CO_2), 27.6 ($(\text{CH}_3)_3\text{C}$), 30.6 ($(\text{CH}_3)_3\text{C}$), 33.5 (CH_3N), 128.5 (CN), 129.3, 132.4, 133.0 (Ph-C), 188.7 (CO_2).

$^{31}\text{P}\{^1\text{H}\}$ NMR (ppm, CD_2Cl_2): δ 99.7 (s).

4: EA $\text{C}_{68}\text{H}_{62}\text{B}_2\text{F}_8\text{Mo}_2\text{N}_2\text{O}_4\text{P}_4$ (1488.7)

Calcd: C, 54.90; H, 4.24; N, 3.77.

Found: C, 54.56; H, 4.03; N, 3.59.

IR (KBr, cm^{-1}): 3049 w, 2934 w, 2235 m ($\nu(\text{C}\equiv\text{N})$), 1619 m, 1482 m, 1436 vs, 1186 m, 1124 vs, 1083 vs, 998 m, 882 s, 763 m, 746 s, 698 s, 668 m, 642 m, 525 s, 501 m, 471 m.

^1H NMR (ppm, CD_2Cl_2): δ 2.26 (s, 6, CH_3C), 2.43 (m, 6, CH_3N), 7.50 – 7.73 (m, 50, Ph-H).

^{13}C NMR (ppm, CD_2Cl_2): δ 23.0 (CH_3C), 30.7 (CH_3N), 120.4 (CN), 129.6, 132.6, 133.1 (Ph-C), 189.0 (CO_2).

$^{31}\text{P}\{^1\text{H}\}$ NMR (ppm, CD_2Cl_2): δ 99.1 (s).

5: EA: $\text{C}_{72}\text{H}_{62}\text{B}_2\text{F}_8\text{Mo}_2\text{N}_2\text{O}_4\text{P}_4$ (1535.4)

Calcd: C, 56.27; H, 4.04; N, 3.65.

Found: C, 56.38; H, 3.91; N, 3.49.

IR (KBr, cm^{-1}): 3244 s ($\nu(\text{C}\equiv\text{C}-\text{H})$), 3092 w, 3056 w, 2939 w, 2235 s ($\nu(\text{C}\equiv\text{N})$), 2106 w ($\nu(\text{C}\equiv\text{C})$), 1601 w, 1438 vs, 1403 m, 1099 vs, 1070 vs, 998 m, 878 s, 850 m, 748 m, 698 m, 668 s, 642 m, 562 m, 524 m, 502 m, 469 m.

^1H NMR (ppm, CD_2Cl_2): δ 2.20 (s, 6, CH_3C), 2.36 (m, 6, CH_3N), 3.39 (s, 2, CCH), 7.39 – 7.67 (m, 48, Ph-H).

^{13}C NMR (ppm, CD_2Cl_2): δ 23.7 (CH_3C), 33.8 (CH_3N), 82.0 (CCH), 112.0 (Ph-C), 119.9 (CN), 129.6, 132.4, 133.0, 133.4 (Ph-C), 189.1 (CO_2).

$^{31}\text{P}\{^1\text{H}\}$ NMR (ppm, CD_2Cl_2): δ 101.0 (s).

□ ***trans*-[Mo₂(μ -O₂CCH₃)₂(μ -dppma)₂][NC-M(CO)₅]₂ (M = Cr, **6**; Mo, **7**; W, **8**).**

A solution of **1** (0.14 g, 0.11 mmol) and Na[NC-M(CO)₅] (M = Cr, Mo, W, 0.22 mmol) in 10 cm^3 of acetonitrile was stirred at room temperature for 2 h, leading to a red precipitate which was collected and washed with small portions of methanol for several times. Yield: 0.14 g, 81% for **6**; 0.08 g, 47% for **7** and 0.16 g, 78% for **8** based on **1**.

6: EA: C₆₆H₅₂Cr₂Mo₂N₄O₁₄P₄ (1544.9)

Calcd.: C, 51.27; H, 3.37; N, 3.62.

Found: C, 50.92; H, 3.30; N, 3.46.

IR (KBr, cm^{-1}): 3061w, 2923w, 2101 m ($\nu(\text{C}\equiv\text{N})$), 2048 s, 1972 m, 1926 vs, 1902 vs, 1630 w, 1482 m, 1434 s, 877 m, 745 m, 696 m, 678 s, 663 s, 642 m, 526 m, 502 m, 470 m.

^1H NMR (ppm, CD_2Cl_2): δ 2.25 (s, 6, CH_3C), 2.38 (m, 6, CH_3N), 7.23 – 7.41 (m, 40, Ph-H).

^{13}C NMR (ppm, CD_2Cl_2): δ 22.5 (CH_3C), 32.0 (CH_3N), 127.2 (CN), 130.2, 131.1, 131.2, 132.2 (Ph-C), 187.0 (CO_2), 215.5 (CO).

$^{31}\text{P}\{^1\text{H}\}$ NMR (ppm, CD_2Cl_2): δ 103.2 (s).

7: EA: $\text{C}_{66}\text{H}_{52}\text{Mo}_4\text{N}_4\text{O}_{14}\text{P}_4$ (1632.8)

Calcd: C, 48.51; H, 3.18; N, 3.43.

Found: C, 48.13; H, 2.97; N, 3.17.

IR (KBr, cm^{-1}): 3060 w, 2931 w, 2099 m ($\nu(\text{C}\equiv\text{N})$), 2055 s, 1978 m, 1928 vs, 1901 vs, 1636 w, 1483 m, 1436 vs, 881 m, 746 m, 694 m, 668 s, 642 m, 608 m, 594 m, 526 m, 499 m, 472 m.

^1H NMR (ppm, CD_2Cl_2): δ 2.25 (s, 6, CH_3C), 2.63 (s, 6, CH_3N), 7.48 – 7.56 (m, 40, Ph-H).

^{13}C NMR (ppm, CD_2Cl_2): δ 24.0 (CH_3C), 31.0 (CH_3N), 125.0 (CN), 129.7, 132.0, 133.1, 134.0 (Ph-C), 188.5 (CO_2), 194.1, 217.4 (CO).

$^{31}\text{P}\{^1\text{H}\}$ NMR (ppm, CD_2Cl_2): δ 101.2 (s).

8: EA: $\text{C}_{66}\text{H}_{52}\text{Mo}_2\text{N}_4\text{O}_{14}\text{P}_4\text{W}_2$ (1808.6)

Calcd: C, 43.79; H, 2.88; N, 3.10.

Found: C, 43.31; H, 2.39; N, 2.92.

IR (KBr, cm^{-1}): 3061 w, 2962 w, 2101 m ($\nu(\text{C}\equiv\text{N})$), 2052 s, 1967 m, 1918 vs, 1896 vs, 1653 w, 1436 s, 882 m, 800 m, 747 m, 693 m, 668 s, 643 m, 598 m, 584 m, 525 m, 499 m, 471 m. **^1H NMR** (ppm, CD_2Cl_2): δ 2.08 (s, 6, CH_3C), 2.19 (s, 6, CH_3N), 7.16 – 7.36 (m, 40, Ph-H). **^{13}C NMR** (ppm, CD_2Cl_2): δ 24.1 (CH_3C), 30.1 (CH_3N), 125.2 (CN), 129.0, 131.8, 133.6 (Ph-C), 189.0 (CO_2), 219.1 (CO).

$^{31}\text{P}\{^1\text{H}\}$ NMR (ppm, CD_2Cl_2): δ 101.2 (s).

□ *trans*- $[\text{Mo}_2(\mu\text{-O}_2\text{CCH}_3)_2(\mu\text{-dppma})_2][\text{NC-Fe}(\text{CO})_2\text{Cp}]_2[\text{BF}_4]_2$ **9**.

To a solution of 0.13 g (0.10 mmol) of **1** in methylene chloride was added $\text{Cp}(\text{CO})_2\text{Fe-CN}$ (41 mg, 0.20 mmol) at room temperature. The solution was stirred for 2 h. The solvent was removed in vacuo to give the pink-red product, which was washed with diethyl ether. Yield: ca. 100 % based on **1**.

9: EA: $\text{C}_{70}\text{H}_{62}\text{B}_2\text{F}_8\text{Fe}_2\text{Mo}_2\text{N}_4\text{O}_8\text{P}_4$ (1688.4)

Calcd: C, 49.75; H, 3.67; N, 3.32.

Found: C, 49.29; H, 3.93; N, 3.06.

IR (KBr, cm^{-1}): 3115 w, 3053 w, 2923 w, 2117 m ($\nu(\text{C}\equiv\text{N})$), 2056 vs, 2008 vs, 1616 w, 1483 m, 1436 vs, 1083 vs, 878 m, 749 m, 696 m, 641 m, 609 m, 526 m, 499 m, 470 m.

^1H NMR (ppm, CD_2Cl_2): δ 2.21 (s, 6, CH_3C), 2.37 (s, 6, CH_3N), 4.47 (s, 10, Cp), 7.43 – 7.67 (m, 40, Ph-H).

^{13}C NMR (ppm, CD_2Cl_2): δ 23.9 (CH_3C), 33.9 (CH_3N), 85.7 (Cp), 129.7 (CN), 132.7, 133.0 (Ph-C), 189.1 (CO_2), 208.7, 224.6 (CO).

$^{31}\text{P}\{^1\text{H}\}$ NMR (ppm, CD_2Cl_2): δ 100.5 (s).

4.3.2 Dimolybdenum(II) Complexes Linked by Pyridine and Its Derivatives

□ *trans*- $[\text{Mo}_2(\mu\text{-O}_2\text{CCH}_3)_2(\mu\text{-dppma})_2(\text{NC}_5\text{H}_4\text{-R})_2][\text{BF}_4]_2$ (R = H, **10**; $\text{C}(\text{CH}_3)_3$, **11**; C_6H_5 , **12**; $\text{CH}=\text{CHC}_6\text{H}_5$, **13**; CCH, **14**; CN, **15**).

To a solution of *trans*-[Mo₂(μ-O₂CCH₃)₂(μ-dppma)₂(CH₃CN)₂][BF₄]₂ (**1**, 0.20 g, 0.15 mmol) in 20 mL of methylene chloride was added 0.32 mmol of the pyridine derivatives, resp.. The solution was stirred at room temperature for 4 h. After being concentrated to ca. 5 mL, the solution was treated with 20 mL of diethyl ether to precipitate a red solid. The crude product was washed with portions of diethyl ether and then recrystallized from methylene chloride/diethyl ether. Yields are ca. 90 to 95%.

10: EA: C₆₄H₆₂B₂F₈Mo₂N₄O₄P₄ (1439.4)

Calc. C 53.36, H 4.31, N 3.89

Found C 52.98, H 3.96, N 4.00

IR (KBr, cm⁻¹): 3052 w, 1594 m, 1482 m [v_{asym}(OCO)], 1440 vs [v_{sym}(OCO)], 1220 w, 1096 vs, 1055 vs, 998 m, 880 s, 753 m, 700 s, 669 m, 640 m, 616 w, 523 m, 500 m, 468 m.

Raman (ν, Mo-Mo): 345 cm⁻¹

¹H-NMR (CD₂Cl₂, ppm): δ 2.29 (t, 6H, CH₃C), 2.49 (s, 6H, CH₃N), 7.20 (t, 4H, py-H_γ), 7.31 (s, 2H, py-H), 7.53 – 7.71 (m, 40H, Ph-H), 8.21 (s, 4H, py-H).

¹³C-NMR (CD₂Cl₂, ppm): δ 24.1 (CH₃C), 33.9 (CH₃N), 125.0 (py-C_γ), 129.8, 132.7, 132.9, 133.0, 133.1, 133.2 (Ph-C), 139.3 (py-C_β), 148.6 (py-C_α), 189.7 (CO₂).

³¹P{¹H}-NMR (CD₂Cl₂, ppm): δ 95.6 (s).

11: EA: C₇₂H₇₈B₂F₈Mo₂N₄O₄P₄ (1551.4)

Calc. C 55.69, H 5.03, N 3.61

Found C 55.26, H 4.67, N 3.44

IR (KBr, cm^{-1}): 3055 m, 2965 m, 2869 w, 1620 s, 1483 m [$\nu_{\text{asym}}(\text{OCO})$], 1437 vs [$\nu_{\text{sym}}(\text{OCO})$], 1276 m, 1185 m, 1084 vs, 1066 vs, 1000 m, 969 m, 880 s, 750 m, 698 s, 670 m, 645 m, 570 m, 533 m, 500 m, 469 m.

Raman (ν , Mo-Mo): 350 cm^{-1} .

$^1\text{H-NMR}$ (CD_2Cl_2 , ppm): d 1.15 (s, 18H, $(\text{CH}_3)_3\text{C}$), 2.30 (m, 6H, CH_3C), 2.39 (s, 6H, CH_3N), 7.24 (d, 4H, py- H_β), 7.53 – 7.73 (m, 40H, Ph-H), 7.94 (d, 4H, py-H).

$^{13}\text{C-NMR}$ (CD_2Cl_2 , ppm): δ 24.8 (CH_3CO_2), 30.1 ($(\text{CH}_3)_3\text{C}$), 34.0 ($(\text{CH}_3)_3\text{C}$), 35.5 (CH_3N), 123.3 (py- C_γ), 129.7, 129.8, 129.9, 132.9, 133.2, 133.3 (Ph-C), 149.7 (py- C_β), 166.1 (py- C_α), 190.6 (CO_2).

$^{31}\text{P}\{^1\text{H}\}$ -NMR (CD_2Cl_2 , ppm): δ 98.9 (s).

12: EA: $\text{C}_{67}\text{H}_{64}\text{B}_2\text{F}_8\text{Mo}_2\text{N}_4\text{O}_4\text{P}_4$ (1477.4)

Cal. C 54.42, H 4.33, N 3.79

Found C 54.82, H 4.18, N 3.43

IR (KBr, cm^{-1}): 3056 m, 1614 m, 1602 m, 1483 m [$\nu_{\text{asym}}(\text{OCO})$], 1437 vs [$\nu_{\text{sym}}(\text{OCO})$], 1224 w, 1188 m, 1097 vs, 1056 vs, 1000 m, 884 s, 764 m, 751 m, 700 s, 668 m, 642 m, 614 m, 526 m, 500 m, 469 m.

Raman (ν , Mo-Mo): 344 cm^{-1} .

$^1\text{H-NMR}$ (CD_2Cl_2 , ppm): δ 2.30 (m, 6H, CH_3C), 2.59 (s, 6H, CH_3N), 7.46 (d, 4H, py- H_β), 7.51 – 7.70 (m, 50H, Ph-H), 7.99 (d, 4H, py- H_α).

^{13}C -NMR (CD_2Cl_2 , ppm): δ 24.5 (CH_3C), 34.0 (CH_3N), 122.2 (py-C_γ), 127.3, 129.5, 129.6, 129.9, 130.8, 133.0, 133.1, 133.2, 136.8 (Ph-C), 149.8 (py-C_β), 151.1 (py-C_α), 190.0 (CO_2).

$^{31}\text{P}\{^1\text{H}\}$ -NMR (CD_2Cl_2 , ppm): δ 95.6 (s).

13: EA: $\text{C}_{80}\text{H}_{74}\text{B}_2\text{F}_8\text{Mo}_2\text{N}_4\text{O}_4\text{P}_4$ (1643.4)

Calc. C 58.42, H 4.50, N 3.41

Found C 58.30, H 4.31, N, 3.14

IR (KBr , cm^{-1}): 3056 m, 1602 s, 1482 m [$\nu_{\text{asym}}(\text{OCO})$], 1436 vs [$\nu_{\text{sym}}(\text{OCO})$], 1188 m, 1098 vs, 1061 vs, 999 m, 882 s, 815 m, 749 s, 696 vs, 669 m, 642 m, 527 s, 500 m, 470 m.

Raman (ν , Mo-Mo): 347 cm^{-1} .

^1H -NMR (CD_2Cl_2 , ppm): δ 2.30 (m, 6H, CH_3C), 2.57 (s, 6H, CH_3N), 6.93 (s, 2H, PhCH), 6.97 (s, 2H, pyCH), 7.24 (d, 4H, py-H_β), 7.34 – 7.74 (m, 50H, Ph-H), 7.91 (d, 4H, py-H_α).

^{13}C -NMR (CD_2Cl_2 , ppm): δ 24.5 (CH_3C), 33.9 (CH_3N), 121.8 (py-C_γ), 124.5, 127.8, 129.3, 129.8, 130.0, 133.0, 133.1, 133.2, 135.7 (PhCH), 136.9 (pyCH), 148.5 (py-C_β), 149.0 (py-C_α), 189.9 (CO_2).

$^{31}\text{P}\{^1\text{H}\}$ -NMR (CD_2Cl_2 , ppm): δ 95.6 (s).

14: EA: $\text{C}_{68}\text{H}_{62}\text{B}_2\text{F}_8\text{Mo}_2\text{N}_4\text{O}_4\text{P}_4$ (1487.4):

Calc. C 54.86, H 4.17, N 3.77

Found C 54.79, H 4.26, N, 3.45

IR (KBr, cm^{-1}): 3293 m (CC-H), 3056 m, 2112 w ($\text{C}\equiv\text{C}$), 1598 s, 1483 m [$\nu_{\text{asym}}(\text{OCO})$], 1436 vs [$\nu_{\text{sym}}(\text{OCO})$], 1188 m, 1098 vs, 1061 vs, 998 m, 888 s, 849 w, 752 m, 700 s, 668 m, 641 s, 525 s, 500 m, 470 s.

Raman (ν , Mo-Mo): 349 cm^{-1} .

$^1\text{H-NMR}$ (CD_2Cl_2 , ppm): δ 2.31 (s, 6H, CH_3C), 2.37 (s, 6H, CH_3N), 3.39 (s, 2H, CCH), 7.15 (s, 4H, py- H_β), 7.38 – 7.66 (m, 40H, Ph-H), 8.16 (s, 4H, py- H_α).

$^{13}\text{C-NMR}$ (CD_2Cl_2 , ppm): δ 24.0 (CH_3C), 30.1 (CH_3N), 66.0 (CCH), 126.5 (py- C_γ), 129.3, 129.7, 130.3, 131.3, 132.3, 132.6, 132.8, 133.0, 133.3 (Ph-C and py- C_β), 150.3 (py- C_α), 189.0 (CO_2).

$^{31}\text{P}\{^1\text{H}\}\text{-NMR}$ (CD_2Cl_2 , ppm): δ 98.9 (s).

15: EA: $\text{C}_{66}\text{H}_{60}\text{B}_2\text{F}_8\text{Mo}_2\text{N}_6\text{O}_4\text{P}_4$ (1489.4)

Calc. C 53.18, H 4.03, N 5.64

Found C 53.39, H 4.18, N 5.32

IR (KBr, cm^{-1}): 3049 w, 2932 w, 2239 w ($\text{C}\equiv\text{N}$), 1639 s, 1600 m, 1508 m, 1482 m [$\nu_{\text{asym}}(\text{OCO})$], 1436 vs [$\nu_{\text{sym}}(\text{OCO})$], 1189 w, 1098 vs, 1083 vs, 1059 vs, 1000 m, 889 s, 748 s, 699 s, 668 m, 642 m, 524 s, 498 m, 472 m.

Raman (ν , Mo-Mo): 353 cm^{-1} .

$^1\text{H-NMR}$ (CD_2Cl_2 , ppm): δ 2.34 (t, 6H, CH_3C), 2.63 (s, 6H, CH_3N), 7.30 (d, 4H, py- H_β), 7.37 – 7.66 (m, 40H, Ph-H), 8.71 (d, 4H, py- H_α).

^{13}C -NMR (CD_2Cl_2 , ppm): δ 23.9 (CH_3C), 31.0 (CH_3N), 116.8 (CN), 124.3 (py- C_γ), 125.6 (py- C_β), 128.6, 129.6, 132.5, 132.7, 133.1, 133.4 (Ph-C), 151.1 (py- C_α), 189.2 (CO_2).

$^{31}\text{P}\{^1\text{H}\}$ -NMR (CD_2Cl_2 , ppm): δ 98.9 (s).

4.3.3 Dimolybdenum and Dirhodium Complexes Bearing 2-Pyridylphosphine Ligands, PPhPy₂ and PPy₃

□ $\text{Mo}_2(\mu\text{-O}_2\text{CCF}_3)_3(\text{O}_2\text{CCF}_3)(\text{PPhPy}_2)$ (**16a**)

To a stirred solution of $\text{Mo}_2(\mu\text{-O}_2\text{CCF}_3)_4$ (0.322g, 0.5mmol) in 15ml of CH_2Cl_2 was added an equimolar amount of PPhPy₂ (0.132g, 0.5mmol) in 10 ml of CH_2Cl_2 . An immediate reaction took place with the formation of a bright red precipitate, which was collected after two hours stirring, washed with portions of CH_2Cl_2 and dried under oil pump vacuum. Yield: 90%.

EA: $\text{C}_{24}\text{H}_{13}\text{F}_{12}\text{Mo}_2\text{N}_2\text{O}_8\text{P}$ (908.2)

Calc: C 31.74, H 1.44, N 3.08;

Found C 31.82, H 1.42, N 2.96

IR (KBr, cm^{-1}): 1654 s, 1608 vs, 1431 m, 1192 vs, 1161 vs, 984 m, 854 m, 723 s, 597 w, 543 w, 518 m.

□ *trans*- $\text{Mo}_2(\mu\text{-O}_2\text{CCF}_3)_2(\text{O}_2\text{CCF}_3)_2(\text{PPhPy}_2)_2$ (**16b**)

The same procedure was applied as described for compound **16a**, only the molar ratio of the $\text{Mo}_2(\mu\text{-O}_2\text{CCF}_3)_4$: PPhPy₂ being 1:4. The resulting compound was of purple color. Yield: 85%. Violet prisms crystals suitable for X-ray crystallography were obtained by slow diffusion of solution of $\text{Mo}_2(\mu\text{-O}_2\text{CCF}_3)_4$ in CH_2Cl_2 into PPhPy₂ dissolved in diethyl ether after two days.

EA: $\text{C}_{40}\text{H}_{26}\text{F}_{12}\text{Mo}_2\text{N}_4\text{O}_8\text{P}_2$ (1172.5)

Calc: C 40.97, H 2.24, N 4.77

Found: C 42.46, H 2.10, N 4.22

IR (KBr, cm^{-1}): 1690 vs, 1650 sh, 1607 m, 1192 vs, 1166 s, 856 m, 831 m, 791 m, 597 w, 425 w, 379 w, 331 w, 223 w, 137 vw.

Raman (ν , cm^{-1}): 1693 vw, 1670 vw, 1589 vs, 1203 w, 1144 m, 865 w, 831 w, 772 w, 619 w, 430 w, 376 w, 344 s, 303 vs.

□ **$\text{Mo}_2(\mu\text{-O}_2\text{CCF}_3)_3(\text{O}_2\text{CCF}_3)(\text{PPy}_3)$ (**17a**)**

The synthetic procedure applied was similar to that used for compound **16a**. PPy_3 was employed instead of PPhPy_2 . Yield: 87%.

EA: $\text{C}_{23}\text{H}_{12}\text{F}_{12}\text{Mo}_2\text{N}_3\text{O}_8\text{P}$ (909.5)

Calc: C 30.37, H 1.33, N 4.62

Found: C 29.85, H 1.45, N 4.60

IR (KBr, cm^{-1}): 1647 s, 1608 s, 1452 m, 1426 s, 1193 vs, 1164 sh, 990 w, 856 m, 803 m, 777 w, 730 s, 520 m.

□ ***trans*- $\text{Mo}_2(\mu\text{-O}_2\text{CCF}_3)_2(\text{O}_2\text{CCF}_3)_2(\text{PPy}_3)_2$ (**17b**)**

The procedure was similar to that described for compound **16a** with the following exceptions: the molar ratio of starting materials used was $\text{Mo}_2(\mu\text{-O}_2\text{CCF}_3)_4 : \text{PPy}_3 = 1:4$. And the reaction mixture was refluxed for 4 hours. The resulting product was purple. The product yield is 63%, however, the obtained material is mixed with complex **17a** (27% based on elementary analysis). Attempts to isolate clean complex **17b** were not successful due to its insoluble in all common organic solvents. Slow diffusion of PPy_3 in methanol into $\text{Mo}_2(\mu\text{-O}_2\text{CCF}_3)_4$ in CH_2Cl_2 with molar ratio of 2:1 leads to harvest of a few violet prisms crystals.

EA: C₃₈H₂₄F₁₂Mo₂N₆O₈P₂ (1174.5)

Calc: C 38.36, H 2.06, N 7.15

Found: C 35.38, H 1.94, N 6.50

IR (KBr, cm⁻¹): 1684 sh, 1647 s, 1608 vs, 1194 vs, 1164 s, 857 m, 836 w, 795 w, 509 m, 382 w.

Raman (ν, cm⁻¹): 1685 vw, 1648 vs, 1608 vs, 1592 m, 1209 vw, 867 w, 839 w, m, 798 s, 523 vvs, 510 s, 388 vs, 354 s, 307 vs.

□ **Rh₂(μ-O₂CCH₃)₄(PPhPy₂)₂ (18)**

Rh₂(μ-O₂CCH₃)₄ (0.111g, 0.25mmol) was dissolved in 10 ml of THF to produce a bright green solution. The 4-fold stoichiometric amount of PPhPy₂ (0.264 g, 1.00 mmol) in 10 ml of acetone was then added. The red-brownish precipitate was gradually formed and the suspension was stirred for 2 hours. The crude product was washed several times with THF (3x5ml), acetone (3x5ml), and then dried in oil pump vacuum. The yield is 83% based on Rh₂(μ-O₂CCH₃)₄.

EA: C₄₀H₃₉N₄O₈P₂Rh₂ (971.8)

Calc: C 49.44, H 4.04, N 5.76

Found: C 46.42, H 3.53, N 5.28

IR (KBr, cm⁻¹): 1596 vs, 1434 vs, 1422 vs, 1374 s, 1320 m, 1128 w, 1015 w, 650 w, 380 w, 289 w

Raman (ν, cm⁻¹): 1587 m, 1438 w, 1386 vw, 1327 w, 1128 s, 580 vw, 337 s, 287 vvs, 240 sh.

¹H-NMR (CD₂Cl₂, ppm): δ 1.63 (s, 12H, CH₃C), 7.26(dd, 4H, H₇), 7.44(m, 6H, H₂, H₃), 7.62(dt, 4H, H₁), 7.88(d, 4H, H₅), 8.02(d, 4H, H₆), 8.70(d, 4H, H₈)

$^{13}\text{C-NMR}$ (CD_2Cl_2 , ppm): δ 24.2(CH_3C), 123.6(C_7), 128.4(C_2), 130.4(C_3), 131.8(C_1), 133.3(C_5), 135.3(C_6), 136.5(C_4), 150.2(C_8), 159.5(C_9), 193.0(CO_2)

$^{31}\text{P}\{^1\text{H}\}$ -NMR (CD_2Cl_2 , ppm): δ -8.99(s)

UV/Vis (CH_2Cl_2 solution): $\lambda_{\text{max}} = 496 \text{ nm}$ ($\epsilon = 600 \text{ M}^{-1}\text{cm}^{-1}$), $\lambda_{\text{max}} = 318 \text{ nm}$, ($\epsilon = 36500$

$\text{M}^{-1}\text{cm}^{-1}$), $\lambda = 356 \text{ nm}$ (sh).

□ **$\text{Rh}_2(\mu\text{-O}_2\text{CCH}_3)_4(\text{PPy}_3)_2$ (**19**)**

The procedure applied was analogous as described for complex **18**. PPy_3 was used instead of PPhPy_2 as the ligand. The yield based on $\text{Rh}_2(\mu\text{-O}_2\text{CCH}_3)_4$ is 92 %.

EA: $\text{C}_{38}\text{H}_{37}\text{N}_6\text{O}_8\text{P}_2\text{Rh}_2$ (973.8)

Calc: C 46.87, H 3.83, N 8.67

Found: C 42.96, H 3.40, N 7.53

IR (KBr , cm^{-1}): 1594 vs, 1422 vs, 1284 m, 1129 vw, 1086 m, 1066 vvw, 695 s, 382 m, 303 vw, 278 w

Raman (ν , cm^{-1}): 1421 s, 1278 m, 581 vw, 527 m, 338 s, 289 vvs

$^1\text{H-NMR}$ (CD_2Cl_2 , ppm): δ 1.63 (s, 12H, CH_3C), 7.29 (dt, 6H, H_7), 7.67 (dt, 6H, H_5), 7.99 (d, 6H, H_6), 8.69 (d, 4H, H_8)

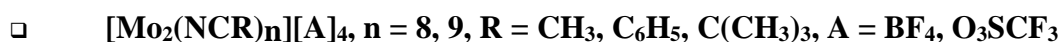
$^{13}\text{C-NMR}$ (CD_2Cl_2 , ppm): δ 24.0 (CH_3C), 123.6 (C_7), 132.0 (C_5), 135.2 (C_6), 150.2 (C_8), 158.3 (C_9), 192.7 (CO_2)

$^{31}\text{P}\{^1\text{H}\}$ -NMR (CD_2Cl_2 , ppm): δ -2.64(s)

UV/Vis (CH₂Cl₂ solution): $\lambda_{\max} = 568 \text{ nm}$ ($\epsilon = 250 \text{ M}^{-1} \text{ cm}^{-1}$), $\lambda_{\max} = 318 \text{ nm}$ ($\epsilon = 28100 \text{ M}^{-1} \text{ cm}^{-1}$), $\lambda = 370 \text{ nm}$ (sh).

4.3.4 Solvent Stabilized Metal-Metal Bonded Catalysts

Preparation of these complexes was according to literature procedures. Compound **20** according to ref. ^[9a], complex **21** as described in ^[10a], compounds **22** and **24-26** according to ^[10b], complex **23** analogous to ^[10c], derivative **27** as described in ^[10d], compound **28** as described in **4.3**, Complex **29** according to ^[10e] and derivatives **30**, **30a**, **30b** as given in ^[13]. The identity of all complexes has been proven by elementary analysis, NMR- and IR spectroscopy. The received data have been in all cases been identical with the data given in the literature. In all examined cases the depicted structural formulas are in agreement with the X-ray data of the particular complexes.



Dimolybdenum (II) tetraacetate, (1.2 g, 2.80 mmol), was suspended in a solution consisting of the appropriate nitrile (20 mL) and methylene chloride (40 mL). To this vigorously stirring yellow solution was added HBF₄•Et₂O (6.0 mL, 85 % HBF₄ solution) or a solution of HO₃SCF₃ (10 mmol in 5 mL of CH₃CN/CH₂Cl₂), resp.. The color changed immediately to red, then to purple and within less than 30 min to blue. The reaction mixture was then heated and refluxed for 4 h. Then the reaction mixture was cooled to room temperature and the blue precipitate which had formed during the course of the reaction was isolated by filtering off the mother liquor. The precipitate was washed several times with diethyl ether, methylene chloride and n-pentane or n-hexane. Then it was dried for 12 h in oil pump vacuum. Prolonged drying leads to complexes containing only 8 nitrile ligands or less. Drying for less than 1 h usually leads to a compound with 10 nitrile ligands. The yield is in all cases nearly quantitative.



EA: C₆₃H₄₅N₉B₄F₁₆Mo₂ (1417.22)

Calcd.: C 51.57, H 3.09, N 8.59

Found: C 51.31, H 2.99, N 8.44

IR (KBr, cm⁻¹): 3008 w, 2962 w, 2279 m, 2231 w, 1262 s, 1084 vs, 1023 vs, 802 s, 760 m, 684 m, 555 w, 515w.

¹H NMR (CH₂Cl₂, ppm): δ 7.71 (m, 2H), 7.62 (m, 1H), 7.51 (m, 2H).

□ **[Mo₂(NCC(CH₃)₃)₉][BF₄]₄ (20c):**

EA: C₄₅H₈₁N₉B₄F₁₆Mo₂ (1287.31)

Calcd.: C 41.99, H 6.34, N 9.79

Found: C 41.71, H 6.21, N 9.68

IR (KBr, cm⁻¹): 2929 m, 2729 m, 2259 s, 2222 w, 1266 s, 1085 vs, 1022 s, 811 s, 731 m, 677 m, 550 m.

¹H NMR (CD₂Cl₂, ppm) δ 1.28 (s, C(CH₃)₃).

□ **[Mo₂(NCCH₃)₈][O₃SC₃F]₄ (20d):**

EA: C₂₀H₂₄N₈F₁₂Mo₂O₁₂S₄ (1116.56)

Calcd.: C 21.54, H 2.17, N 10.04

Found: C 21.91, H 2.02, N 10.13

IR (KBr, cm^{-1}): 2971 w, 2917 w, 2277 w, 1258 vs, 1173 s, 1034 s, 802 w, 766 w, 647 s, 579 m, 520 m.

^1H NMR (CD_2Cl_2 , ppm) δ 1.95 (s, CH_3).

4.3.5 Solvent Stabilized Monomeric Catalysts

All examined complexes are prepared according to literature procedures. Compounds **31** was prepared according to ref. ^[8], complex **32** as described in ref. ^[9], and **33-36** and **39-40** were prepared according to ref. ^[10], **33a** and **34a** were prepared by employing MnCl_2 and FeBr_2 to interact with AgBPh_4 in acetonitrile under darkness; complex **37** was prepared by using PdCl_2 upon reaction with AgBF_4 in the same condition as **33a** and **34a**; **33b** according to ref. ^[14]. The identity of all complexes has been proven by elementary analyses, **Raman**- and **IR** spectroscopy. The received data have in all cases been identical with the data given in the literature. The depicted structural formulae are in agreement with the X-ray data of the particular complexes, in all cases examined by this method.

4.3.6 Mesoporous MCM-41

Purely siliceous MCM-41 was synthesized as described previously using $[(\text{C}_{14}\text{H}_{29})\text{NMe}_3]\text{Br}$ as the templating agent.^[15] After calcination ($540^\circ\text{C}/6\text{h}$), the material was characterized by XRD, N_2 adsorption and IR spectroscopy. Prior to the grafting experiments, calcined MCM-41 was activated at 160°C in vacuum (10^{-2} Pa) for 3 hours. This treatment is sufficient to achieve complete thermodesorption of physically adsorbed water molecules from the silica surface.^[18]

4.4 Characterization of the Grafting Homogeneous Catalysts

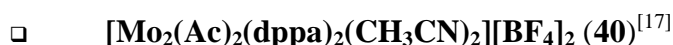
In addition to the preparation and characterization of the heterogeneous catalysts, some necessary characterized data of the homogeneous catalysts are also given as follows for comparison:

- $[\text{Mo}_2(\text{CH}_3\text{CN})_{10}][\text{BF}_4]_4$ (**20**)^[9a]

^{13}C CP MAS NMR (25 °C, ppm): δ 149.5, 148.1 (NCCH₃, equatorial), 123.6 (NCCH₃, axial), 3.5, 0.8 (NCCH₃; equatorial and axial).



^{13}C CP MAS NMR (25°C, ppm): δ 187.6 (O₂CCH₃), 148.9, 146.5 (NCCH₃), 121.9, 119.7, 118.3 (NCCH₃), 22.68 (O₂CCH₃), 5.0, 2.1, -0.1 (NCCH₃).



^{13}C CP MAS NMR (25 °C, ppm): δ 189.3 (s, O₂CCH₃), 134.2, 131.1, 129.5 (dppa), 24.6, 22.4 (s, O₂CCH₃), 1.9, 0.1 (NCCH₃)

^{31}P MAS NMR (25 °C, ppm): δ 82.6.



Calcined MCM-41 (0.5 g) was dehydrated and treated with a 0.012 M solution of $[\text{Mo}_2(\text{MeCN})_{10}][\text{BF}_4]_4$ in acetonitrile (30 mL). The mixture was stirred at room temperature for 2 days. The solution was then filtered off and the blue solid washed four times with 20 mL portions of NCMe, before drying in vacuum (10^{-2} Pa) at room temperature for several hours. Gradually, over a period of several days, the product became blue-violet. Exposure of a sample to air resulted in a color change to grey-brown within a few minutes.

EA: 2.36 mass% Mo.

IR (KBr, cm^{-1}): 3742 w, 3455 vs, 2946 m, 2322 w, 2298 m, 2266 m, 1647 s, 1409 s, 1377 s, 1233 vs, 1084 vs, 966 s, 793 m, 743 m, 668 m, 549 w, 458 vs.

^{29}Si MAS NMR spectrum exhibited two broad resonances at $\delta = -101.9$ (Q₃) and $\delta = -110.1$ (Q₄). Deconvolution/integration gave a Q₃/Q₄ ratio of 0.26.

²⁹Si CP MAS NMR spectrum were consist of three broad resonances at $\delta = -93.7$ (Q₂), $\delta = -100.5$ (Q₃) and $\delta = -109.9$ (Q₄).

¹³C CP MAS NMR (25 °C, ppm): $\delta = 140.0$

(NCCH₃, equatorial), 120 (NCCH₃, axial), 1.6, -1.5 (NCCH₃).

□ **[Mo₂(Ac)₂(CH₃CN)₆][BF₄]₂-MCM-41 (22/MCM-41)**

Calcined MCM-41 (0.4 g) was dehydrated and treated with a 0.014 M solution of [Mo₂(μ-O₂CCH₃)₂(MeCN)₆][BF₄]₂ in NCCH₃ (20 mL). The mixture was stirred at room temperature for 2 days. The solution was then filtered off and the pink solid washed four times with 20 mL portions of NCCH₃, before drying in vacuum (10⁻² Pa) at room temperature for several hours. Exposure of a sample to air resulted in an immediate (< 30 seconds) color change to grey-brown.

EA: 3.62 mass% Mo.

IR (KBr, cm⁻¹): 3455 vs, 2984 m, 2941 m, 2894 m, 2298 w, 2266 w, 1656 s, 1531 m, 1489 m, 1444 s, 1387 s, 1232 vs, 1083 vs, 966 m, 797 m, 752 m, 673 w, 591 w, 554 w, 460 vs.

²⁹Si MAS NMR spectrum exhibited one broad resonance at $\delta = -109.8$ (Q₄).

²⁹Si CP MAS NMR spectrum were consist of three broad resonances at $\delta = -91.8$ (Q₂), $\delta = -101.2$ (Q₃) and $\delta = -109.3$ (Q₄).

¹³C CP MAS NMR (25 °C, ppm): $\delta = 186.5$ (s, O₂CCH₃), 146.0 (NCCH₃), 129.4 (NCCH₃), 19.4 (s, O₂CCH₃), 4.7, 2.2, 1.0, -0.70 (NCCH₃).

□ **[Mo₂(Ac)₂(dppa)₂(MeCN)₂][BF₄]₂-MCM-41 (40/MCM-41)**

Calcined MCM-41 (0.5 g) was dehydrated and mixed with a 0.011 M solution of [Mo₂(μ-O₂CCH₃)₂(dppa)₂(MeCN)₂][BF₄]₂ in NCCH₃ (20 mL). The mixture was stirred at room

temperature for 2 days. The solution was then filtered off and the pink solid washed three times with 30 mL portions of NCCH_3 , before drying in vacuum (10^{-2} Pa) at room temperature for several hours. Gradually, over a period of several days, the product became pink-light brown. Exposure of a sample to air resulted in a color change to gray within one to two hours.

EA: 2.21 mass% Mo.

IR (KBr, cm^{-1}): 3742 vw, 3457 vs, 2926 m, 2857 m, 2264 w, 1656 s, 1592 m, 1483 m, 1440 vs, 1410 s, 1236 vs, 1083 vs, 967 m, 797 s, 743 m, 697 m, 669 m, 527 m, 455 vs.

^{29}Si MAS NMR spectrum exhibited one broad resonance at $\delta = -109.6$ (Q_4).

^{29}Si CP MAS NMR spectrum exhibited two broad resonances at $\delta = -101.0$ (Q_3) and $\delta = -109.7$ (Q_4).

^{13}C CP MAS NMR (25 °C, ppm): $\delta = 176.3$ (s, O_2CCH_3), 130.2, 128.7 (dppa), 13.0 (s, O_2CCH_3), -1.4 (NCCH_3).

^{31}P MAS NMR spectrum (25 °C, ppm): $\delta = 87.3$.

4.5 Cationic Polymerization of Olefins

4.5.1 Polymerization of Cyclopentadiene

In a dry round bottom flask under argon atmosphere (glove box) 40 mL of a solution of dry cyclopentadiene ($c(\text{Cyclopentadiene}) = 2.24$ mol/L for complexes **20-30** and 2.27 mol/L for **31-40**) in dry methylene chloride (drying agent = CaH_2) was added to 0.1 mmol of a Mo_2 - or Rh_2 complex compound (**20-29**) or 0.1 mmol of a Cr compound (**30, 30a, 30b**), or to 0.05 mmol of a other divalent compounds **31-40** resp. under vigorous stirring at room temperature. After 16 h reaction time 3 mL of methanol were added to stop the reaction. The solvent was removed in oil pump vacuum (10 Pa). The yield was determined gravimetrically after drying in a drying oven

(5d, 2000 Pa, 20 °C). Because of the sensitivity of the polycyclopentadiene to radical induced crosslinking all work up steps were performed under O₂-exclusion.

The GPC has been carried out with the following equipment: Waters 510 pump, columns: Waters Ultrastyrigel 500, 1000, 10000, 100000 Å, RI-detector: Waters 410, eluent: THF, flow rate: 0.5 mL/min, calibration standard: polystyrene.

4.5.2 Polymerization of Methylcyclopentadiene

The manipulation procedure was like those for polymerization of cyclopentadiene. 7.2 g (0.9 mol) of methylcyclopentadiene, 0.0242 g (2.94 μmol) or 0.0478 g (5.88 μmol) of [Mo₂(AN)₁₀][BF₄]₄/MCM-41(**20**/MCM-41), 0.0130 g (2.45 μmol) of [Mo₂(Ac)₂(AN)₆][BF₄]₂/MCM-41(**22**/MCM-41), 0.0222 g (2.56 μmol) of [Mo₂(Ac)₂(dppa)₂(AN)₂][BF₄]₂/MCM-41(**40**/MCM-41), were used.

5. Bibliography

Chapter 1A

[1] (a) A. Werner, *Neuere Anschauungen auf dem Gebiete der anorganischen Chemie*, Braunschweig, **1905**; (b) see P. Pfeiffer in *Great Chemists*, ed. E. Farber, Interscience, New York, **1961**, p.1233; (c) excellent general reviews of Werner's publications are to be found in G. B. Kauffmann, *Coord. Chem. Rev.*, **1973**, 9, 339; **1973**, 11, 161; **1974**, 12, 105; **1975**, 15,1.

[2] C. Brosset, *Ark. Kemi, Mineral, Geol.*, **1946**, A20, No. 7; *Ark. Kemi, Mineral Geol.*, **1946**, A22, No. 11.

[3] (a) J. A. Bertrand, F. A. Cotton and W. A. Dollas, *J. Am. Chem. Soc.*, **1963**, 85, 1349; (b) *idem.*, *Inorg. Chem.*, **1963**, 2, 1166; (c) F. A. Cotton and T. E. Haas, *Inorg. Chem.*, **1964**, 3, 10.

[4] W. T. Robinson, J. E. Fergusson and B. R. Penfold, *Proc. Chem. Soc.*, **1963**, 116.

[5] F. A. Cotton and R. A. Walton, *Multiple Bonds between Metal Atoms*, Oxford University Press, New York, **1993**, 2ed.; (b) F. A. Cotton, *Inorg. Chem.*, **1998**, 37, 5710; (c) F. A. Cotton, *J. Chem. Soc., Dalton Trans.*, **2000**, 1961.

[6] (a) F. A. Cotton and J. T. Mague, *Proc. Chem. Soc.*, **1964**, 233; (b) *idem.*, *Inorg. Chem.*, **1964**, 3, 1402; (c) F. A. Cotton and S. J. Lippard, *J. Am. Chem. Soc.*, **1964**, 86, 4497; (d) F. A. Cotton, S. J. Lippard and J. T. Mague, *Inorg. Chem.*, **1965**, 4, 508; (e) J. Gelinek and W. Rudorff, *Naturwiss.*, **1964**, 51, 85.

[7] (a) V. G. Tronev and S. M. Bondin, *Dokl. Akad. Nauk SSSR*, **1952**, 86, 87; (b) A. S. Kotel'nikova and V. G. Tronev, *Zh. Neorg. Khim.*, **1958**, 3, 1008; *Russ. J. Inorg. Chem.*, **1958**, 3, 268; (c) V. G. Kuznetzov and P. A. Koz'min, *Zh. Strukt. Khim.*, **1963**, 4, 55; *J. Struct. Chem.*, **1963**, 4, 49.

[8] (a) F. A. Cotton, N. F. Curtis, B. F. G. Johnson and W. R. Robinson, *Inorg. Chem.*, **1965**, 4, 326; (b) F. A. Cotton and C. B. Harris, *Inorg. Chem.*, **1965**, 4, 330.

- [9] F. A. Cotton, N. F. Curtis, C. B. Harris, B. F. G. Johnson S. J. Lippard, J. T. Mague, W. R. Robinson and J. S. Wood, *Science*, **1964**, 145, 1305.
- [10] F. A. Cotton, G. Wilkinson, C. A. Murillo and M. Bochmann, *Advanced Inorganic Chemistry*, 6th ed., A Wiley-Interscience Publication, John Wiley & Sons, Inc., **1999**.
- [11] (a) F. A. Cotton and F.E. Kühn, *J. Am. Chem. Soc.*, 1996, 118, 5826; (b) F.A. Cotton, J. Eglin, K.J. Wiesinger, *Inorg. Chim. Acta*, **1992**, 195, 11; (c) D.I. Arnold, F.A. Cotton, F.E. Kühn, *Inorg. Chem.*, **1996**, 35, 4733; (d) F.A. Cotton, F.E. Kühn, A. Yokochi, *Inorg. Chim. Acta*, **1996**, 252, 251; (e) Y.Y. Wu, J.D. Chen, L.S. Liou, J.C. Wang, *Inorg. Chim. Acta*, **1997**, 258, 193; (f) D.I. Arnold, F.A. Cotton, F.E. Kühn, *Inorg. Chem.*, **1996**, 35, 5764; (g) F.A. Cotton, F.E. Kühn, *Inorg. Chim. Acta*, **1996**, 252, 257; (h) L. J. Farrugia, A. McVitie and R. D. Peacock, *Inorg. Chem.*, **1988**, 27, 1257.
- [12] M. McCann, in *Catalysis by Di- and Polynuclear Metal Cluster Complexes*, ed. R. D. Adams and F. A. Cotton, Wiley-VCH, New York, **1998**, p. 145-166.
- [13] M. Bakir and R. A. Walton, *Polyhedron*, **1988**, 7, 1279.
- [14] (a) D.I. Arnold, F.A. Cotton, F.E. Kühn, *Inorg. Chem.*, **1996**, 35, 4733; (b) Y.Y. Wu, J.D. Chen, L.S. Liou, J.C. Wang, *Inorg. Chim. Acta*, **1997**, 258, 193; (f) D.I. Arnold, F.A. Cotton, F.E. Kühn, *Inorg. Chem.*, **1996**, 35, 5764.
- [15] (a) L.J. Farrugia, A. McVitie, R.D. Peacock, *Inorg. Chem.*, **1988**, 27, 1257; (b) F.A. Cotton, J. Eglin, K.J. Wiesinger, *Inorg. Chim. Acta*, **1992**, 195, 11;
- [16] (a) R. H. Cayton and M. H. Chisholm, *J. Am. Chem. Soc.*, **1989**, 111, 8921; (b) R. H. Cayton, M. H. Chisholm, J. C. Huffman and E. B. Lobkovsky, *Angew. Chem., Int. Ed. Engl.*, **1991**, 30, 862; (c) R. H. Cayton, M. H. Chisholm and F. D. Darrington, *Angew. Chem., Int. Ed. Engl.*, **1990**, 29, 1481; (d) K. Mashima, M. Tanaka, Y. Kaneda, A. Fukumoto, H. Mizomoto, K. n Tani, H. Nakono, A. Nakamura, T. Sakagushi, K. Kamada and K. Ohta, *Chem. Lett.*, **1997**, 411; (e) R. H. Cayton, M. H. Chisholm, J. C. Huffman and E. B. Lobkovsky, *J. Am. Chem. Soc.*, **1991**, 113, 8709; (f) M. H. Chisholm, *Acc. Chem. Res.* **2000**, 33, 53.

[17] (a) F. A. Cotton and T. R. Felthouse, *Inorg. Chem.*, **1980**, *19*, 328; (b) M. C. Kerby, B. W. Eichhorn, J. A. Creighton and K. P. C. Vllhardt, *Inorg. Chem.*, **1990**, *29*, 1319; (c) F. A. Cotton and T. R. Felthouse, *Inorg. Chem.*, **1981**, *20*, 600.

[18] M. McCann in *Catalysis by Di- and Polynuclear Metal Cluster Complexes*, (Eds.: R. D. Adams, F. A. Cotton), Wiley-VCH, New York, **1998**.

[19] P. Legzdins, G. L. Rempel and G. Wilkinson, *J. Chem. Soc., Chem. Commun.*, **1969**, 825.

[20] (a) M. McCann, P. Guinan, *Polyhedron*, **1991**, *10*, 2283; (b) M. McCann, E. Mac Giolla Coda, *J. Mol. Catal.*, **1996**, *A 109*, 99; (c) F. L. Lufa, I. A. Poleteava, V. A. Korner, B. D. Babitsky, M. I. Lobach, V. V. Markova and L. A. Churlyaeva, British Patent 1338155 (1973).

[21] (a) J. G. Hamilton, K. J. Iviv, M. McCann and J. J. Rooney, *Makromol. Chem.*, **1985**, *186*, 1477; (b) H. E. Ardrill, R. M. E. Greene, J. G. Hamilton, H. T. Ho, K. J. Iviv, G. Lapienis, M. McCann and J. J. Rooney, *Am. Chem. Soc. Symp. Ser.*, 286 (American Chemical Society, Washington, DC, **1985**), P. 275; (c) M. McCann, D. McDonnell, unpublished results, cited by M. McCann in *Catalysis by Di- and Polynuclear Metal Cluster Complexes*, (Eds.: R. D. Adams, F. A. Cotton), Wiley-VCH, New York, **1998**; (d) P. Guinan and M. McCann, *Polyhedron*, **1992**, *11*, 205; (e) E. Whelan, M. Devereux, M. McCann and V. McKee, *J. Chem. Soc. Chem. Commun.*, **1997**, 427; (e) M. McCann, E. Mac Gilloa Coda and K. Maddock, *J. Chem. Soc., Dalton. Trans.*, **1994**, 1489.

[22] (a) K. J. Ivin, *Olefin Metathesis* (Academic Press, London, 1983); (b) V. Dragutan, A. T. Balaban and M. Dimonie, *Olefin Metathesis and Ring-Opening Polymerization of Cyclo-Olefins* (Wiley, New York, 1985 and Editura Academic, Bucarest); (c) R. H. Crabtree, *The Organometallic Chemistry of the transition Metals*, 2nd ed. (Wiley, New York, 1994), Chap. 11; (d) R. Streck, *J. Mol. Catal.*, **1988**, *46*, 305; (e) J. Smith, W. Mowat, D. A. Whan and E. A. V. Ebaworth, *J. Chem. Soc., Dalton Trans.*, **1974**, 1742; (f) R. F. Howe, *J. Chem. Soc., Faraday Trans.*, **1975**, *1*, 1689; (g) Q. Zhang, A. Fukuoka, T. Fujimoto, K. Tanaka and M. Ichikawa, *J. Chem. Soc., Chem. Commun.*, **1991**, 745; (h) A. Morris, H. Thomas and C. J. Attridge, British Patent 1372852 (1972); Imperial Chemical Industries Ltd., French Patent 2130509 (1972); (i) J. P. Candlin, German Patent 2213947 (1973); (j) J. P. Candlin and H. Thomas, *Adv. Chem.*, **1974**,

Ser. 132, 212; (k) Y. Iwasawa, M. Yamagishi and S. Ogasawara, *J. Chem. Soc., Chem. Commun.*, **1980**, 871; (l) Y. Iwasawa, S. Ogasawara, Y. Sato and H. Kuroda, *Proc. Climax 4th. Int. Conf. The Chemistry and Uses of Molybdenum*, **1980**, p. 283; (m) Y. Sato, Y Iwasawa and H. Kuroda, *Chem. Lett.*, **1982**, 1101; (n) Y. Iwasawa and M. Yamagishi, *J. Catal.*, **1983**, 82, 289; (o) Y. Iwasawa, Y. Sato and H. Kuroda, *J. Catal.*, **1983**, 82, 373; (p) W. P. McKenna and E. M. Eyring, *J. Mol. Catal.*, **1982**, 29, 363.

[23] R. F. Vogel, R. J. Rennard and J. A. Tabacek, British Patent 2139913A (**1984**); (b) H. Alper and C. Blais, *J. Chem. Soc., Chem. Commun.*, **1980**,169.

[24] (a) M. H. Chisholm in *Metal-Metal Bonds and Clusters in Chemistry and Catalysis*, J. P. Fackler, Jr.,Ed.(Plenum Press, New York, **1990**), p. 55; (b) M. H. Chisholm and J. A. Klang, *J. Am. Chem. Soc.*, **1989**, 111, 2324.

[25] (a) W. Clegg, G. Pimblett and C. D. Gatner, *polyhedron*, **1986**, 5, 31; (b) G. Pimblett, C. D. Gatner and W. Clegg, *J. Chem. Soc., Dalton Trans.*, **1986**, 1257; (c) F. A. Cotton, A. H. Reid and W. Schwotzer, *Inorg. Chem.*, **1985**, 24, 3965.

Chapter 2A

[1] F. A. Cotton and R. A. Walton, *Multiple Bonds between Metal Atoms*, Oxford University Press, New York, **1993**, 2ed.

Chapter 2A.1

[1] M. Bakir., R.A. Walton, *Polyhedron*, **1988**, 7, 1279.

[2] (a) L.J. Farrugia, A. McVitie, R.D. Peacock, *Inorg. Chem.*, **1988**, 27, 1257; (b) F.A. Cotton, J. Eglin, K.J. Wiesinger, *Inorg. Chim. Acta*, **1992**, 195, 11; (c) D.I. Arnold, F.A. Cotton, F.E. Kühn, *Inorg. Chem.*, **1996**, 35, 4733; (d) F.A. Cotton, F.E. Kühn, A. Yokochi, *Inorg. Chim. Acta*, **1996**, 252, 251; (e) Y.Y. Wu, J.D. Chen, L.S. Liou, J.C. Wang, *Inorg. Chim. Acta*, **1997**, 258, 193; (f) D.I. Arnold, F.A. Cotton, F.E. Kühn, *Inorg. Chem.*, **1996**, 35, 5764; (g) F.A. Cotton, F.E. Kühn, *Inorg. Chim. Acta*, **1996**, 252, 257.

[3] F.E. Kühn, I.S. Gonçalves, A.D. Lopes, J.P. Lopes, C.C. Romão, W. Wachter, J. Mink, L. Hajba, J.A. Parola, F. Pina, J. Sotomayor, *Eur. J. Inorg. Chem.*, **1999**, 295.

- [4] F.A. Cotton, R.A. Walton, *Multiple Bonds between Metal Atoms*, 2nd ed.; Oxford University Press, London 1993 and references cited therein.
- [5] A. L. Spek, *PLATON*, A Multipurpose Crystallographic Tool, Utrecht University, **1999**.
- [6] A. Carvill, P. Higgins, G.M. McCaan, H.Ryan, A. Shiels, *J. Chem. Soc., Dalton Trans.*, **1989**, 2435.
- [7] A. Das, J.C. Jeffery, J.P. Maher, J.A. McCleverty, E. Schatz, M.D. Ward, G. Wollermann, *Inorg. Chem.* **1993**, **32**, 2145.
- [8] P. Vella, J. Zubietta, *J. Inorg. Nucl. Chem.*, **1978**, **40**, 477.

Chapter 2A.2

- [1] (a) M. Handa, H. Matsumoto, D. Yoshioka, R. Nukada, M. Mikuriya, I. Hiromitsu, K. Kasuga, *Bull. Chem. Soc. Jpn.*, **1998**, **71**, 1811; (b) M. Handa, M. Mikuriya, T. Kotera, K. Yamada, T. Nakao, H. Matsumoto, K. Kasuga, *Bull. Chem. Soc. Jpn.*, **1995**, **68**, 2567; (c) X. Ouyang, C. Campana, K.R. Dunbar, *Inorg. Chem.*, **1996**, **35**, 7188; (d) M. Handa, H. Matsumoto, T. Namura, T. Nagaoka, K. Kasuga, M. Mikuriya, T. Kotera, R. Nukada, *Chem. Lett.*, **1995**, 903; (e) F.A. Cotton, Y. Kim, J. Lu, *Inorg. Chim. Acta*, **1994**, **221**, 1; (f) M. Handa, M. Mikuriya, R. Nukada, H. Matsumoto, K. Kasuga, *Bull. Chem. Soc. Jpn.*, **1994**, **67**, 3125; (g) F.A. Cotton, Y. Kim *J. Am. Chem. Soc.*, **1993**, **115**, 8511; (h) M. Handa, K. Yamada, T. Nakao, K. Kasuga, M. Mikuriya, T. Kotera, *Chem. Lett.*, **1993**, 1969; (i) M. Handa, K. Kasamatsu, K. Kasuga, M. Mikuriya, T. Fujii, *Chem. Lett.*, **1990**, 1753; (j) M.C. Kerby, B.W. Eichorn, J.A. Creighton, K.P.C. Vollhardt, *Inorg. Chem.*, **1990**, **29**, 1319.
- [2] F.A. Cotton, R.A. Walton, *Multiple Bonds between Metal Atoms*, 2nd ed.; Oxford University Press, London 1993 and references cited therein.
- [3] F.A. Cotton, E. A. Hillard, C. A. Murillo and H.-C. Zhou, *J. Am. Chem. Soc.*, **2000**, **122**, 416.
- [4] (a) D.I. Arnold, F.A. Cotton, F.E. Kühn, *Inorg. Chem.*, **1996**, **35**, 4733; (b) F.A. Cotton, F.E. Kühn, A. Yokochi, *Inorg. Chim. Acta*, **1996**, **252**, 251; (c) Y.Y. Wu, J.D. Chen, L.S. Liou, J.C. Wang, *Inorg. Chim. Acta*, **1997**, **258**, 193; (d) F.A. Cotton, F.E. Kühn, *Inorg. Chim. Acta*, **1996**, **252**, 257.
- [5] F.A. Cotton, T.R. Felthouse, *Acta Cryst.*, 1984, **C40**, 42.

Chapter 2A.3

- [1] (a) Z.-Z. Zhang and H. Cheng, *Coord. Chem. Rev.*, **1996**, 147, 1; (b) G. R. Newcomer, *Chem. Rev.*, **1993**, 93, 2067.
- [2] (a) C.-Y. Kuo, Y.-S. Fuh., J.-Y. Shiue, S. J. Yu, G.-H. Lee and S.-M. Peng, *J. Organomet. Chem.*, **1999**, 588, 260; (b) N. D. Jones, K. S. MacFarlane, M. B. Smith, R. P. Schutte, S. J. Rettig and B. R. James, *Inorg. Chem.*, **1999**, 38, 3956; (c) T. Nicholson, M. Hirsch-Kuchma, A. Shellenbarger-Jones, A. Davison, and A., Jones, *Inorg. Chim. Acta*, **1998**, 267, 319; (d) R. P. Schutte, S. J. Rettig, A. M. Joshi and B. R. James, *Inorg. Chem.*, **1997**, 36, 5809; (e) I. R. Baird, M. B. Smith and B. R., James, *Inorg. Chim. Acta*, **1995**, 235, 291; (f) P. Braustein, D. G. Kelly, A. Tiripicchio and F. Ugozzoli, *Bull. Soc. Chim. Fr.*, **1995**, 132, 1083; (g) Y. Xie, C.-L. Lee, Y. Yang, S. J. Rettig and B. R. James, *Can. J. Chem.*, **1992**, 70, 751.
- [3] (a) G. Franciò, R. Scopelliti, C. G. Arena, G. Bruno, D. Drommi, and F. Faraone, *Organometallics*, **1998**, 17, 338; (b) W.-H. Chan, Z.-Z. Zhang, T. C. W. Mak and C.-M. Che, *J. Chem. Soc., Dalton Trans.*, **1998**, 803; (c) S.-M. Kuang, F. Xue, Z.-Z. Zhang, W.-M. Xue, C.-M. Che and , T. C. W. Mak, *J. Chem. Soc., Dalton Trans.*, **1997**, 3409; (d) S.-M. Kuang, H. Cheng, L.-J. Sun., Z.-Z. Zhang, , Z. Y. Zhou, B.-M. B.-M. Wu and T. C. W. Mak, *Polyhedron*, **1996**, 15, 3417; (e) L. Y. Xie and B. R. James, *Inorg. Chim. Acta*, **1994**, 217, 209; (f) E. Rotondo, G. Bruno, F. Nicolò, S. Lo Schiavo, and P. Piraino, *Inorg. Chem.*, **1991**, 30, 1195; (g) P. W. Schrier, D. R. Derringer, P. E. Fanwick, and R. A. Walton, *Inorg. Chem.*, **1990**, 29, 12290; (h) F. A. Cotton, and M. Matusz, *Inorg. Chim. Acta*, **1988**, 143, 45; (i) F. A. Cotton, and M. Matusz, *Polyhedron*, **1988**, 7, 2201; (j) T. J. Barder, F. A. Cotton, G. L. Powell, S. M. Tetrick and R. A. Walton, *J. Am. Chem. Soc.*, **1984**, 106, 1323.
- [4] (a) R. Gobetto, C. G. Arena, D. Drommi and F. Faraone, *Inorg. Chim. Acta*, **1996**, 248, 257; (b) A. J. Deeming and , M. B. Smith, *J. Chem. Soc., Chem. Commun.*, **1993**, 844 and references therein.
- [5] P. Braustein, M. Knorr, M. Strmpfer, A. De Cian and J. Fischer, *J. Chem. Soc., Dalton Trans.*, **1994**, 117.
- [6] N. W. Alcock, P. Moore, P. A. Lampe and K. F. Mok, *J. Chem. Soc., Dalton Trans.*, **1982**, 207.

- [7] (a) W.-J. Zao, T.-Q. Fang, S.-Q. Zhang, Z.-Z. Zhang and L.-M. Yang, *J. Chem. Eng. Natural Gas*, **1992**, 17, 3; through Ref. 1b. (b) CA: **119**,P 202967.
- [8] (a) J. San Filippo, Jr and H. J. Sniadoch, *Inorg. Chem.*, **1973**, 12, 2326; (b) F. A. Cotton and J. G. Norman, Jr, *J. Am. Chem. Soc.*, **1972**, 94, 5697.
- [9] F.A. Cotton, R.A. Walton, *Multiple Bonds between Metal Atoms*, 2nd ed.; Oxford University Press, London 1993 and references cited therein.
- [10] M. C. Kerby, B. W. Eichhorn, J. A. Creighton, and K. P. C. Vollhardt, *Inorg. Chem.*, **1990**, 29, 1319.

Chapter 2B:

- [1] O. Nuyken, St. D. Pask (**1989**), *Comprehensive Polymer Science*, Vol. 3, P629-630, Pergamon Press plc., Oxford, England.
- [2] I. Kuntz, in H. F. Mark, N. Bikales and C. G. Overberger (ed.), *Encyclopedia of Polymer Science and Engineering*, 2nd Ed. Vol. 4, Wiley, New York, 1990, p. 537-542, and references therein.
- [3] D. W. Klosiewicz, US Pat. 4400340 (1983); R. P. Geer and R. D. Stoutland, *Plastics* 85. Proceedings of the SPE 43rd Annual Technical Conference, ANTEC '85 (1985) 1232.
- [4] H. Staudinger and H. A. Bruson, *Ann.*, **1926**, 447, 110.
- [5] U. Schädeli and M. Neunschwander, *Chimia*; **1986**, 40, 239.

Chapter2B.1

- [1] H. Staudinger and H. A. Bruson, *Ann.*, **1926**, 447, 97.
- [2] (a) B. Eisler, A. Wassermann, F. D. Farnsworth, D. Kendrink and Schnurminn, *Nature*, **1951**, 180, 459; (b) P. V. French, L. Roubinek and A. Wassermann, *J. Chem. Soc.*, **1961**, 1953; (c) J. Murphy, L. Roubinek and A. Wassermann, *J. Chem. Soc.*, **1961**, 1964.
- [3] S.-P. S. Yen., *Polym. Prep.*, **1963**, 4, 82.

[4] (a) S. Kohjiya, A. Terada and S. Yamashita, *Chem. Lett.*, **1972**, 671; (b) S. Kohjiya and S. Yamashita, *Chem. Lett.*, **1973**, 1007.

[5] (a) J. F. Brown, Jr. and D. M. White, *J. Am. Chem. Soc.*, **1960**, 82, 5671; (b) C. Aso, T. Kunitake and Y. Ishimoto, *Bull. Chem. Soc. Jpn.*, **1967**, 40, 2894.

[6] H. Tsutsumi, M. Miyata and K. Takemoto, *Polym. J.*, **1987**, 19, 1321.

[7] (a) M. McCann in *Catalysis by Di- and Polynuclear Metal Cluster Complexes*, (Eds.: R. D. Adams, F. A. Cotton), Wiley-VCH, New York, **1998**, 145-166; (b) M. McCann, P. Guinan, *Polyhedron*, **1991**, 10, 2283; (c) M. McCann, E. Mac Giolla Coda, *J. Mol. Catal.* **1996**, A 109, 99.

[8] (a) C. Aso, T. Kunitake, Y. Ishimoto, *J. Polym. Sci., Part A: Polym. Chem.*, **1968**, 6, 1163; (b) C. Aso, T. Kunitake, Y. Ishimoto, *J. Polym. Sci., Part A: Polym. Chem.*, **1968**, 6, 1175; (c) C. Aso, T. Kunitake, K. Ito, Y. Ishimoto, *J. Polym. Sci., Part B: Polym. Lett.*, **1966**, 4, 701; (d) G. Heublein, G. Albrecht, G. Knöppel, *J. Macromol. Sci. Chem.*, **1984**, A21, 1355; (e) G. Heublein, G. Knöppel, D. Stadermann, *Polym. Bull. (Berlin)*, **1988**, 20, 109; (f) S. Spange, E. Langhammer, *Macromol. Chem. Phys.*, **1997**, 198, 431; (g) S. Spange, E. Langhammer, *Macromol. Chem. Phys.*, **1997**, 198, 2993; (h) J. P. Kennedy, *Cationic Polymerisation of Olefins: A Critical Inventory*, John Wiley & Sons, INC., New York, pp. 178-185 and refs cited therein (**1975**).

[9] (a) F. A. Cotton, C. A. Murillo, L. Daniels, X. Wang, *Polyhedron*, **1998**, 17, 2781; (b) F. A. Cotton, L. Daniels, S. C. Haefner, F. E. Kühn, *Inorg. Chimia Acta*, **1999**, 287, 159.

[10] R. T. Henriques, E. Herdtweck, F. E. Kühn, A. D. Lopes, J. Mink, C. C. Romão, *J. Chem. Soc., Dalton Trans.*, **1998**, 1293.

Chapter 2B.2

[1] DE 19729817 (1997), BASF AG., Erf.: W. Risse, C. Mehler, E. Conner., Chem. Abstr. Vol. 190, No. 9, (1999) Chem. Abstr. No. 130.110748.

[2] R. T. Henriques, E. Herdtweck, F. E. Kühn, A. D. Lopes, J. Mink, C. C. Romão, *J. Chem. Soc., Dalton Trans.*, **1998**, 1293.

- [3] S. J. Anderson, F. J. Wells, G. Wilkinson, B. Hussain, M. B. Hursthouse, *Polyhedron*, **1988**, 7, 2615.
- [4] B. J. Hathaway, D. G. Holah, A. E. Underhill, *J. Chem. Soc.*, **1962**, 2444.
- [5] B. J. Hathaway, D. G. Holah, *J. Chem. Soc.*, **1964**, 2400.
- [6] B. J. Hathaway, D. G. Holah, *J. Chem. Soc.*, **1964**, 2408.
- [7] J. P. Fackler, D. G. Holah, *Inorg. Chem.*, **1965**, 4, 945.
- [8] W. E. Buschmann, J. S. Miller, *Chem. Eur. J.*, **1998**, 4, 1731.
- [9] (a) M. W. Duckworth, G. W. A. Fowles and R. A. Hoodless, *J. Chem. Sci.*, **1963**, 5665; (b) Simon J. Anderson, Fionna J. Wells and Geoffery Wikinson, *Polyhedron*, **1988**, 7(24), 2615.
- [10] J. Reedijk, A. P. Groeneveld, *Rec. Trav. Chim.*, **1967**, 86, 1127.
- [11] L. E. Orgel, *An introduction to transition-metal chemistry*, Wiley, New York, pp 69 – 85 (**1960**).
- [12] F. A. Cotton, L. Daniels, S. C. Haefner, F. E. Kühn, *Inorg. Chimia Acta*, **1999**, 287, 159.
- [13] (a) F. A. Cotton, K. J. Wiesinger, *Inorg. Chem.*, **1991**, 30, 871; (b) F. A. Cotton, F. E. Kühn, *Inorg. Chim. Acta*, **1996**, 252, 257; (c) F. A. Cotton, F. E. Kühn, *J. Am. Chem. Soc.*, 1996, 118, 5826.
- [14] (a) C. Aso, T. Kunitake, Y. Ishimoto, *J. Polym. Sci., Part A: Polym. Chem.*, **1968**, 6, 1163; (b) C. Aso, T. Kunitake, Y. Ishimoto, *J. Polym. Sci., Part A: Polym. Chem.*, **1968**, 6, 1175; (c) C. Aso, T. Kunitake, K. Ito, Y. Ishimoto, *J. Polym. Sci., Part B: Polym. Lett.*, **1966**, 4, 701;

Chapter 2B.3

- [1] M. McCann, in *Catalysis by Di- and Polynuclear Metal Cluster Complexes*, ed. R. D. Adams and F. A. Cotton, Wiley-VCH, New York, **1998**, p. 145–166;
- [2] (a) M. McCann and E. M. G. Coda, *J. Mol. Catal. A: Chemical*, **1996**, 109, 99; (b) M. McCann, E. M. G. Coda and K. Maddock, *J. Chem. Soc., Dalton Trans.*, **1994**, 1489.
- [3] (a) J. Smith, W. Mowat, D. A. Whan and E. A. V. Ebsworth, *J. Chem. Soc., Dalton Trans.*, **1974**, 1742; (b) Q. Zhuang, A. Fukuoka, T. Fujimoto, K. Tanaka and M. Ichikawa, *J. Chem. Soc., Chem. Commun.*, **1991**, 745.
- [4] Y. Iwasawa, S. Ogasawara, Y. Sato and H. Kuroda, *Proc. Climax 4th Int. Conf. The Chemistry and Uses of Molybdenum*, **1980**, p. 283.

- [5] (a) K. Moller and T. Bein, *Chem. Mater.*, **1998**, *10*, 2950; (b) T. Maschmeyer, *Curr. Opin. Solid State Mater. Sci.*, **1998**, *3*, 71; (c) R. A. Sheldon, I. W. C. E. Arends and H. E. B. Lempers, *Catal. Today*, **1998**, *41*, 387.
- [6] (a) C. T. Kresge, M. E. Leonowicz, W. J. Roth, J. C. Vartuli and J. S. Beck, *Nature*, **1992**, *359*, 710; (b) J.S. Beck, J.C. Vartuli, W.J. Roth, M.E. Leonowicz, C.T. Kresge, K.D. Schmitt, C.T.-W. Chu, D.H. Olson, E.W. Sheppard, S.B. McCullen, J.B. Higgins and J.L. Schlenker, *J. Am. Chem. Soc.*, **1992**, *114*, 10834.
- [7] F. A. Cotton and F. E. Kühn, *Inorg. Chim. Acta*, **1996**, *252*, 257.
- [8] M. McCann, E. M. G. Coda and K. Maddock, *J. Chem. Soc., Dalton Trans.*, **1994**, 1489.
- [9] F. A. Cotton and K. J. Wiesinger, *Inorg. Chem.*, **1991**, *30*, 871.
- [10] F. A. Cotton and R. A. Walton, *Multiple Bonds between Metal Atoms*, Oxford University Press, New York, 1993.
- [11] F. A. Cotton, L. Daniels, S. C. Haefner and F. E. Kühn, *Inorg. Chim. Acta*, **1999**, *287*, 159.
- [12] R. Schmidt, M. Stöcker, E. Hansen, D. Akporiaye and O. H. Ellestad, *Microporous Mater.*, **1995**, *3*, 443.
- [13] B. Marler, U. Oberhagemann, S. Voltmann and H. Gies, *Microporous Mater.*, **1996**, *6*, 375.
- [14] M. Morey, A. Davidson, H. Eckert and G. D. Stucky, *Chem. Mater.*, **1996**, *8*, 486.
- [15] I. J. Shannon, T. Maschmeyer, R. D. Oldroyd, G. Sankar, J. M. Thomas, H. Pernot, J. -P. Balikdjian and M. Che, *J. Chem. Soc., Faraday Trans.*, **1998**, *94*, 1495.
- [16] S. Brunauer, L. S. Deming, W. S. Deming and E. Teller, *J. Am. Chem. Soc.*, **1940**, *62*, 1723.
- [17] (a) O. Franke, G. Schulz-Ekloff, J. Rathousky, J. Starek and A. Zunkal, *J. Chem. Soc., Chem. Commun.*, **1993**, 724; (b) P. J. Branton, P. G. Hall and K. S. W. Sing, *J. Chem. Soc., Chem. Commun.*, **1993**, 1257.
- [18] A. A. Romero, M. D. Alba, W. Zhou and J. Klinowski, *J. Phys. Chem. B*, **1997**, *101*, 5294.
- [19] X. S. Zhao, G. Q. Lu, A. K. Whittaker, G. J. Miller and H. Y. Zhu, *J. Phys. Chem. B*, **1997**, *101*, 6525.
- [20] (a) S. O'Brien, J. M. Keates, S. Barlow, M. J. Drewit, B. R. Payne and D. O'Hare, *Chem. Mater.*, **1998**, *10*, 4088; (b) P. Ferreira, I. S. Gonçalves, F. Mosselmans, M. Pillinger, J. Rocha and A. Thursfield, *Eur. J. Inorg. Chem.*, **2000**, 97.
- [21] P. Ferreira, I. S. Gonçalves, F. E. Kühn., M. Pillinger, J. Rocha, A. M. Santos and A. Thursfield, *Eur. J. Inorg. Chem.*, **2000**, 551.

[22] (a) T. Maschmeyer, F. Rey, G. Sankar and J. M. Thomas, *Nature*, **1995**, 378, 159; (b) L. Marchese, E. Gianotti, V. Dellarocca, T. Maschmeyer, F. Rey, S. Coluccia and J. M. Thomas, *Phys. Chem. Chem. Phys.*, **1999**, 1, 585.

[23] D. L. Arnold, F. A. Cotton and F. E. Kühn, *Inorg. Chem.*, **1996**, 35, 4733.

Chapter 2B.4

[1] Q. Zhuang, A. Fukuoka, T. Fujimoto, K. Tanaka and M. Ichikawa, *J. Chem. Soc., Chem. Commun.*, **1991**, 745.

[2] (a) J. Evans, J. T. Gauntlett and J. F. W. Mosselmans, *Faraday Discuss. Chem. Soc.*, **1990**, 89, 107; (b) K. Zama, Y. Imada, A. Fukuoka and M. Ichikawa, *Appl. Catal. A: General*, **2000**, 194-195, 285.

[3] S. P. Cramer, K. O. Hodgson, W. O. Gillum and L. E. Mortenson, *J. Am. Chem. Soc.*, **1978**, 100, 3398.

[4] F. A. Cotton, A. H. Reid, Jr. and W. Schwotzer, *Inorg. Chem.*, **1985**, 24, 3965.

[5] (a) E. I. Stiefel, *Prog. Inorg. Chem.*, **1976**, 22, 1; (b) S. P. Cramer, P. K. Eidem, M. T. Paffett, J. R. Winkler, Z. Dori and H. B. Gray, *J. Am. Chem. Soc.*, **1983**, 105, 799; (c) K. Wieghardt, M. Hahn, W. Swiridoff and J. Weiss, *Inorg. Chem.*, **1984**, 23, 94.

[6] J. R. Knox and C. K. Prout, *Acta Cryst.*, **1969**, B25, 1857.

[7] Y. Sato, Y. Iwasawa and H. Kuroda, *Chem. Lett.*, **1982**, 1101.

[8] F. A. Cotton and K. J. Wiesinger, *Inorg. Chem.*, **1991**, 30, 871.

[9] M. McCann, in *Catalysis by Di- and Polynuclear Metal Cluster Complexes*, ed. R. D. Adams and F. A. Cotton, Wiley-VCH, New York, **1998**, p. 145–166.

[10] J. Ismeier, Ph. D. thesis, Technische Universität München, 1999.

Chapter 3

[1] F. A. Cotton, R. A. Walton, *Multiple Bonds between Metal Atoms*, 2nd ed., Oxford University Press, Oxford, UK, **1993**.

[2] (a) Y. Xie, R. S. Grev, J. Gu, H. F. Schaeffer III, P. V. R. Schleyer, J. Su, X.-W. Li and G. H. Robinson, *J. Am. Chem. Soc.*, **1998**, 120, 3773; (b) F. A. Cotton, A. H. Cowley and X. Feng, *J. Am. Chem. Soc.*, **1998**, 120, 1795.

[3] M. Bakir and R. A. Walton, *Polyhedron*, **1988**, 7, 1279.

[4] M. McCann in *Catalysis by Di- and Polynuclear Metal Cluster Complexes*, (Eds.: R. D. Adams, F. A. Cotton), Wiley-VCH, New York, **1998**, p.145-166 and references therein.

Chapter 4

[1] (a) Z. Otwinowski, W. Minor, "Processing of X-Ray Diffraction Data Collected in Oscillation Mode", *Methods in Enzymology*, **1996**, 276. W. C. Carter, Sweet, Jr. & R. M.; Eds., Academic Press, USA; (b) *International Tables for Crystallography*, Vol. C, Tables 6.1.1.4 (pp. 500-502), 4.2.6.8 (pp. 219-222), and 4.2.4.2 (pp. 193-199), Ed. A.J.C. Wilson, Kluwer Academic Publishers, Dordrecht, The Netherlands, 1992; (c) G. Artus, W. Scherer, T. Priermeier, E. Herdtweck, "STRUX-V", *A Program System to Handle X-Ray Data*, TU München, Germany, **1997**; (d) A.L. Spek, "PLATON", *A Multipurpose Crystallographic Tool*, Utrecht University Utrecht, The Netherlands, **1999**; (e) A. Altomare, G. Cascarano, C. Giacovazzo, A. Guagliardi, M.C. Burla, G. Polidori, M. Camalli "SIR92", *J. Appl. Cryst.*, **1994**, 27, 435; (f) G.M. Sheldrick, "SHELXL-97", University of Göttingen, Göttingen, Germany, **1998**.

[2] N. Binsted, EXCURV98, CCLRC Daresbury Laboratory computer programme, 1998.

[3] S. J. Gurman, N. Binsted and I. Ross, *J. Phys. C*, 1984, 17, 143; 1986, 19, 1845.

[4] F. W. Lytle, D. E. Sayers and E. A. Stern, Report of the International Workshop on Standards and Criteria in X-ray Absorption Spectroscopy, *Physica B*, 1989, 158, 701-722

[5] M.-C. Chiang, W. H. Hartung, *J. Org. Chem.*, **1945**, 10, 21.

[6] D. Ciana, A. Haim, *J. Heterocyclic Chem.*, **1984**, 21, 607.

[7] H. Schmidbauer and Y. Inoguchi, *Z. Naturforsch.*, **1980**, 35b, 1329.

[8] F. R. Keene, M. R. Snow, P. J. Stephenson and E. R. T. Tiekink, *Inorg. Chem.*, **1988**, 27, 2040.

[9] (a) F.A. Cotton, K. Wiesinger, *Inorg. Chem.*, **1991**, 30, 871; (b) F.A. Cotton, K. Wiesinger, *Inorg. Synth.*, **1992**, 29, 134; (c) F.A. Cotton, F.E. Kühn, *J. Am. Chem. Soc.*, **1996**, 118, 5826; (d)

F.A. Cotton, C.A. Murillo, L. Daniels, X. Wang, *Polyhedron*, **1998**, *17*, 2781; (e) G. Pimblett, C.D. Garner and W. Clegg, *J. Chem. Soc., Dalton Trans.*, **1986**, 1257.

[10] (a) F. A. Cotton, L. Daniels, S. C. Haefner, F. E. Kühn, *Inorg. Chimica Acta*, **1999**, 287, 159; (b) F. A. Cotton, F. E. Kühn, *Inorg. Chim. Acta* , **1996**, 252, 257; (c) J. C. Menezes, C. C. Romão, *Polyhedron*, , **1990**, 9, 1237; (d) (c) F. A. Cotton, F. E. Kühn, *J. Am. Chem. Soc.* , **1996**, *118*, 5826-5827; (e) K. R. Dunbar, *J. Am. Chem. Soc.* , **1988**, *110*, 8247; (f) R. T. Henriques, E. Herdtweck, F. E. Kühn, A. D. Lopes, J. Mink, C. C. Romão, *J. Chem. Soc., Dalton Trans.* , **1998**, 1293;

[11] (a) M.W. Duckworth, G. W. A. Fowles and R: A. Hoodless, *J. Chem. Sci.*, **1963**, 5665; (b) Simon J. Anderson, Fionna J. Wells and Geoffery Wilkinson, *Polyhedron*, **1988**, 7(24) 2615.

[12] R. T. Henriques, E. Herdtweck, F. E. Kühn, A. D. Lopes, J. Mink, C. C. Romão, *J. Chem. Soc., Dalton Trans.*, **1998**, 1293.

[13] B. J. Hathaway, D. G. Holah, A. E. Underhill, *J. Chem. Soc.*, **1962**, 2444.

[14] W. E. Buschmann, J. S. Miller, *Chem. Eur. J.*, **1998**, *4*, 1731.

[15] (a) C. T. Kresge, M. E. Leonowicz, W. J. Roth, J. C. Vartuli and J. S. Beck, *Nature*, **1992**, *359*, 710; (b) J.S. Beck, J.C. Vartuli, W.J. Roth, M.E. Leonowicz, C.T. Kresge, K.D. Schmitt, C.T.-W. Chu, D.H. Olson, E.W. Sheppard, S.B. McCullen, J.B. Higgins and J.L. Schlenker, *J. Am. Chem. Soc.*, **1992**, *114*, 10834.

[16] (a) C. P. Jaroniec, R. K. Gilpin and M. Jaroniec, *J. Phys. Chem. B*, **1997**, *101*, 6861; (b) C. P. Jaroniec, M. Kruk, M. Jaroniec and A. Sayari, *J. Phys. Chem. B*, **1998**, *102*, 5503.

[17] F. A. Cotton, A. H. Reid and W. Schwotzer, *Inorg. Chem.*, **1985**, *24*, 3965.

[18] (a) C. P. Jaroniec, R. K. Gilpin and M. Jaroniec, *J. Phys. Chem. B*, **1997**, *101*, 6861; (b) C. P. Jaroniec, M. Kruk, M. Jaroniec and A. Sayari, *J. Phys. Chem. B*, **1998**, *102*, 5503.

Appendix

Table 1. Crystallographic data for **1**·4(CH₃CN), **2**·2(CH₂Cl₂), **2**·1/2(C₄H₁₀O, C₆H₁₄), **4** and **5**

	1 ·4(CH ₃ CN)	2 ·2(CH ₂ Cl ₂)	2 ·1/2(C ₄ H ₁₀ O, C ₆ H ₁₄)	4	5
Chemical formula	C ₆₆ H ₇₀ B ₂ F ₈ Mo ₂ N ₈ O ₄ P ₄	C ₁₁₂ H ₁₁₂ B ₄ Cl ₈ F ₁₆ Mo ₄ N ₄ O ₈ P ₈	C ₁₁₈ H ₁₂₈ B ₄ F ₁₆ Mo ₄ N ₄ O ₉ P ₈	C ₆₈ H ₆₂ B ₂ F ₈ Mo ₂ N ₄ O ₄ P ₄	C ₇₂ H ₆₂ B ₂ F ₈ Mo ₂ N ₄ O ₄ P ₄
Molecular weight	1528.68	2904.42	2725.01	1488.60	1536.64
Crystal system	Monoclinic	Triclinic	Triclinic	Monoclinic	Monoclinic
Space group	P 2 ₁ /c	P $\bar{1}$	P $\bar{1}$	P 2 ₁ /n	P 2 ₁ /n
a/pm	1257.0(5)	1371.1(1)	1580.37(3)	1371.89(4)	1330.57(3)
b/pm	2413.5(5)	1400.3(1)	1913.09(3)	1619.30(5)	1641.02(3)
c/pm	2296.9(9)	1782.2(2)	2226.22(4)	1544.51(5)	1639.23(4)
α /°		68.73(1)	77.758(1)		
β /°	93.75(2)	77.20(1)	69.838(1)	105.437(1)	103.550(1)
γ /°		89.44(1)	77.453(1)		
V/10 ⁶ pm ³	6953(4)	3100.0(5)	6097.9(2)	3307.3(2)	3479.6(1)
Z	4	1	2	2	2
T/K	163	163	143	163	143
ρ calcd/g cm ⁻³	1.460	1.556	1.484	1.495	1.467
μ /mm ⁻¹	4.451	0.750	0.588	0.550	0.525
Data collected (<i>h, k, l</i>)	+15, +25, \pm 27	\pm 16, \pm 16, \pm 21	\pm 19, \pm 23, \pm 27	\pm 17, \pm 20, \pm 19	\pm 17, \pm 19, \pm 21
No. of reflections collected	13023	30270	45149	20864	14627
No. of independent reflections	12451	10855	24833	6982	7325
R _{int}	0.0306	0.0276	0.0280	0.0400	0.0306

Table 1 *continued*

R1 ^a	0.0479	0.0542	0.0554	0.0580	0.0420
wR2 ^b	0.1044	0.1293	0.0877	0.1099	0.0775
GOF ^c	1.157	1.075	1.019	1.052	1.011

^a $RI = \sum(|F_o| - |F_c|) / \sum|F_o|$; ^b $wR2 = [\sum_w (F_o^2 - F_c^2)^2 / \sum_w (F_o^2)^2]^{1/2}$; ^c $GOF = [\sum_w (F_o^2 - F_c^2)^2 / (NO - NV)]^{1/2}$.

Table 2. Selected interatomic distances (pm), angles ($^{\circ}$) and torsion angles ($^{\circ}$) for **1**·4(CH₃CN), **2**·2(CH₂Cl₂), **2**·1/2(C₄H₁₀O, C₆H₁₄), **4** and **5**

		1 ·4(CH ₃ CN)	2 ·2(CH ₂ Cl ₂)	2 ·1/2(C ₄ H ₁₀ O, C ₆ H ₁₄) ^a	4	5
Mo - Mo'	A	211.33(9)	211.52(5)	211.51(3)		213.15(3)
	B	212.95(9)	211.09(6)	211.61(3)		
Mo - P1	A	255.90(14)	257.61(11)	258.17(9)	255.32(9)	257.03(5)
	B	257.25(14)	257.81(13)	257.05(9)	258.02(9)	
Mo - P2'	A	256.07(14)	258.60(12)	260.28(9)	260.27(9)	258.39(5)
	B	257.09(14)	259.43(11)	259.18(9)	258.38(9)	
Mo - O1	A	209.7(2)	208.3(3)	208.2(2)	208.7(2)	209.50(15)
	B	207.9(3)	208.1(3)	209.6(2)	209.5(2)	
Mo - O2'	A	209.5(2)	211.0(3)	210.7(2)	211.3(2)	210.12(15)
	B	209.6(3)	211.2(3)	210.8(2)	209.9(2)	
Mo - L	A	264.8(4)	250.5(5)	252.0(2)	258.0(3)	258.2(2)
	B	263.9(4)		252.7(2)	259.2(2)	
P1 - N1	A	168.8(3)	169.5(3)	169.4(3)	169.4(3)	169.4(2)
	B	169.1(3)	170.0(4)	169.2(3)	169.4(3)	
P2 - N1	A	168.1(3)	168.6(4)	169.6(3)	170.3(3)	169.9(2)
	B	168.3(3)	169.0(4)	169.7(3)	169.1(3)	
O1 - C2	A	126.2(5)	126.4(4)	127.5(4)	127.6(4)	127.3(3)
	B	126.6(4)	126.9(4)	127.9(4)	127.7(4)	
O2 - C2	A	127.4(4)	127.9(5)	128.4(4)	127.5(4)	127.6(3)
	B	127.8(4)	126.7(5)	127.3(4)	127.8(4)	

Table 2 continued

		1·4(CH ₃ CN)	2·2(CH ₂ Cl ₂)	2·1/2(C ₄ H ₁₀ O, C ₆ H ₁₄) ^a	4	5
N1 - C3	A	147.3(5)	148.4(6)	148.0(5)	148.6(4)	147.8(5)
	B	147.1(5)	148.9(6)	148.3(4)	148.1(4)	
C2 - C1	A	149.5(5)	149.3(6)	147.9(5)	149.4(5)	149.8(5)
	B	148.1(5)	148.2(7)	149.6(4)	149.2(4)	150.0(4)
Mo' - Mo - L	A	175.56(9)	177.79(15)	177.13(6)	177.56(7)	179.40(9)
	B	178.06(10)		175.57(6)	175.17(6)	178.03(6)
Mo - L - X	A	144.5(4)	172.5(5)	175.1(2)	166.1(3)	156.8(4)
	B	162.5(4)		156.7(2)	173.3(2)	164.9(2)
P1 - Mo - P2'	A	161.63(4)	160.13(4)	160.60(3)	160.43(3)	161.22(3)
	B	160.77(4)	160.28(4)	163.62(3)	163.53(3)	161.61(2)
O1 - Mo - O2'	A	177.43(10)	177.04(10)	176.72(8)	177.16(8)	177.57(9)
	B	177.64(9)	177.31(11)	176.95(8)	176.60(8)	177.42(6)
P1 - N1 - P2	A	117.72(16)	117.9(2)	118.62(16)	116.81(16)	117.58(17)
	B	118.31(16)	118.3(2)	117.10(16)	118.38(16)	117.85(11)
O1 - C2 - O2	A	121.0(3)	121.7(4)	121.1(3)	121.4(3)	121.1(3)
	B	121.1(3)	121.1(3)	121.2(3)	121.5(3)	121.6(2)
P1 - Mo - Mo' - P2	A	-7.23(4)	-11.19(4)	-9.02(3)	10.32(3)	-8.80(3)
	B	-10.14(4)	-10.00(4)	13.22(3)	10.47(3)	-7.34(2)
O1 - Mo - Mo' - O2	A	-0.26(10)	-0.67(11)	0.77(8)	1.29(9)	-0.08(9)
	B	-0.18(9)	-0.12(19)	3.98(9)	3.72(8)	0.32(7)

^a The bond distances and angles given in column 6 are caused by loss of crystallographic symmetry

Table 3. Selected interatomic distances (pm), angles (°) and torsion angles (°) for **10·CH₂Cl₂^a**

Distances		Angles	
Mo - Mo'	215.04(2)	Mo' - Mo - N2	174.53(4)
Mo - P1	258.49(5)	Mo - N2 ... C6	173.83(9)
Mo - P2'	258.70(5)	P1 - Mo - P2'	162.39(2)
Mo - O1	210.65(14)	O1 - Mo - O2'	178.05(5)
Mo - O2'	208.79(14)	P1 - N1 - P2	118.11(10)
Mo - N2	259.44(18)	O1 - C2 - O2	121.51(17)
P1 - N1	169.68(18)		
P2 - N1	169.55(18)	P1 - Mo - Mo' - P2	-5.85(2)
O1 - C2	126.9(2)	O1 - Mo - Mo' - O2	0.23(4)
O2 - C2	127.7(2)		
N1 - C3	147.8(3)		
C2 - C1	149.1(3)		

^a Translation of symmetry code to equivalent positions: (1-x, 1-y,1-z).

Table 4. Crystallographic data for **10**·CH₂Cl₂

Chemical formula	C ₆₅ H ₆₄ B ₂ Cl ₂ F ₈ Mo ₂ N ₄ O ₄ P ₄
Formula weight	1525.48
Crystal size (mm)	0.25 × 0.13 × 0.05
Crystal system	Monoclinic
Space group	P2 ₁ /n
<i>a</i> (pm)	1307.68(2)
<i>b</i> (pm)	1659.30(3)
<i>c</i> (pm)	1571.52(3)
<i>b</i> (°)	106.982(1)
<i>V</i> (10 ⁶ pm ³)	3261.3(1)
<i>Z</i>	4
<i>r</i> _{calcd} (g cm ⁻³)	1.553
<i>μ</i> (mm ⁻¹)	0.639
<i>F</i> 000	1548
<i>I</i> (pm)	71.073
Data collected (<i>h</i> , <i>k</i> , <i>l</i>)	±16, ±20, ±19
No. of parameters refined	433
<i>R</i> _{int}	0.0212
<i>R</i> ^a	0.0306
<i>WR</i> ₂ ^b	0.0667
GOF ^c	1.058
Weights <i>a</i> / <i>b</i> ^d	0.0148 / 3.6194
<i>Dr</i> max/min (e Å ⁻³)	0.59 / -0.44

^a $R_1 = \Sigma(|F_o| - |F_c|) / \Sigma|F_o|$; ^b $wR_2 = [\Sigma w (F_o^2 - F_c^2)^2 / \Sigma w (F_o^2)^2]^{1/2}$; ^c $GOF = [\Sigma w (F_o^2 - F_c^2)^2 / (NO - NV)]^{1/2}$;

^d $w = 1 / [\sigma^2(F_o^2) + (a * P)^2 + b * P]$ with $P: [\max(0 \text{ or } F_o^2) + 2F_c^2] / 3$.

Table 5. Proposed assignments of vibrational spectra of **16b**.

IR	Raman	Assignment
1690 vs	1693 rw	terminal $\nu_a(\text{CO}_2)$
1650 sh	1670 vw	
1507 vv	1589 rs	bridging $\nu_a(\text{CO}_2)$
1466 vw 1283 vw	1453 vs 1436 w,sh (1282 m)	$\nu_{as}(\text{CO}_2)$
1192 vs	1203 w	$\nu_a(\text{CF}_3)$
1166 s ~ 1110 sh	1144 m 1095 s 1025 vvs 1001 s	$\nu_{as}(\text{CF}_3)$
856 m 831 m 796 m	865 w 831 w 772 vw	$\nu(\text{CO}_2)$
730 s 719 s	737 m 724 m	$\nu_{as}(\text{CF}_3)$
647 w	647 vs	$\nu(\text{CO}_2)$
597 w	619 w,n	$\nu_a(\text{CF}_3)$
455 vv	504 m	
425 w	430 w	$\nu(\text{MoO})$
379 w	376 w	$\nu(\text{MoMo})$
331 w	344 s	$\nu(\text{MoO})$
	303 vs	$\nu(\text{MoMo})$
268 w,m	289 s	$\nu(\text{CF}_3)$
223 w		$\nu(\text{MoO})$
137 vw		$\nu(\text{MoP})$

Table 6. Proposed assignments of vibrational spectra for **17b**.

IR	Raman	Assignment
1684 sh 1647 s	1685 vw 1648 vs	terminal $\nu_a(\text{CO}_2)$
1608 vs	1592 m	bridging $\nu_a(\text{CO}_2)$
1466 vw	1456 vvs 1436 m, s	$\nu_{as}(\text{CO}_2)$
1194 vs	1209 vw	$\nu_{as}(\text{CF}_3)$
1164 s 1008 vw	1148 w 1097 wm 1025 vs	$\nu_a(\text{CF}_3)$
	991 m, b	
857 m 836 w 795 w	867 w 839 w, m 798 s	$\nu(\text{CO}_2)$
731 s 721 w	773 s 745 s 720 w	$\nu_{as}(\text{CF}_3)$
648 rw	649 s	$\nu(\text{CO}_2)$
620 w	632 w 620 vw	$\nu(\text{CO}_2)$
509 m	523 vvs 510 s	$\nu(\text{CO}_2)$
445 vw	440 m	$\nu_{as}(\text{MoO})$
382 w	388 vs	$\nu(\text{MoMo})$
331 vw	354 s	$\nu(\text{CF}_3)$
	307 vs	$\nu(\text{MoMo})$
264 w	295 w	$\nu(\text{CF}_3)$
231 w 223	167 m	other skeletal modes

Table 7. Preliminary assignments of vibrational spectra of **18**

IR	Raman	Assignment
1596 vs	1587 m	$\nu_a(\text{CO}_2)$
1434 vs	1438 w	$\nu_{as}(\text{CO}_2)$
1422 vs		$\nu_a(\text{CH}_3)$
1374 s	1386 vw	$\nu_{as}(\text{CH}_3)$
1320 m	1327 w	
1140 w	1155 m	
1128 w	1128 s	$\nu(\text{CC})$
1015 w		
916 vw		
	917 vw	
	843 vw	
650 w		$\nu(\text{CO}_2)$
	580 vw	$\nu(\text{CO}_2)$
542 s		$\nu(\text{CO}_2)$
(467 w)	~450 m, b	
	389 w	
380 w		
	337 s	$\nu_{as}(\text{RhO}_4)$
307 vw		
289 w		$\nu_a(\text{RhO}_4)$
	240 sh	$\nu(\text{RhRh})$
	287 vvs	
232 vw		
	222 w	other skeletal modes
	172 w	
	159 w	
157 vw		

Table 8. Preliminary assignments of vibrational spectra for **19**.

IR	Raman	Assignment
1594 vs	not found	$\nu_a(\text{CO}_2)$
1422 vs	1421 s	$\nu_{as}(\text{CO}_2)$
(1422 vs)	1453 m	$\nu_a(\text{CH}_3)$
1284 m	1278 m	$\nu_{as}(\text{CH}_3)$
1129 vw 1066 vvw	(1129 s) ~1061 vw	$\nu(\text{CC})$
695 s	not found	$\nu(\text{CO}_2)$
561 w	581 vw	$\nu(\text{CO}_2)$
525 s	527 m	$\nu(\text{CO}_2)$
(487 m) 467 vw	461 m (432 w)	
399 vw	399 m	
382 m		
	338 s	$\nu_{as}(\text{RhO}_4)$
323 w	325 sh	
303 vw		
	289 vvs	$\nu(\text{RhRh})$
278 w		$\nu_a(\text{RhO}_4)$
214 vw (?) 171 w, b	164 s 126 vs	other skeletal modes $\nu_a(\text{RhL})$

Table 9. Crystallographic data for **16b** and **17b**.

	16b	17b
Chemical formula	C ₄₀ H ₂₆ F ₁₂ Mo ₂ N ₄ O ₈ P ₂	C ₄₀ H ₂₆ F ₁₂ Mo ₂ N ₄ O ₈ P ₂
Formula weight	1172.47	1174.45
Crystal size(mm)	0.13×0.15×0.20	0.24×0.28×0.33
Crystal system	Triclinic	Triclinic
Space group	P $\bar{1}$	P $\bar{1}$
a/pm	966.60(3)	913.27(2)
b/pm	1046.78(3)	987.29(2)
c/pm	1203.17(3)	1287.91(4)
α /°	110.453(1)	111.895(1)
β /°	91.656(2)	91.209(1)
γ /°	105.882(1)	100.520(1)
V(10 ⁶ pm ⁻³)	1086.58(5)	1054.31(5)
Z	1	1
$\rho_{\text{calcd.}}$ (g.cm ⁻³)	1.792	1.850
μ (mm ⁻¹)	0.760	0.784
F ₀₀₀	580	580
λ (pm)	71.073	71.073
Diffractometer	Kappa CCD	Kappa CCD
Θ range(°)	1.82 to 26.07	2.26 to 27.50
Data collected (<i>h,k,l</i>)	±11, ±12, ±14	±11, ±12, ±16
No. of reflections	20571	24437
No. of independent reflections	3797	4821
No. of parameters refined	348	355
R _{int}	0.017	0.020
R ₁ ^a	0.0737	0.0561
GOF ^c	1.029	1.049
Weights a/b ^d	0.0241/1.8741	0.0087/0.9617
$\Delta\rho_{\text{max/min}}$ (eÅ ⁻³)	0.91/-0.55	0.66/-0.45

^a $R_1 = \Sigma(|F_o| - |F_c|) / \Sigma|F_o|$; ^b $wR_2 = [\Sigma w (F_o^2 - F_c^2)^2 / \Sigma w (F_o^2)^2]^{1/2}$; ^c $GOF = [\Sigma w (F_o^2 - F_c^2)^2 / (\text{NO} - \text{NV})]^{1/2}$; ^d $w = 1 / [\sigma^2(F_o^2) + (a * P)^2 + b * P]$ with $P: [\max(0 \text{ or } F_o^2) + 2F_c^2] / 3$.

Table 10. Selected interatomic distances (pm) and angles (°) for **16b** and **17b**.

16b		17b	
Mo-P	250.85(8)	Mo-P	252.54(5)
Mo-O2	210.5(2)	Mo-O2	212.65(13)
Mo-O3	239.9(29)	Mo-O3	234.92(13)
Mo-Moa	219.01(3)	Mo-Moa	218.84(2)
Mo-O1a	211.8(2)	Mo-O1a	211.23(13)
Mo-N1a	221.2(2)	Mo-N1a	220.56(16)
P-C11	182.1(3)	P-C11	183.13(19)
O1-C2	126.1(4)	O1-C2	126.5(2)
O2-C2	125.4(4)	O2-C2	125.4(2)
O3-C4	125.3(4)	O3-C4	125.9(2)
O4-C4	120.6(5)	O4-C4	121.9(3)
N1-C11	134.6(4)	N1-C11	135.8(2)
P-Mo-O2	94.36(6)	P-Mo-O2	91.57(4)
P-Mo-O3	74.75(5)	P-Mo-O3	73.18(4)
Moa-Mo-P	83.48(2)	Moa-Mo-P	83.96(1)
P-Mo-O1a	88.39(6)	P-Mo-O1a	90.96(4)
P-Mo-N1a	166.93(6)	P-Mo-N1a	167.46(49)
O2-Mo-O3	98.52(7)	O2-Mo-O3	84.17(5)
Moa-Mo-O2	91.23(5)	Moa-Mo-O2	89.74(4)
O1a-Mo-O2	177.11(8)	O1a-Mo-O2	177.15(5)
O2-Mo-N1a	90.70(8)	O2-Mo-N1a	89.79(5)
Moa-Mo-O3	156.69(5)	Moa-Mo-O3	156.11(4)
O1a-Mo-O3	81.32(7)	O1a-Mo-O3	95.33(5)
O3-Mo-N1a	92.60(7)	O3-Mo-N1a	94.57(5)
Moa-Mo-O1a	89.98(5)	Moa-Mo-O1a	91.81(4)
Moa-Mo-N1a	108.49(6)	Moa-Mo-N1a	108.51(4)
O1a-Mo-N1a	86.42(8)	O1a-Mo-N1a	87.46(5)
O1-C2-O2	125.6(3)	O1-C2-O2	126.33(17)
P-C11-N1	112.3(2)	P-C11-N1	112.01(13)

Translation of Symmetry Code to Equiv. Pos. a = [2556.00] = -x, -y, 1-z

Parts of this work have been published in scientific journals or presented as posters in scientific meetings

1. Publications:

1. Martyn Pillinger, Isabel S. Gonçalves, Paula Ferreira, João Rocha, **Guofang Zhang**, Marcus Schäfer, Oskar Nuyken and Fritz E. Kühn, in preparation (XAFS analysis and catalytic activity of MCM-41-supported dimolybdenum complexes containing metal-metal bonds)
2. **Guofang Zhang**, Fritz E. Kühn, E. Herdtweck, in preparation (Synthesis and Characterization of Dimolybdenum and Dirhodium Complexes Bearing 2-Pyridylphosphine Ligands, PPhPy₂ or PPy₃ (Ph = Phenyl; Py = 2-Pyridyl))
3. Paula Ferreira, Isabel S. Gonçalves, Fritz E. Kühn, Martyn, Pillinger, João Rocha, Alan Thursfield, Wen-Mei Xue and **Guofang Zhang**, *J. Mater. Chem.*, **2000**, *10*, 1395-1401 (Synthesis and characterization of MCM-41-supported dimolybdenum complexes)
4. F. E. Kühn, D. Schön, **Guofang Zhang**, O. Nuyken, *J. Macromol. Sci.*, **2000**, *A37 (9)*, 971-981 (Monometallic Solvent Stabilized Transition Metal Cations as Initiators for Cyclopentadiene Polymerization).
5. W. M. Xue, F. E. Kühn, **Guofang Zhang**, E. Herdtweck, *J. Organomet. Chem.*, **2000**, *596*, 177-182 (Synthesis and characterization of [trans-di(μ -acetato)(μ -bis(diphenylphosphino)ethylamine)bis(pyridine)dimolybdenum(II)]bis(tetrafluoroborate) and derivatives).
6. W. M. Xue, F. E. Kühn, **Guofang Zhang**, E. Herdtweck, G. Raudaschl-Sieber, *J. Chem. Soc., Dalton Trans.*, **1999**, 4103-4110 (Dimolybdenum(II) complexes linked by axial cyano bridges to organic and organometallic ligands: syntheses, structures, and characterization).
7. F. E. Kühn, J. R. Ismeier, D. Schön, W. M. Xue, **Guofang Zhang**, O. Nuyken, *Macromol. Rapid Commun.*, **1999**, *20*, 555 (Solvent Stabilized Transition Metal Cations as Initiators for Cyclopentadiene Polymerization).

2. Poster Presentations:

1. Synthesis, Characterization and Catalytic Properties of MCM-41-Supported Dimolybdenum Complexes. P. Ferreira, I.S. Gonçalves, F. E. Kuehn, M. Pillinger, J. Rocha, W.-M. Xue, **Guofang Zhang**, poster presentation at the *XVII Ibero-American Symposium of Catalysis*, July 2000.

2. Synthesis and Characterization of [*trans*-di(*m*-acetato)(*m*-bis(diphenylphosphino)methylamine)bis(pyridine) dimolybdenum(II)] bis(tetrafluoroborate) and Derivatives. W.-M. Xue, F. E. Kuehn, **Guofang Zhang**, E. Herdtweck, poster presentation at the *Royal Society of Chemistry Annual Conference 1999* held in Edinburgh, UK, September 1999, P08.
3. Structure and Spectroscopy of Mo(II)-Mo(II) Quadrupty Bonded Complexes Linked by Axial Cyano Bridges to Organic and Organometallic Ligands. W.-M. Xue, **Guofang Zhang**, E. Herdtweck, F. E. Kuehn, poster presentation at the *7th Austrian Hungarian International Conference on Vibrational Spectroscopy* held in Balatonfüred, Hungary, April 1999, P54.

Curriculum Vitae

Name: Guofang Zhang
Date of Birth: 06 July, 1967
Place of Birth: Shaanxi, P. R. China
Nationality: Chinese
Civil Status: Married to Xinyan Li
Child: Muqi Zhang, was born on 03. 08. 2001

1974-1985 Elementary and High School in Xingping, Shaanxi, P. R. China
1985-1989 Bachelor Degree of Science, Study of Chemistry at Normal University
Shaanxi, Xi'an, P. R. China
1989-1992 Master Degree of Science, Study of Inorganic Chemistry at Normal
University East China, Shanghai, P. R. China
1992-1997 Teaching Chemistry at Normal University Shaanxi, Xi'an, P. R. China
1998-2001 Ph. D. at the Technische Universität München under the supervision of
Priv.-Doz. Dr. F. E. Kühn in the group of Prof. Dr. Dr. h.c. mult. W.
A. Herrmann